LAUNCH VEHICLE PROPULSION PARAMETER DESIGN MULTIPLE SELECTION CRITERIA

by

JOEY DEWAYNE SHELTON

A DISSERTATION

Submitted in partial fulfillment of the requirements
for the degree of Doctor of Philosophy
in
The Department of Mechanical and Aerospace Engineering
to
The School of Graduate Studies
of
The University of Alabama in Huntsville

HUNTSVILLE, ALABAMA

2004

In presenting this dissertation in partial fulfillment of the requirements for a doctoral degree from The University of Alabama in Huntsville, I agree the Library of this University shall make it freely available for inspection. I further agree that permission for extensive copying for scholarly purposes may be granted by my advisor or, in his/her absence, by the Director of the Program or Dean of the School of Graduate Studies. It is also understood that due recognition shall be given to me and to The University of Alabama in Huntsville in any scholarly use which may be made of any material in this dissertation.

_____ _____

Joey Dewayne Shelton (date)

DISSERTATION APPROVAL FORM

Submitted by Joey D. Shelton in partial fulfillment of the requirements for the degree of Doctor of Philosophy in Mechanical Engineering and accepted on behalf of the Faculty of the School of Graduate Studies by the dissertation committee.

We, the undersigned members of the Graduate Faculty of the University of Alabama in Huntsville, certify that we have advised and/or supervised the candidate on the work described in this dissertation. We further certify that we have reviewed the dissertation manuscript and approve it in partial fulfillment of the requirements of the degree of Doctor of Philosophy in Mechanical Engineering.

_____ Committee Chair

(Date)

_____

_____

_____

_____

_____ Department Chair

_____ College Dean

_____ Graduate Dean

ABSTRACT
The School of Graduate Studies
The University of Alabama in Huntsville

Degree Doctor of Philosophy College/Dept Engineering/Mechanical and Aerospace Engineering

Name of Candidate Joey D. Shelton
Title Launch Vehicle Propulsion Parameter Design Multiple Selection Criteria

The optimization tool described herein addresses and emphasizes the use of computer tools to model a system and focuses on a concept development approach for a liquid hydrogen/liquid oxygen single-stage-to-orbit system, but more particularly the development of the optimized system using new techniques. This methodology uses new and innovative tools to run Monte Carlo simulations, genetic algorithm solvers, and statistical models in order to optimize a design concept.

The concept launch vehicle and propulsion system were modeled and optimized to determine the best design for weight and cost by varying design and technology parameters. Uncertainty levels were applied using Monte Carlo Simulations and the model output was compared to the National Aeronautics and Space Administration Space Shuttle Main Engine. Several key conclusions are summarized here for the model results. First, the Gross Liftoff Weight and Dry Weight were 67% higher for the design case for minimization of Design, Development, Test and Evaluation cost when compared to the weights determined by the minimization of Gross Liftoff Weight case. In turn, the Design, Development, Test and Evaluation cost was 53% higher for optimized Gross Liftoff Weight case when compared to the cost determined by case for minimization of Design, Development, Test and Evaluation cost. Therefore, a 53% increase in Design,

Development, Test and Evaluation cost results in a 67% reduction in Gross Liftoff Weight. Secondly, the tool outputs define the sensitivity of propulsion parameters, technology and cost factors and how these parameters differ when cost and weight are optimized separately. A key finding was that for a Space Shuttle Main Engine thrust level the oxidizer/fuel ratio of 6.6 resulted in the lowest Gross Liftoff Weight rather than at 5.2 for the maximum specific impulse, demonstrating the relationships between specific impulse, engine weight, tank volume and tank weight. Lastly, the optimum chamber pressure for Gross Liftoff Weight minimization was 2713 pounds per square inch as compared to 3162 for the Design, Development, Test and Evaluation cost optimization case. This chamber pressure range is close to 3000 pounds per square inch for the Space Shuttle Main Engine.

Abstract Approval: Committee Chair _____

Department Chair _____

Graduate Dean _____

ACKNOWLEDGMENTS

My wife, Susanna, has been so supportive of me through the years of graduate school. It has been a long road and but one that has provided great rewards in return. I also mention my children, Torianne, Hannah, Kaelie, Seth, and Alania because they are also a part of this. I love you all very much.

Pursuing my doctoral degree has been a rewarding privilege. I would like to thank Dr. Robert Frederick for his guidance and leadership over the last several years. And also Dr. Alan Wilhite who helped direct and focus me toward my research topic. I have been so fortunate to have such an outstanding committee. Thanks to you all.

I also want to acknowledge the advice from Joe Leahy/MSFC. Joe shared his insight into the P-Star tool being developed and used by the NASA MSFC Space Transportation Directorate and was always available for questions and suggestions. I also want to thank Dr. Christian Smart/SAIC-Huntsville for his help in understanding the NAFCOM cost uncertainty approaches and his sharing insights on lognormal distributions. Thanks so much.

TABLE OF CONTENTS

LIST OF FIGURES

LIST OF TABLES

LIST OF SYMBOLS

a	The 'a' coefficient for a power series regression curve
AR	Nozzle Area Ratio
AR_1	Nozzle Area Ratio of Engine One
AR_2	Nozzle Area Ratio of Engine Two
ART	Area Ratio Transition
A^*	Nozzle Throat Area
α	Alpha Angle
b	'b' coefficient for regression curve
BAC	Boeing Aircraft Corporation
β	Response Surface Model Coefficient
CAIV	Cost as and Independent Variable
CEA	Chemical Equilibrium with Applications
Cequel	Chemical EQUilibrium in excEL
C_f	Thrust Coefficient
C_{f1}	Thrust Coefficient of Engine 1
C_{f2}	Thrust Coefficient of Engine 2
CIF	Cost Influence Factor
CLO	Closed Loop Optimization
CompFactor	Cost Complexity Factor
C_{star}	Characteristic Exhaust Velocity
D	Drag

DDTE	Design Development Test and Engineering
D_{mani}	Manifold Diameter
DNA	Deoxyribonucleic acid
DOE	Design of Experiments
D_R	Tube Diameter
D^*	Engine Throat Diameter
Δr	Change in the Value of 'r'
ΔX_1	Change in the Value of 'X_1'
ΔX_2	Change in the Value of 'X_2'
ΔX_J	Change in the Value of 'X_J'
∂r	Partial Derivative of 'r'
∂x	Partial Derivative of 'x'
E	Error
$E(x)$	Expected Value
e	Logarithmic Exponent
ε	Error due to Response Surface
FOM	Figure of Merit
FPL	Full Power Level
ft^2	Feet Squared
ft^3	Feet Cubed
GA	Genetic Algorithm
$GLOW$	Gross Liftoff Weight

g_o	Gravitational Constant
HTO	Horizontal Take-Off
ISP	Specific Impulse
ISP_{sl}	Sea Level Specific Impulse
ISP_{vac}	Vacuum Specific Impulse
ITAR	International Traffic in Arms Regulation
J-2	Saturn Rocket Stage Two Engine
L	Cone Reference Length
lbf	Pounds Force
lbm	Pounds Mass
LE-7	Japanese Rocket Engine LE-7
LE-7A	Japanese Rocket Engine LE-7A
LLC	Life Cycle Cost
L_{mani}	Manifold Diameter
ln	Natural Log
LH2	Liquid Hydrogen
LVSS	Launch Vehicle Sizer and Synthesis
LOX	Liquid Oxygen
γ	Launch Angle
M_{DM}	Engine Jacket Mass
m_{dot}	Engine Mass Flow Rate
M_{DR}	Engine Tube Mass
m_f	Final Vehicle Mass

m_i	Initial Vehicle Mass
M_{mani}	Manifold Mass
m_p	Propellant Mass
MMC	Martin Marietta Corporation
MR	Vehicle Mass Ratio
MSFC	George C. Marshall Space Flight Center
μ	Mean Value
n	Number of Cases and/or Examples
NAFCOM	NASA/Air Force Cost Model
$NAFCOM_{unc}$	NASA/Air Force Cost Model Uncertainty
NASA	National Aeronautics and Space Administration
NPL	Normal Power Level
OF	Oxidizer/Fuel
OF_1	Oxidizer/Fuel Ratio of Engine One
OF_2	Oxidizer/Fuel Ratio of Engine Two
OMS	Orbital Maneuvering System
O_R	Integrated Surface
P_c	Chamber Pressure
P_{c1}	Chamber Pressure of Engine 1
P_{c2}	Chamber Pressure of Engine 2
PGG_{inj}	Pressure of Gas Generator Injector
psi	Pounds per square inch

PSTAR	Propulsion Sizing, Thermal Analysis and Weight Relationship
r	Unspecified Variable
RD-0120	Russian Rocket Engine RD-0120
R&D	Research and Development
R^2	Sample Coefficient of Determination
ρ_c	Density of Jacket Material
ρ_{mani}	Density of Manifold Material
RCS	Reaction Control System
RSM	Response Surface Modeling/Model
RS-68	Russian Engine Number 68
σ	Standard Deviation
$\sigma_{zul\ R}$	
SAIC	Science Application International Corporation
SE	Standard Error
s_{mani}	Manifold Wall Thickness
S_M	Jacket Average Thickness
S_R	Tube Average Thickness
SSME	Space Shuttle Main Engine
SSTO	Single-Stage-to-Orbit
S_{xx}	Standard Deviation for x^2 terms
S_{xy}	Standard Deviation for xy terms

S_{yy}	Standard Deviation for y^2 terms
T	Thrust
T_c	Chamber Temperature
TCA	Thrust Chamber Assembly
TEP	Thermal Equilibrium Program
TF	Technology Factor
TPS	Thermal Protection System
T_{sl}	Sea Level Thrust
T_{vac}	Vacuum Thrust
Twi	Initial Thrust-to-Weight Ratio
T1_T	Set 1 Thrust versus Total Thrust
θ	Theta Angle
U_r	Uncertainty With Respect to 'r'
U_X	Uncertainty With Respect to 'X'
U_{X1}	Uncertainty With Respect to 'X1'
U_{X2}	Uncertainty With Respect to 'X2'
U_{XJ}	Uncertainty With Respect to 'J^{th}' Variable
Var	Variance
VTO	Vertical Take-off
Vulcain	European Rocket Engine Vulcain
Vulcain 2	European Rocket Engine Vulcain 2
W	Weight

W_B	Bare Engine Weight
W_{dot}	Propellant Flow Rate
W_{nozzle}	Nozzle Weight
$W_{nozzle\text{-}ext}$	Nozzle Extension Weight
$W_{nozzle\text{-}act}$	Nozzle Actuator Weight
$W_{PR,FD}$	Engine Pressure and Feed System Weight
W_{pump1}	Weight of Pump One
W_{pump2}	Weight of Pump Two
Wt_{unc}	Weight Uncertainty
W_{total}	Total Engine Weight
x	Unspecified Variable 'x'
y	Unspecified Variable 'y'
Y	Response Surface Equation Value
Z	Response Surface Output
2-POS	Two Position Nozzle

CHAPTER 1

INTRODUCTION

Studies in propulsion techniques for hypersonic flight regimes are adding considerable information leading to the possibility of a Single Stage to Orbit (SSTO) space vehicle. Ramjet-Scramjet technology has also provided numerous alternative proposals to current space vehicle concepts. But little is known about the system cost, performance and reliability of Ramjet-Scramjet engines. An exhaustive study in the optimization of current liquid propulsion systems could prove beneficial in reducing cost and increasing the reliability of space flight.

Significant research and development dollars have focused on methodologies to analyze preliminary designs for rocket propulsion systems of concept space vehicles. One such vehicle analysis technique is termed Closed Loop Optimization (CLO). CLO is very simply a process or strategy that explicitly allows for incorporating internal feedback into the system in order to provide the best results for a specified variable used in the design of a vehicle. An example illustration of an optimization flow process is shown in Figure 1.1.

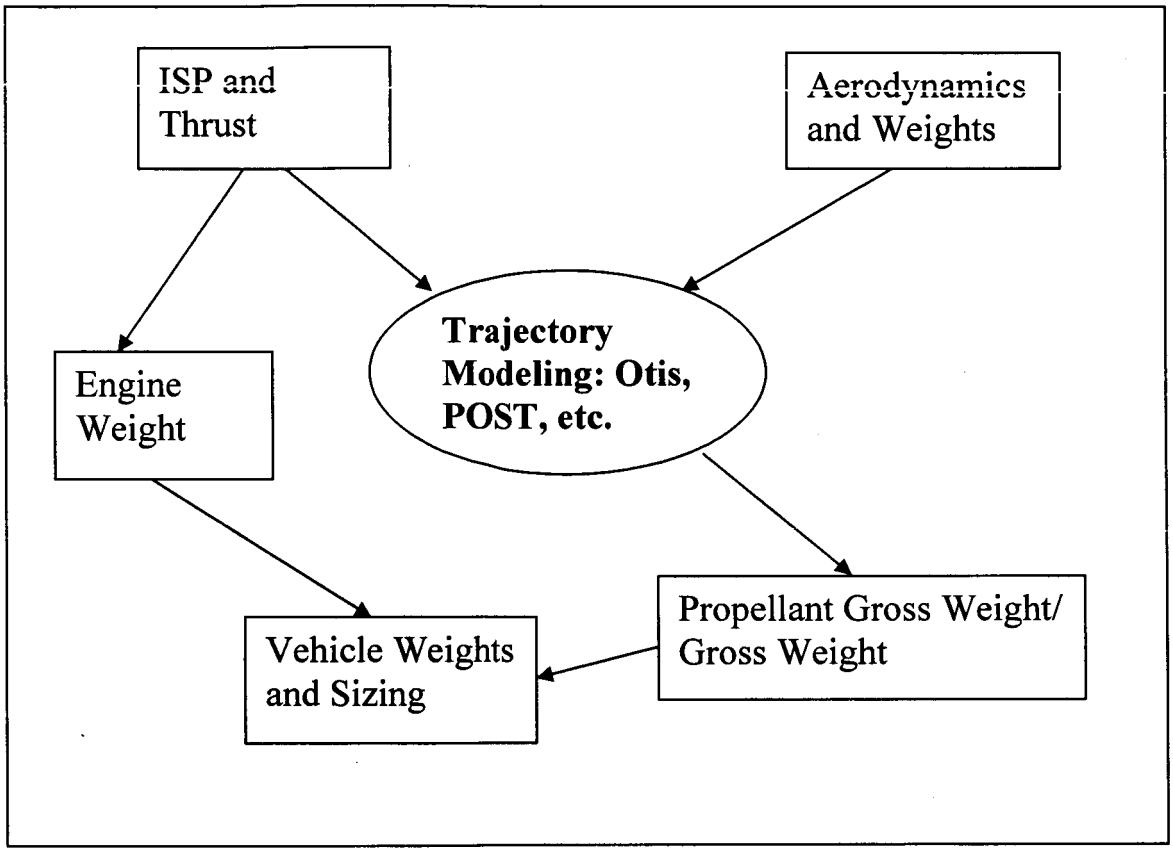

Figure 1.1 Vehicle Modeling Process

To date, no modeling tools are available that incorporate key propulsion system variables in a totally iterative and optimum way. Propulsion variables such as Specific Impulse (*ISP*), Engine Mass, Propellant Mass/Gross Lift off Weight (*GLOW*), Nozzle Area Ratio (*AR*), Chamber Temperature (T_c), Chamber Pressure (P_c), Thrust (T), Initial Thrust-to-Weight Ratio (*Twi*), and Oxidizer/Fuel (*OF*) Ratio, have not been fully integrated into the modeling for closed loop analysis of launch vehicle concepts. The

performance characteristics for propulsion optimization are measured by weight, reliability and cost of operations. The primary goal of the optimization studies herein are based upon the weight savings in the propulsion system but will also focus on cost. This study will focus on the use of rocket engines that utilize a liquid hydrogen fuel and liquid oxygen oxidizer. Reduction in the overall Research and Development (R&D) cost can be accomplished by proving that you can optimize propulsion system components using an existing rocket system, and then comparing the known system with the optimization tool outputs. This enables the system designer to understand the limitations of a vehicle concept. The subject of launch vehicle optimization concludes in the evaluation of a pre-defined system and its analytical results.

The model methodology described is formed for an SSTO system that uses liquid oxygen and liquid hydrogen and focused on the minimization of key parameters relating to vehicle weight and cost. Key performance measures are defined for *GLOW* minimization, Dry Weight minimization, Dry Weight with Margin minimization, Design, Development, Test and Evaluation cost minimization, Production cost minimization, Operations cost minimization, and Life Cycle cost minimization. The approach uses a combination of historical data for weight relationships, Monte Carlo simulations for uncertainty analysis, technology factors and cost influence factors for trading weight savings for cost savings, thermochemical analysis, and genetic algorithm solvers for concept optimization. The optimized design cases result in a defined set of parameters for chamber pressure, area ratio, oxidizer/fuel ratio, thrust to weight ratio, mass ratio, and also the corresponding technology and cost influence factors. The Monte Carlo

simulation uncertainty is used to determine the performance measures for cost and/or weight based upon lognormal distribution functions at 95% uncertainty. The results of the study reflect the improvements in methodology and the practical use of the tool to measure propulsion parameter sensitivity when compared to the key performance measures.

CHAPTER 2

LITERATURE REVIEW

In recent years there have been numerous accomplishments in the development and use of computer modeling and simulation for launch vehicle analysis. Using a software tool to determine the vehicle, system or component functionality and specification has reduced the overall time for a) research and development, b) conceptual design analysis, c) trade studies development, and d) design, development and test of systems. The use of optimization techniques has been refined in many ways and is described herein using results found during a review of existing work done in this area.

The components of system modeling addressed in Figure 1.1, form the basis of departure for current best practices. The focus of this modeling approach emphasizes the use of not only the best model for a specific aspect of the system but the feasibility of the approach when combined with the integrated model. The techniques/methods examined in this review are defined here in Table 2.1. Each is defined as either applicable or not applicable to the model described herein. The literature review focused on the methods with potential application to the integrated model. Several of the possible methods were not chosen because of the limited ability to link with other model components and/or the utility being performed by the function was not necessary for the integrated model.

Table 2.1 Modeling Techniques and Methods Utilized

Method	**Applicable**	**Not Applicable**
Technology Factors	CR2866	-
Uncertainty	Monte Carlo (Lognormal Distributions)	Numerical Uncertainty, Monte Carlo (Normal and Triangular Distributions)
Response Surface Modeling	-	Response Surface Modeling
Genetic Algorithm	Genetic Algorithm Solver	-
Propulsion Engine Mass	NASA Langley, U.S. Air Force, Rocketdyne, Historical Data Curves, Nozzle Physical Model	Manski-Martin Method
Trajectory	Rocket Equation	POST, Otis
Weights and Sizing	Parametric Technique	-
Cost	NAFCOM	-
Thermochemical	Cequel	CEA, TEP

2.1 Technology Requirements and Factors

In October 1977, Haefeli, Littler, Hurley and Winter [1] defined the areas of interest for technology development for an earth to orbit transportation system. An assessment was made to define which technologies would be important in the development of an SSTO system. The study defined each particular technology available and used a method to evaluate and to determine which technologies would further the overall vehicle capabilities in meeting the goal of SSTO. Two primary areas of interest were defined: 1) structure and materials and 2) propulsion system performance.

The significant technology areas are defined in greater detail by graphing historical data on existing and previous vehicle systems. The graphs have important design parameters on the y-axis that show the level of a measured variable versus the x-axis that defines the applicable calendar year, surface area, volume, or subsystem parameter used to determine technology projections. Several examples of the technology projection curves are shown in Figures 2.1, 2.2 and 2.3. Figure 2.3 defines the historical curves for Orbital Maneuvering System (OMS) and Reaction Control System (RCS) *ISP* levels and weight levels. Using the historical data, each component of a system (wing, tail, body, etc.) is assigned a technology factor based upon the historical weight and technology projection data. A factor of 1.0 assumes no improvement in baseline technology; where as a factor of .5 would assume a 50% better result. The technology factor (TF) approach will be used to formulate weights and sizing models later in Section 3.1.1.

The technology factors described by Haefeli, Littler, Hurley and Winter [1] show the value of projecting technology enhancements in the design of a future SSTO system. This approach is a key component of the methodology and will later prove that technology enhancements can be traded against a vehicle cost increase in order to optimize the concept vehicle. The accuracy of the technology factor results is shown when examining the regression values for the data curve fits. A more current and up-to-date assessment of the technology enhancements, since 1979, would greatly enhance the fidelity of the data used in formulating the value or projection of weight, cost, etc., savings for a specified technology on into the future.

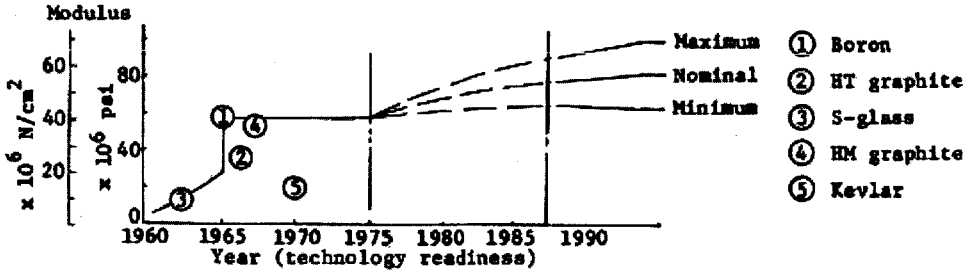

Figure 2.1 Advanced Composite Fibers - Modulus History and Projection [1]

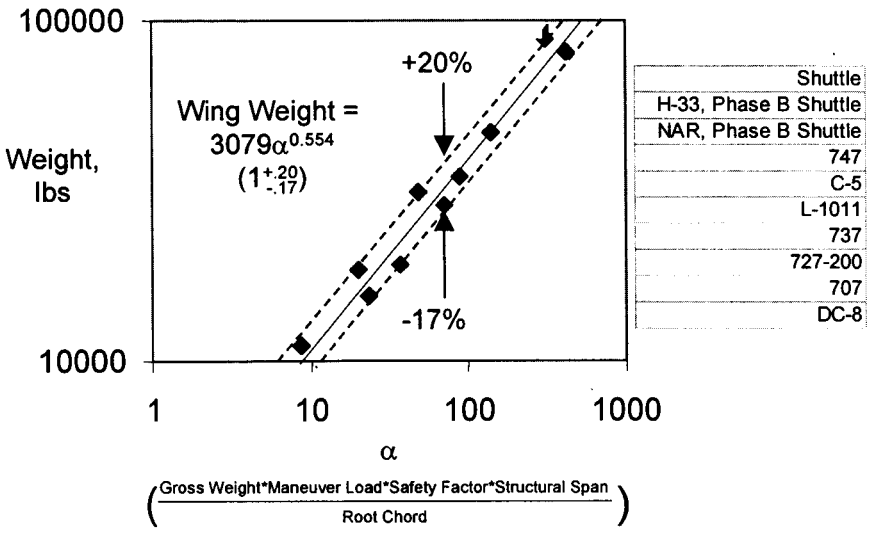

Figure 2.2 Historical Wing Structure Weight and Regression Curve [2]

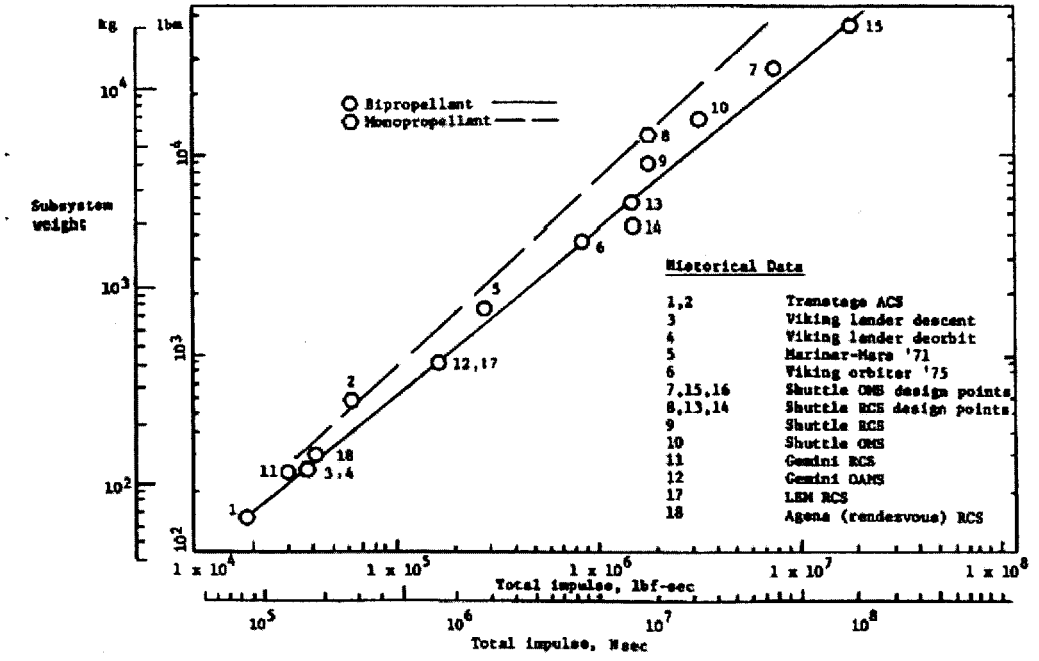

Figure 2.3 OMS/RCS Weight and History Projection [1]

2.2 Uncertainty Methodology

Typically, uncertainty levels can be computed using simple numerical techniques or by more robust methods that utilize Monte Carlo simulations. Classical uncertainty methods use a derivative approach to define an overall uncertainty value. The basic concept is to change an input variable by some specified amount and measure the magnitude of the change in the result being computed, in this case vehicle dry weight. An example of the numerical uncertainty data output is defined in Appendix A. The appendix data shows the results of a numerical dry weight uncertainty at a given condition by combining the component uncertainties into a total value for a given parameter.

The Monte Carlo simulation approach provides the flexibility to establish the distribution function such as normal, uniform, triangular, etc. This method also allows the user to define the bounds of the simulation for number of iterations and tolerances for the uncertainty results. The simulation is not restricted to the number of variables or inputs and the Monte Carlo approach can use a large number of inputs while still producing an overall system level uncertainty result.

Wilhite, Gholston, Farrington and Swain [2] performed an uncertainty analysis for both a SSTO and Bimese concept vehicles. The study utilized the Monte Carlo approach to do an uncertainty calculation. The analysis used a version of the LVSS model and @RISK^{TM} Risk Analysis and Simulation Software [3]. Propulsion, Overall Body, Thermal Protection System (TPS), Systems, Liquid Oxygen (LOX) Tank, Liquid

Hydrogen (LH2) Tank, Tail, Wing, and Landing Gear components were part of study. The results showed that a 95% probability for the vehicle dry weight resulted in an uncertainty range of +/- 25 percent. The @Risk tool was used to produce a sensitivity table for the components and is defined in Figure 2.4. The cumulative probability results are shown in Figure 2.5.

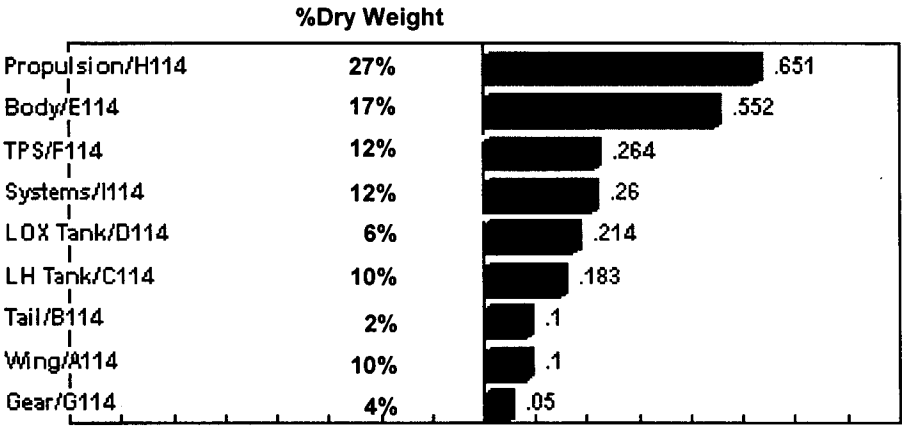

Figure 2.4 Component Sensitivity on Vehicle Dry Weight [2]

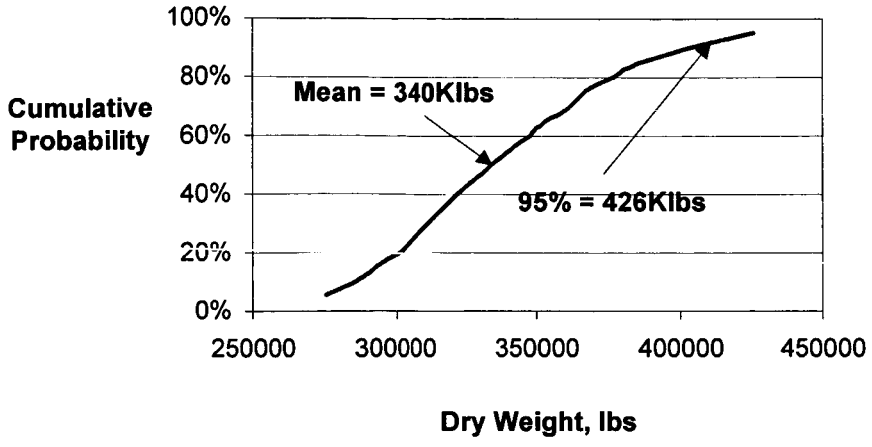

Figure 2.5 Vehicle Dry Weight Range at 95% Certainty [2]

A modified method of the uncertainty calculation defined by Smart [4] is based upon the use of lognormal distribution functions as Monte Carlo @Risk distribution. The regression curves defined in Section 2.1 represent a power regression fit and the lines are plotted on a log-log scale to show them as a linear curve fit. Since the regression curves are plotted in log-space, the distribution function should also be lognormal in order to remain in log-space as well. By using a triangular, normal or uniform distribution during the Monte Carlo operation, the accuracy of the results is diminished. In particular, in an explanation by Smart [4], the triangular distribution accuracy is lower because it focuses on defining only an upper and lower estimate and the distribution is not weighted based upon the remaining estimates and or data that reside within the overall range of data results used in the regression analysis. On the other hand, a lognormal distribution factors in the combined results into the mean and standard deviation of the distribution. The use of lognormal distributions, derived from the historical data, results in a much

more closely aligned distribution and gives a greater accuracy when the overall uncertainty is computed. The mean or expected value and the standard deviation or variance are calculated using the following equations (2.1 and 2.2) as defined by Walpole, Myers, Myers and Ye [5],

$$E(x) = e^{\mu + \frac{\sigma^2}{2}} \tag{2.1}$$

and

$$Var(x) = e^{2\mu+\sigma^2} * \left(e^{\sigma^2} - 1\right). \tag{2.2}$$

The review shows the feasibility of using Monte Carlo simulations to derive an uncertainty range for the vehicle by analyzing the individual uncertainty levels produced by each component. The Monte Carlo approach provides a more accurate solution to the uncertainty than the numerical approach and allows the option to choose thousands of iterations when computing the end result. The numerical approach is limited in that it does not integrate well with the other components of the model and has proven historically to be less accurate than a Monte Carlo simulation.

2.3 Response Surface Modeling

The Response Surface Modeling (RSM) technique allows the model or simulation designer to develop an equation that represents the model or some components of the model. This method is understood by considering the impact of a model input change, to the overall output of the model using Design of Experiment (DOE) techniques and is defined by Box and Draper [6]. In most cases a specified input (x_1) has a combined effect with input (x_2). This requires that the model utilize not only the

contribution of input (x_1) and input (x_2), but the combined impact that inputs (x_1) and (x_2) have on the model result. The response surface is an approximation of the model solution that is formed using a curve fit. The general form of the response surface equation, shown here in equation (2.3), is a relationship to link the model output (Y), the mean value of the output of the response surface (Z), which is a function of some set of known input variables (x_1, x_2) defined by Box and Draper [6],

$$E(Y) = Z = f(x_1, x_2). \tag{2.3}$$

The process steps for preparing a response surface model include recognition of the output to be studied, the definition of the parameters of interest, along with the experimental or theoretical highs and lows for the input parameters. The method defines 4 trials for the standard layout of a full-factorial using 2 input parameters (x_1 and x_2). The number of trials is driven by the number of (X) input parameters and is given by the expression in equation (2.4),

$$Trials = 2^X. \tag{2.4}$$

A half factorial would reduce the number of trials by ½. For example, in an 8-parameter study, the number of trials is equal to 256, with the ½ factorial equaling 128 trials. A corresponding ¼ fraction would further reduce the number or trials to 64. This is important to understand because the number of trials could have a significant impact upon the total cost to a particular project or program being analyzed. If the runs were simplistic and relatively easy to accomplish, then a complete run or 256 for an 8-parameter example case would be best. The total run would give you better accuracy than a reduced number of runs. So, the experiment designer has to determine whether the

number of runs or accuracy is the driving factor and must decide based upon individual circumstances.

The most common forms of the response surface model equation are either linear of quadratic. Montgomery [7] defines the linear form of the RSM for a two-variable study in equation (2.5),

$$Y = \beta_0 + \beta_1 x_1 + \beta_2 x_2 + \beta_{12} x_1 x_2 + \varepsilon . \qquad (2.5)$$

The value of β_0 is the point where x_1 and x_2 are equal to zero. The β_1 and β_2 are the coefficients for the effects of x_1 and x_2 on the result (Y). The β_{12} is the coefficient for the combined effect of x_1 and x_2 on the result (Y). The error or difference between the $E(Y)$ and the response surface is defined as error (ε). The ε should be minimized in order to maintain an accurate representation of the computer model using the response surface. The quadratic form of the RSM for a three-variable system is given by Montgomery [7] in equation (2.6),

$$\hat{y} = \beta_0 + \beta_1 x_1 + \beta_2 x_2 + \beta_3 x_3 + \beta_{12} x_1 x_2 + \beta_{13} x_1 x_3 + \beta_{23} x_2 x_3 + \beta_{11} x_1^2 + \beta_{22} x_2^2 + \beta_{33} x_3^2 . \qquad (2.6)$$

The advantage of the DOE tool is the fact that a RSM can replace the actual computer model and in doing so reduce computation time and difficulty of managing input and output to the model. The RSM representation of the output can then be incorporated into a more complicated vehicle modeling process to effectively represent

the result. The RSM takes the inputs and places them into a single equation that relays the output immediately. The negative aspect of the response surface is that any changes to the core model are not readily input into the RSM without going back and computing a new RSM using the DOE tools. Also, the RSM does introduce some errors due to numerical approximation. In most cases the RSM is determined at a 95% probability level. Since the RSM approach diminishes the accuracy of the results by approximately 5%, it is likely that this technique will not be utilized in the integrated model. The use of RSM is better served when time and money are important to the system designer. In the case describe herein, there is no need to use the RSM in the integrated model.

2.4 Genetic Algorithms

Obitko [8] points out that John Holland invented Genetic Algorithms (GA) in 1975 as a technique in support of the artificial intelligence efforts. According to Obitko [8], the GA methodology relies upon the understanding that a solution can be evolved based upon a population of inputs. The principles of chromosomes and DNA strings served as the guideline in the development of GAs. During human reproduction a recombination of DNA occurs when the parent's combine to form a new chromosome. The new creation results from DNA having changed form from the parents. The changes are caused by genetic copying errors, but the goodness of the organism is measured by the survival of the new life.

Schoonover, Crossley and Heister [9] provide a detailed technical description of the GA implementation and process as applied to hybrid rockets. A large hybrid rocket concept was designed to minimize the *GLOW* and inert mass of the system. The

optimizer included the variation of tank pressure, chamber pressure, and oxidizer mass flux along with discrete variables such as the propellant combination and the number of fuel ports. The results showed that GA solvers assigned to a broad array of vehicle design options can produce optimization results without the expense of exploring a large number of design options separately.

The optimized solution is defined as the best of all possible solutions given specified constraints. Therefore the inputs selected for the solution include not only the variables themselves but also the range (space) in which the inputs are defined. The GA technique begins by guessing a solution in the search space using the minimum and maximum point for each input and having the algorithm search for the best result out of all possible solutions. The approach uses an extreme value (or maximum/minimum) to help find the solution. Once a crossover point is found, the solution will iterate back and forth while converging toward the solution. The crossover point is a phenomenon whereby the current best guess is exceeded then reduced above and below the best guess. Schoonover, Crossley and Heister [9] define this crossover process in the illustration defined in Figure 2.6. The low point in the trough is the location of the optimum design solution. If the convergence of the crossover is steep, then the solution is more clear and easier to define. If the slope is shallow, then a solution with 95% certainty could have wide range depending upon the inputs. Inputs normally have varying degrees of impact on the solution. The inputs, with larger impacts, define a more narrow range for the solution, if numerous solutions are performed using the identical system.

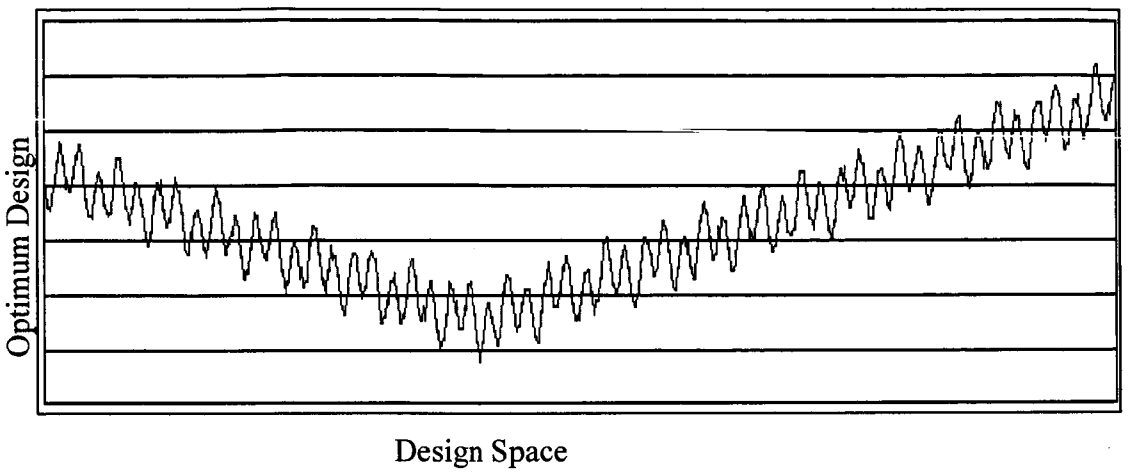

Figure 2.6 Genetic Algorithm Cross Over [9]

An advantage in using GAs is that the trade space is very wide since each input has its own unique design space. This helps the user because it is less likely for the solver to reach an extreme point and stop computing. A small negative aspect of using GAs is that it will take more time to compute a solution and is generally slower than other methods. The Palisades Software Evolver Tool [3] includes a GA solution technique that allows you to stop the computation at any time, thus allowing the user to make a decision to terminate computation after a specified number of runs or a pre-determined time period. The user may also choose to terminate the solver tool if there is not a noticeable change in the optimized solution over a long period of time. There is flexibility in the solution approach that allows the user to determine what degree of accuracy they wish to achieve.

The GA solver applicability is the key component in allowing the optimization of an output based upon select inputs. The solver gives the system user the ability to set constraints and ranges for design parameters that are consistent with current technology and design practices. The GA solver is extremely important to an integrated model methodology and without it the user is constrained to playing what-if scenarios by manually changing inputs and measuring the effects on the output.

2.5 Propulsion System Parameter Optimization

Vehicle computer models and analysis tools have been developed to integrate and to optimize specified parameter(s) of the launch vehicle system. In Phase A studies, numerous proposed configurations are evaluated to determine which design option possesses the best attributes for cost, weight, reliability, etc. Models and tools often include numerical solvers, genetic algorithm solutions, RSM techniques to simulate a model by using an equation, and integration tools to combine inputs and outputs of various modules within design model. Wilhite, McKinney, Farrington and Lovell [10] utilized RSMs, along with system modeling components for trajectory, weights and sizing, and aerodynamics to determine the sensitivity of parameters critical to the launch process such as Mass Ratio (MR) which is the *GLOW* divided by the Dry Weight plus Margin, *Twi* which is the initial vehicle thrust level divided by the initial weight of the vehicle, and flight path angle. Integration of modeling tools has become much more common among the propulsion and launch vehicle community as a cost effective way to evaluate conceptual systems.

Historically, math or analytical models have been used to analyze and determine engine mass and performance. These models utilize equations that relate specified parameters from the engine data in order to determine the overall mass and or size of the engine. Three methods are defined here and sample equations are shown within each method. Parameters of interest are the P_c, OF Ratio, T, and AR that are either provided by the engine or derived for the engine. In many cases the impact of these variables on the mass of the engine are not known. This causes difficulty when modeling a launch system because there is a need to optimize the projected engine mass prior to the actual design and weighing of the real rocket engine.

2.5.1 Propulsion System Mass Model Methodology

Manski and Martin [11] developed a method to optimize propulsion cycles using analytical models to determine the overall engine mass. The approach distributed the engine masses into categories of a) control and turbo-pump system and b) thrust chamber assembly as shown in Figure 2.7. The control and turbo-pump system included the mass of the gas-generator or preburner, turbopumps, valves, hot gas manifold, and auxiliary nozzles. The thrust chamber assembly included the masses for the thrust chamber and regeneratively cooled nozzle. The technique for evaluating the regeneratively cooled nozzle mass is shown below for illustration purposes. The remaining equations are not shown herein but are defined by Manski and Martin [11].

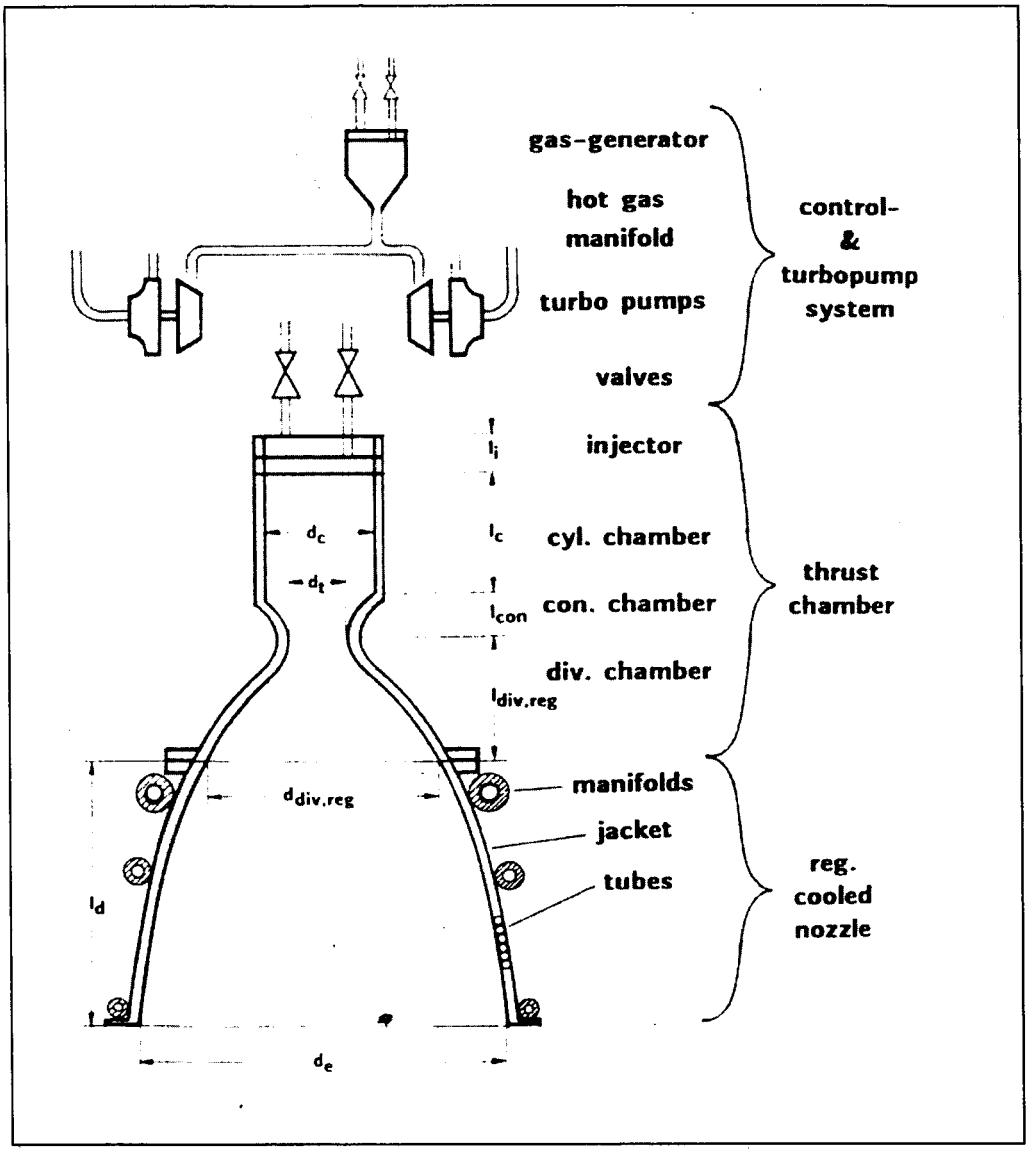

Figure 2.7 Engine Assembly Components [11]

The regeneratively cooled nozzle total mass estimations utilize the combined masses from the manifolds, jackets and tubes. The mass of the tubes is determined using the basic vessel equation for cylindrical shapes given in equation (2.7) by Manski and Martin [11],

$$S_R = \frac{PGG_{inj} * D_R}{2\sigma_{zul\,R}}. \tag{2.7}$$

The engine tube mass is determined using the integrated nozzle surface (O_R) and tube average thickness (S_R) as shown in equation (2.8) by Manski and Martin [11],

$$M_{DR} = \pi * S_R * O_R. \tag{2.8}$$

The overall nozzle surface value is calculated using AR, P_c, thrust level, propellant selection and OF Ratio.

The manifold mass is determined using the relationship between the manifold length, diameter and thickness. Manski and Martin [11] defined the relationships and equations used to obtain these three variable inputs listed above. Manski and Martin [11] defined the manifold mass equation in (2.9),

$$M_{mani} = 3s_{mani} * \pi * D_{mani} * L_{mani} * \rho_{mani}. \tag{2.9}$$

The manifold mass is dependent upon the cooling flow, thrust level, propellant selection and OF Ratio, and pre-burner injection pressure.

The engine jacket mass is determined by the chamber pressure and not the pre-burner pressure. Manski and Martin [11] utilize the vessel equation to determine the thickness. The approach used a minimum thickness of .1 mm for analysis purposes. The jacket mass equation (2.10) is given by Manski and Martin [11] based upon the average thickness, nozzle surface and density of the material,

$$M_{DM} = s_M * O_R * \rho_c . \tag{2.10}$$

2.5.2 Langley Research Center Engine Weight Studies

Engineers at the NASA Langley Research Center [12] developed a series of equations to determine the engine masses using the propellant flow rate (W_{dot}), P_c, and AR for Vertical Take-off (VTO), LH2 and LOX engines. The study was completed using comparison study results from Boeing and Aerojet techniques to determine engine masses. Equations were developed for the a) nozzle mass for $AR < 40$, b) mass of nozzle extension, c) mass of nozzle actuator, d) mass of the bare engine, e) mass of the pressurization and feed system. The total propulsion system mass was determined based upon the components above, including W_{dot} and a correlation coefficient for the bare engine mass. The equations (2.11) to (2.16) are used to calculate the components mentioned above.

$$W_{nozzle} = .01194 * (AR - 1) * W_{dot}, \tag{2.11}$$

$$W_{nozzle-ext} = 9.943 * (AR - 40) * \frac{W_{dot}}{P_c}, \tag{2.12}$$

$$W_{nozzle-act} = 60.54 * (\sqrt{AR} - 1) * \sqrt{\frac{W_{dot}}{P_c}}, \tag{2.13}$$

$$W_B = 4.73 * W_{dot}, \tag{2.14}$$

$$W_{PR,FD} = .59 * W_{dot}, \tag{2.15}$$

and

$$W_{Total} = 1.113 * (\frac{W_B}{W_{dot}}) * W_{dot} + W_{nozzle} + W_{nozzle-ext} + W_{nozzle-act} + (\frac{W_{PR,FD}}{W_{dot}}) * W_{dot}. \tag{2.16}$$

The data and results from the study are shown here in Table 2.2. The data shows a range of uncertainties for the model results between –27.08% and 27.18% error when comparing the actual weight (quoted weight) to the calculated weight.

Table 2.2 NASA Langley Engine Weight Study

Engine	Vacuum Thrust (lb)	ISP (sec)	Pc (lb/in^2)	AR	Quoted Weight (lb)	Calculated Weight (lb)	Error (%)
SSME, NPL	470,000	455.2	2970	77.5	6339	6026	-5.19%
SSME, FPL	512,000	456.6	3237	77.5	6339	6615	4.17%
Rocketdyne	500,000	455.2	3000	80	6650	6427	-3.47%
Rocketdyne	500,000	469	3000	200	8480	6673	-27.08%
BAC, HTO, 2-POS	695,000	465.2	3500	150	9913	9978	0.65%
BAC, VTO	1,056,874	442.8	3800	39.9	11590	14980	22.63%
BAC, VTO, 2-POS	1,100,000	460.9	3800	110	13654	15872	13.97%
MMC	600,400	436.1	4500	35	6769	9295	27.18%
MMC, 2-POS	638,125	463.5	4500	160	9084	10132	10.34%

A concern with the Langley method is that increasing chamber pressure results in very little change in Bare Engine Weight (W_B) when the results should reflect that an increase in the chamber pressure increases the W_B. This is not the case for the solution methodology. Also recognized was the fact that the ranges of AR lower than 40 and

higher than 100 resulted in significantly higher error values when comparing the actual weight to the calculated weight.

2.5.3 U.S. Air Force Engine Modeling

Paulson, Burkhardt, Mysko and Jenkins [13] developed an analytical approach to derive rocket engine masses based upon engine performance parameters. The method relies upon the use of historical engine data for non-Hydrogen, and Hydrogen based engines. Historical data produced equation correlations to determine the mass of engine components for Thrust Chamber Assembly (TCA), Turbomachinery, Preburner, and Lines/Ducts/Valves/Miscellaneous Hardware. The results show that the approach produces an engine mass that closely matches the actual design masses for the engines used in the study.

The TCA mass, including nozzle mass, is derived using a physical model of the nozzle. Once a physical representation is made for the chamber and nozzle, the weight measurements are made based upon material density. The total engine mass is obtained by adding the component masses, along with the nozzle mass, together. The focus on using known engine design parameters to determine the overall mass of the engine is useful in determining what parameters impact the overall engine mass. This is important to engine design since engine mass is a key factor in the design of a launch system.

2.5.4 Rocketdyne Power Balance Model

In the early 1960's, Wells [14] derived a method for determining engine component masses by comparing design parameters of an operating engine with the design parameters of a theoretical engine. NASA used the power balance approach in the development of the Space Shuttle Main Engine (SSME). Combinations of functioning engine components are used with the concept components and form a relationship using coefficients as exponents for the parameter ratios of P_c, thrust coefficient (C_f), AR and OF Ratio. An example would be to define the mass of the concept engine fuel pump by using the relationship defined here in equation (2.17),

$$W_{Pump1} = W_{pump2} * \left(\frac{C_{f1}}{C_{f2}}\right)^{.54} * \left(\frac{P_{c1}}{P_{c2}}\right)^{.03} * \left(\frac{AR_2}{AR_1}\right)^{.2} * \left(\frac{OF_1}{OF_2}\right)^{.16} . \tag{2.17}$$

Equation (2.17) is given here for illustration purposes only and does not reflect the equation used in determining the pump mass. Equations of mass relationships are developed for Pumps, Valves, Lines and Ducts, Fuel Preburner, Oxide Preburner, Thrust Chamber and Thrust Cell Array, and the Nozzle.

2.5.5 Engine Mass Historical Data

The resulting relationships for old or currently used engine systems provides ample data necessary to build regression curves that relate some unknown or approximated value based upon a known variable for the system. An example of this is the relationship between the values for engine P_c, AR and OF Ratio as related to the

overall engine mass. This relationship shows that for a particular engine design, a power series regression curve provides insight into the predicted engine mass based upon these three parameters mentioned above. Table 2.3 illustrates this relationship by showing the actual mass versus the predicted mass of LOX/H2 engines with high thrust values. The results are conclusive because the regression relationship sample coefficient of determination is approximately .85. The only outlier was the LE-7 engine system that produced a percentage error of 43.1%. But the fact that the remaining systems closely matched the curve fit proves the relationship between P_c, AR and OF Ratio is reliable in estimating engine mass.

Table 2.3 Engine Mass Versus P_c*AR*OF Ratio

Engine	O/F*PC*AR	Engine Mass	Predicted Mass (Pc*AR*OF)	Error
SSME Block IA	1,454,810	7445	7450	0.1%
SSME Full Power Level	1,444,492	7004	7413	5.8%
SSME Block II	1,185,610	7813	6481	-17.0%
SSME Block IIA	1,185,610	7607	6481	-14.8%
SSME Return to Flight	1,447,347	7094	7424	4.6%
SSME Block I	1,443,025	7445	7408	-0.5%
SSME 1st Flight	1,399,315	6846	7251	5.9%
RD-0120	1,625,812	7606	8066	6.0%
LE-7A	536,900	3750	4146	10.6%
LE-7	752,400	3440	4922	43.1%
Vulcain 2	595,203	4497	4356	-3.1%
Vulcain	363,825	3249	3523	8.4%
J-2	108,139	3170	2602	-17.9%

2.5.6 Nozzle Weight Computation

In NASA's Propulsion Sizing, Thermal Analysis and Weight Relationship (PSTAR) Model [15], Leahy, et al., utilized the Huzel and Huang [16] approach to model the rocket nozzle in order to determine the mass of the nozzle system. The computation utilizes a surface area calculation of the entire nozzle multiplied by the unit density of the material used to manufacture the nozzle. The inputs required to determine the surface area are the AR, and the nozzle throat area (A^*). The alpha (α) and theta (θ) angles as well as the reference cone length (L) are chosen as standard values for a conical nozzle. The α is set to 15 degrees, the θ is set to 30 degrees, and L is set to 80%. The 80% value for L implies that the remaining 20% of the engine length is dedicated to the thrust chamber, fuel pumps, etc. The unit density of the material is chosen by the designer and is based upon nozzle material properties, understanding of nozzle thickness and historical nozzle design processes. The physical representation of the nozzle has some inherent errors due to assumptions for the nozzle design angles and cone reference length, as well as the integration errors introduced by averaging the incremental area for each integration step. In general, the limitations of this approach are not significant and this physical modeling approach represents the current best practices used by both NASA and the United States Air Force.

2.5.7 Engine Mass Study Summary

The methodology studies reviewed here are necessary to determine the engine mass based upon design and performance parameters of the system. The Manski and Martin approach [11] will not be used because it is complex and did not integrate well

within the integrated model framework. The other engine mass estimating techniques rely upon known parameters and integrate into the model very effectively. The accuracy of each of the approaches defined within this section is normalized by averaging the remaining methods and using the combined result as the engine mass used by the integrated model.

2.6 Trajectory Modeling

The most commonly used form of trajectory modeling utilizes the rocket equation (3.11 and 3.12) to determine the *MR* of a launch vehicle based upon the required system's Delta Velocity (ΔV) to meet the mission needs. Wilhite, McKinney, Farrington, and Lovell [10] describe the trajectory modeling approach in conjunction with an overall analytical process to determine system parameter sensitivities. The rocket equation closure defines a *MR* for a given system of inputs or iterative system input for *Twi*, Orbit Height, Launch Inclination, Drag Reduction, and nozzle *AR* of the propulsion system.

There are numerous approaches to modeling the trajectory but a number of them are not compatible with other modules within an integrated model approach. NASA has historically used the Program to Optimize Simulated Trajectories. This model has proven to be reliable in modeling vehicle trajectories but using this model significant training to become familiar with using the tool. Using a simplified rocket equation model allows a greater degree of flexibility in linking the trajectory inputs and outputs with other modules within the integrated model.

2.7 Weights and Sizing Modeling

The modeling used for vehicle masses and sizing requires a *MR*. The *MR* is defined as the initial vehicle mass (m_i) of the vehicle divided by the final vehicle mass (m_f) as shown in equation (2.18),

$$MR = \frac{m_i}{m_f}. \tag{2.18}$$

The m_f is represented by the difference in m_i minus the propellant mass. The vehicle thrust-to-weight ratio is an important parameter in determining the vehicle mass, particularly the requirement of the propulsion system for overall vehicle thrust required. Wilhite, Gholston, Farrington, and Swain [2] utilized this weight and sizing approach along with historical vehicle data to determine the vehicle *GLOW* and Dry Weight. The approach defined in Section 2.1 above describes the methodology of using historical data curves along with technology enhancements to define component weights for the vehicle system. Using the combination of historical data and relationships between vehicle thrust-to-weight ratio and *MR* is an effective and efficient method to model the weight and size of the vehicle as shown by previous studies. Current best practices rely upon this parametric data relationship to be employed in the modeling of preliminary systems. The technique is proven and will improve as additional historical data is added to the weight model, thus increasing the fidelity.

2.8 Cost Modeling

The NASA Engineering Cost Group and Science Application International Corporation [17] provides ability to derive vehicle Design Development Test and Engineering (DDTE) cost estimates based upon the weight of the component being analyzed. NAFCOM captures a large number of historical weight and cost data and uses regression techniques to fit the data with a regression curve. Since there are a large number of data points that range from orbital vehicles to commercial vehicles, the uncertainty of the results can be large.

The NAFCOM approach for DDTE cost is based upon a power regression curve fits with coefficients A, B, component weight, and also a cost influence factor (CIF). The coefficients are defined directly from the regression fit. The form of the power series equation is given here in equation (2.19),

$$Y = a * X^{b}. \tag{2.19}$$

Where a and b are coefficients of the curve fit and the value X is the weight of the component in question. The component weight is an input into the code. The CIF allows the user the ability to define a multiplying factor for additional complexity due to a new design or new technology used in the development of the component. Each component weight is calculated and totaled to provide an overall weight of the vehicle or system.

The NAFCOM approach is a reliable system employed by NASA and the U.S. Air Force to do cost assessments. The accuracy of the model is represented by the

component standard errors (SEs). These SE values represent the entire envelope of system component weights from aircraft to spacecraft. The NAFCOM database is exhaustive and thorough in capturing the known weight relationships and is the most reliable method available for determining cost. The NAFCOM regression curves are easily integrated into a vehicle model and perform very well during system optimization analysis.

2.9 Thermo-chemical Equilibrium Code

There are a number of commercially available thermal equilibrium codes available for use in the analysis of engine design and performance. The codes function by either using an enthalpy balance and/or using the minimization of Gibbs-Free-Energy. Historically, the outputs of thermochemical codes have been difficult to incorporate into other model codes and have forced the user to cut and paste the data into the necessary location. The creation of Cequel by the Software and Engineering Associates, Inc. [18] and the developments of SpreadsheetWorld, Inc., have allowed the model developer to design and integrate thermo-chemical solutions into their models. The analyst now has the ability to call the Cequel function in Microsoft Excel in a way that any other Excel function is called. This enables the model developer to iterate thermochemical solutions by inputting the *OF* Ratio, P_c and *AR* into the model in order to determine the optimum combination of these 3 input parameters. As the inputs for these values change so does the outputs for *ISP*, C_f, and C_{star}. The impacts of an iterating cycle for these components are key to the sizing of the launch vehicle and the propulsion system for optimum values.

Cequel (Chemical EQUilibrium in excel) was derived from NASA Lewis' Gordon-McBride CEA (Chemical Equilibrium with Applications) code. Cequel provides most of the capabilities presented in CEA but does so as a function within Microsoft Excel. This eliminates the need to cut and paste from external thermodynamics codes' output files into Excel, and provides the additional power of allowing the output of one Cequel function to be used as the input to other Cequel functions. This allows the user to quickly evaluate many "what-if" scenarios as well as to utilize Excel's built in solvers and optimization routines.

2.10 Literature Review Summary

This review focused primarily on modeling techniques but also included reference to historical modeling methodologies. A primary source of difficulty in developing an integrated modeling approach is determining which model components best integrate within the framework of the overall model system. The likelihood is high that certain aspects of the model (weights and sizing, trajectory, thermo-chemical analysis, and cost) will utilize components that are not as accurate as other approaches. Yet if the model designer does not have the ability to integrate the component within the integrated model framework, then the component becomes useless. The idea that a model framework is a set of inputs and outputs between components of the model is the key to understanding, building and utilizing an integrated modeling approach.

CHAPTER 3

APPROACH

An important first step in determining what needs to be assessed is to define the conceptual vehicle or system that provides the most significant results to the aerospace community. Table 3.1 shows the decision making process for SSTO modes to determine the right propulsion system to analyze. Option 1 is a complete SSTO approach as defined by Sutton [20] and shows the multiple propulsion regimes in Figure 3.1. Option 2 is an air-breathing engine based upon current technology or existing design. Option 3 is a ramjet or scramjet engine. Option 4 is a rocket engine, which is based upon current technology or existing design. Each option is ranked according to a pre-determined set of criteria on a scale of 1 to 3, with 3 being the best and 1 being the worst. The availability of existing computer codes, time needed to model the system, fidelity of systems currently in use, and open publication of information was a determining factor in using a Rocket Engine as the basis for the integrated model. In conclusion, the approach defined in Option 4, Rocket Engine analysis, provides a more desirable analysis than the other options and is directly related to current efforts within NASA to develop new and innovative launch systems for access to the International Space Station.

An illustration of the SSTO flight regimes is shown in Figure 3.1. The regimes show what Mach number is required for a particular phase of an orbital flight. If a staged combustion system is not preferred, then the only alternative is using a rocket-based system that can meet all requirements of the SSTO flight modes. A rocket system is the most readily available propulsion system for study, as shown in Table 3.1.

Table 3.1 Propulsion System Decision Matrix

	Option 1 (SSTO)	Option 2 (Air Breather)	Option 3 (Scram/Ramjet)	Option 4 (Rocket)
Code Availability	1	3	1	3
International Traffic in Arms Regulation (ITAR) Restriction	1	2	1	2
Significance	2	2	2	2
Time Needed	1	2	1	3
Fidelity	1	3	1	3
Open Publication	2	3	2	3
Career Topic	3	2	3	2
Totals	11	17	11	18

Key:

1- Bad
2- Fair
3- Good

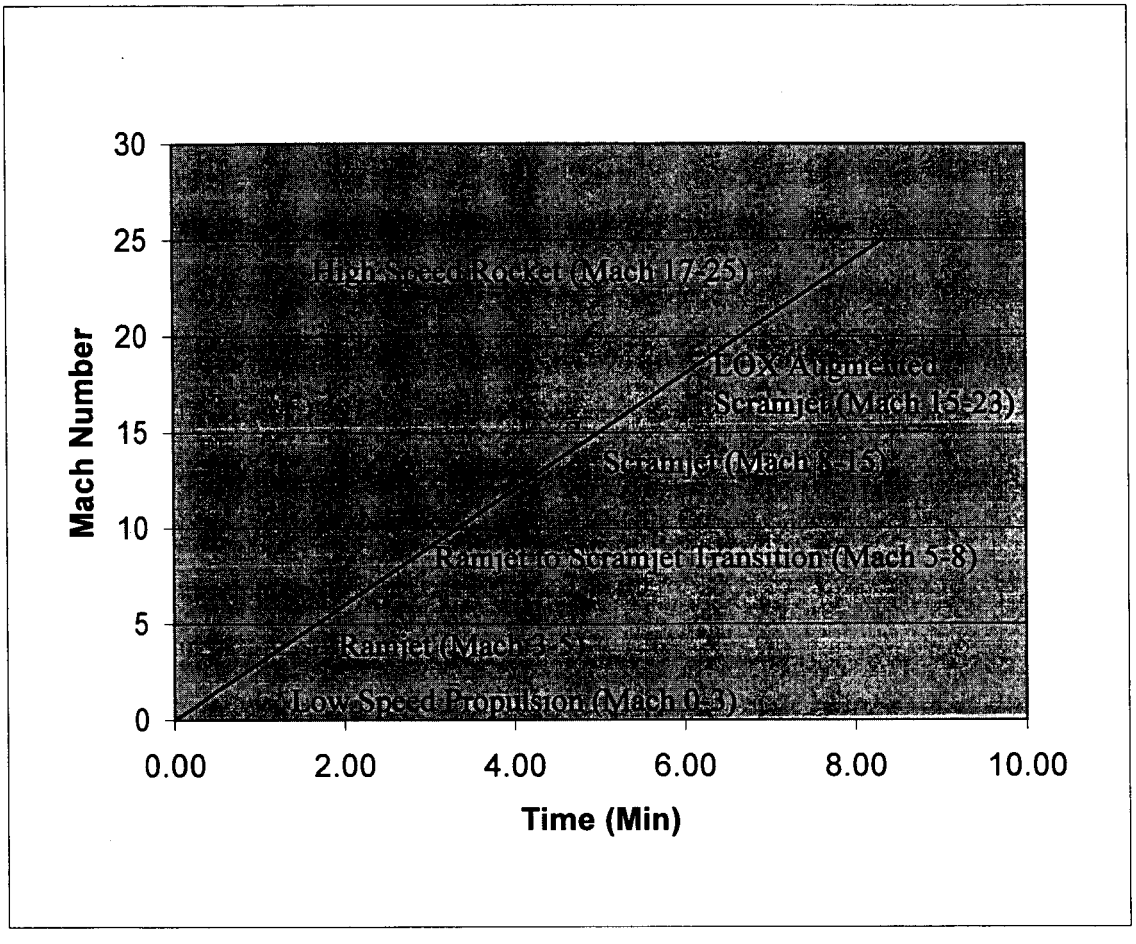

Figure 3.1 SSTO Modes [20]

The optimization of the integrated vehicle SSTO model using rocket engines should focus on several key areas. The first is the overall optimization of the vehicle *Twi*, engine P_c, engine *AR*, engine *OF* Ratio, and TFs for TPS, Autonomous Flight Control, Wing, Tail, LH2 Tank, LOX Tank, Basic Structure, Landing Gear, Engine Accessories, MPS, Engine, and Flight Autonomy. The TFs imply weight reduction for improved technology but also result in a DDTE cost increase due to the time and effort expended in developing the advanced technology. The combination of the propulsion variables and TFs above are used to define the optimum system with respect to the following Figures of Merit (FOMs): 1) Minimum *GLOW*, 2) Minimum Dry Weight, 3) Minimum Dry Weight with Margin, 4) Minimum DDTE Cost, 5) Minimum Production Cost, 6) Minimum Operations Cost, 7) and Minimum Life Cycle Cost (LLC). A table of optimization results will be presented for each of the seven different FOMs defined above. The vehicle *MR*, Main Engine D*, ISP_{vac}, ISP_{sl}, Per Engine Thrust Level, and Per Engine Weight Estimation is defined for each of the seven optimal results that are derived for each FOM case. These levels will vary in each of the seven scenarios due to the fact that the optimization is focused on key FOMs that drive the final optimized propulsion parameters and TFs toward different solutions or goals. In some cases the solutions may be near identical because of the similarity in the parameter being optimized.

A comparison is made between the model output and the SSME main engine design parameters. The information is defined in order to validate the model and show that the solution proposed by the integrated model closely aligns with the current best practices in engine system design used by NASA. The SSME comparison is applicable

based on the fact that the SSME performs from launch vehicle liftoff to space or the entire flight regime needed in a SSTO vehicle concept. Although the Shuttle system relies upon solid rocket boosters, the SSME main engines run continually and should be optimized to perform best throughout the entire vehicle flight path.

The capability of the Evolver Tool Software [3] enables the analyst to define a set of predetermined values for TFs and key propulsion parameters if the technology is not available or if the program or project agrees to use either a new technology or established technology. This optional feature allows the designer the flexibility to also define any of the seven FOMs at a particular value or add a constraint to the optimization. An example would be to include DDTE cost as an independent variable (CAIV) and optimize the vehicle with this cost value set as a constraint. The model will also allow any of the other 7 FOMs to have set values in order to meet a congressional, agency, or industry mandate. The same ability to set pre-defined levels for FOMs or other variables also applies to the propulsion system if for example the use of existing engines was mandated.

The second capability of the model is to show how each of the key engine parameters, P_c, *OF* Ratio, and *AR* are optimized against the FOMs and how significant changes to the system are when the optimized value is not met. The sensitivity of these key propulsion parameters is extremely important to the system designer. The model provides the results to show how changes in each propulsion parameter effects the 7 FOMs mentioned earlier. Understanding the impact that a parameter has on the overall

system is crucial to vehicle system design. Design decisions should never be made without understanding the full impact upon the overall system mass and cost.

The previous methods for combining trajectory, weights and sizing and cost models are shown in Figure 3.2 and the newly defined approach described herein is shown in Figure 3.3. Figure 3.4 illustrates how each of the given propulsion parameters is used as input to determine nozzle mass, engine mass, propellant system mass and vehicle *MR* and illustrates other uses for the propulsion parameters. An overall system flow diagram is shown in Figure 3.5. Each section of the model has inputs and outputs that feed each other and also form the closed loop optimization methodology so desired by a system modeler. The overall schematic shows how mission requirements are fed to the system and how each model component (LVSS-Propulsion Module, Trajectory, Cost and Economics) interacts and what key variables are passed between the models.

The approach utilizes uncertainty principles in order to bind the final outputs with a measure of goodness or certainty. In the case of the weights and sizing model (LVSS) and the DDTE cost, the historical data curves were used to develop estimates for the component vehicle weights and regression curves defined the +/- regression range for each of the curves. Historical engine data used for comparison purposes is defined in Appendix C. The data shows the engine system used for previous launch vehicles and the corresponding design parameters for each system. The engines are all LOX/LH2 and were used on multi-stage rockets and/or systems that required the engine to remain with the vehicle until it reached orbit, or re-useable engines.

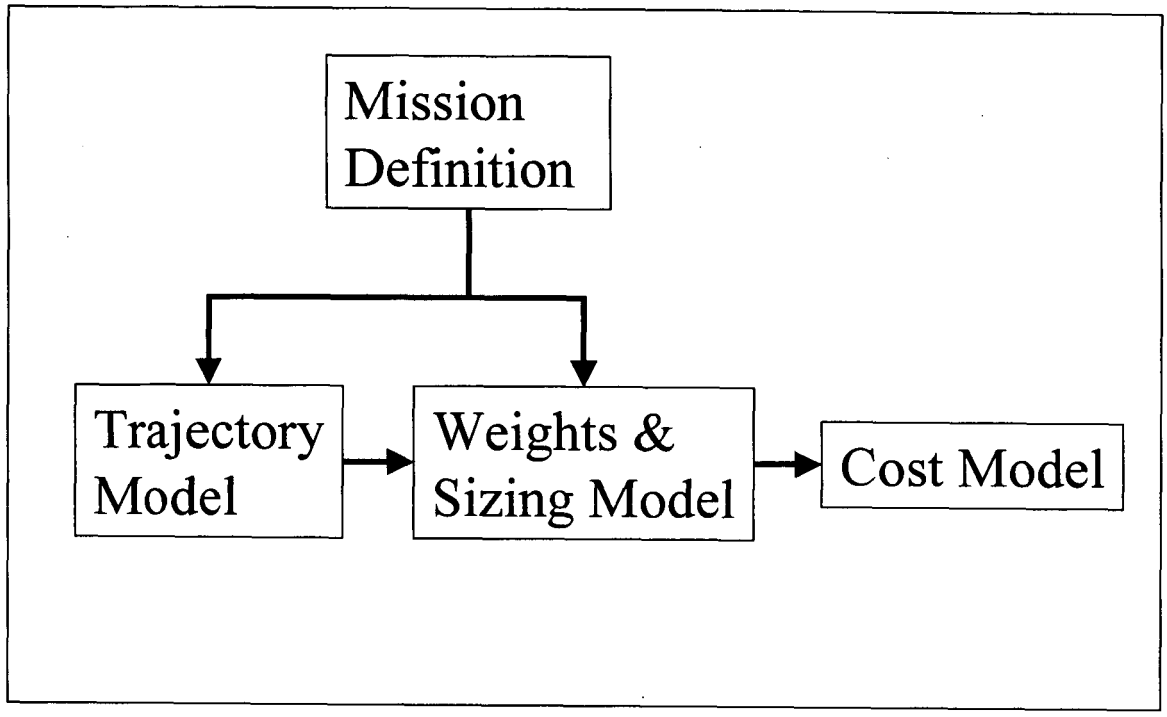

Figure 3.2 Top Level Schematic-Previous

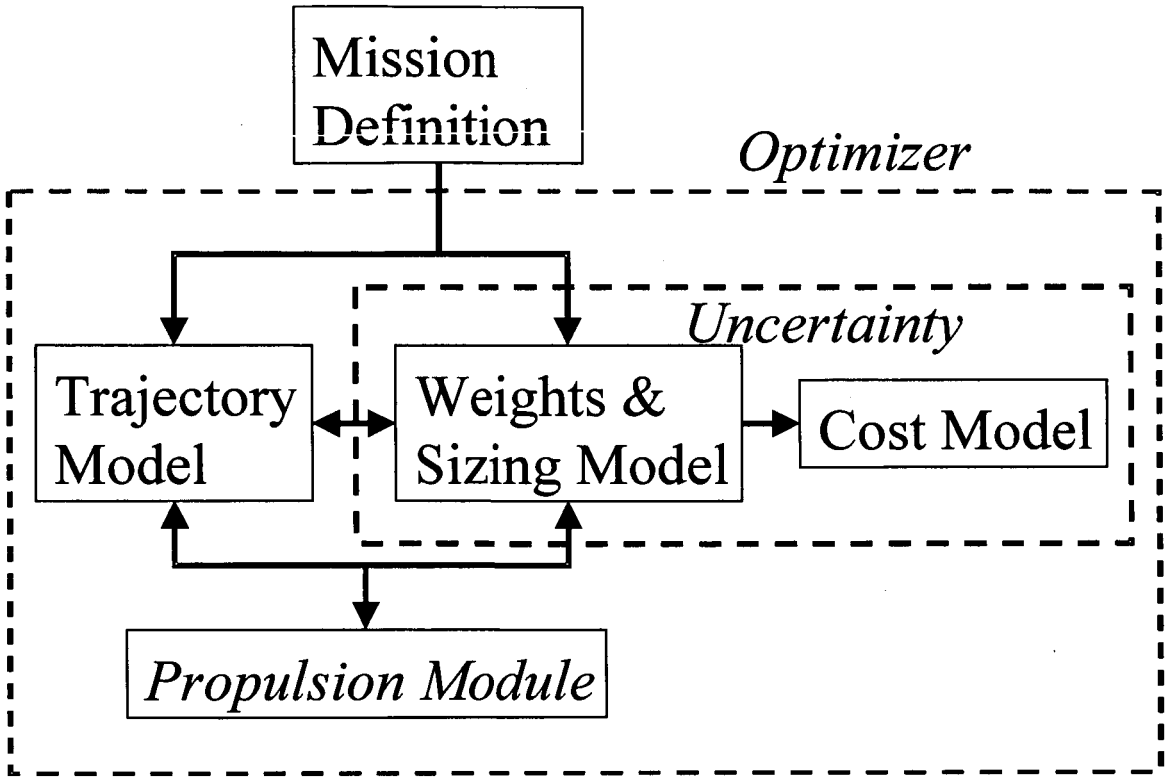

Figure 3.3 Top Level Schematic-New

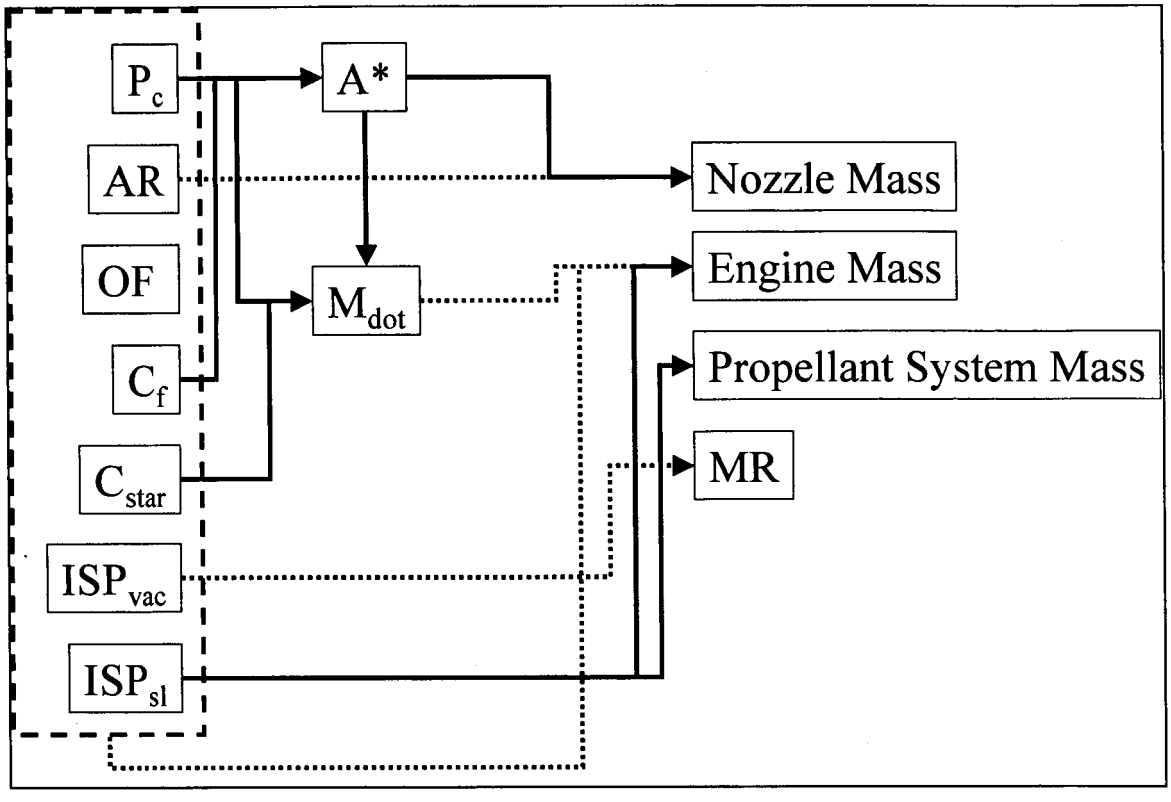

Figure 3.4 Integrated Propulsion Module Parameter Schematic

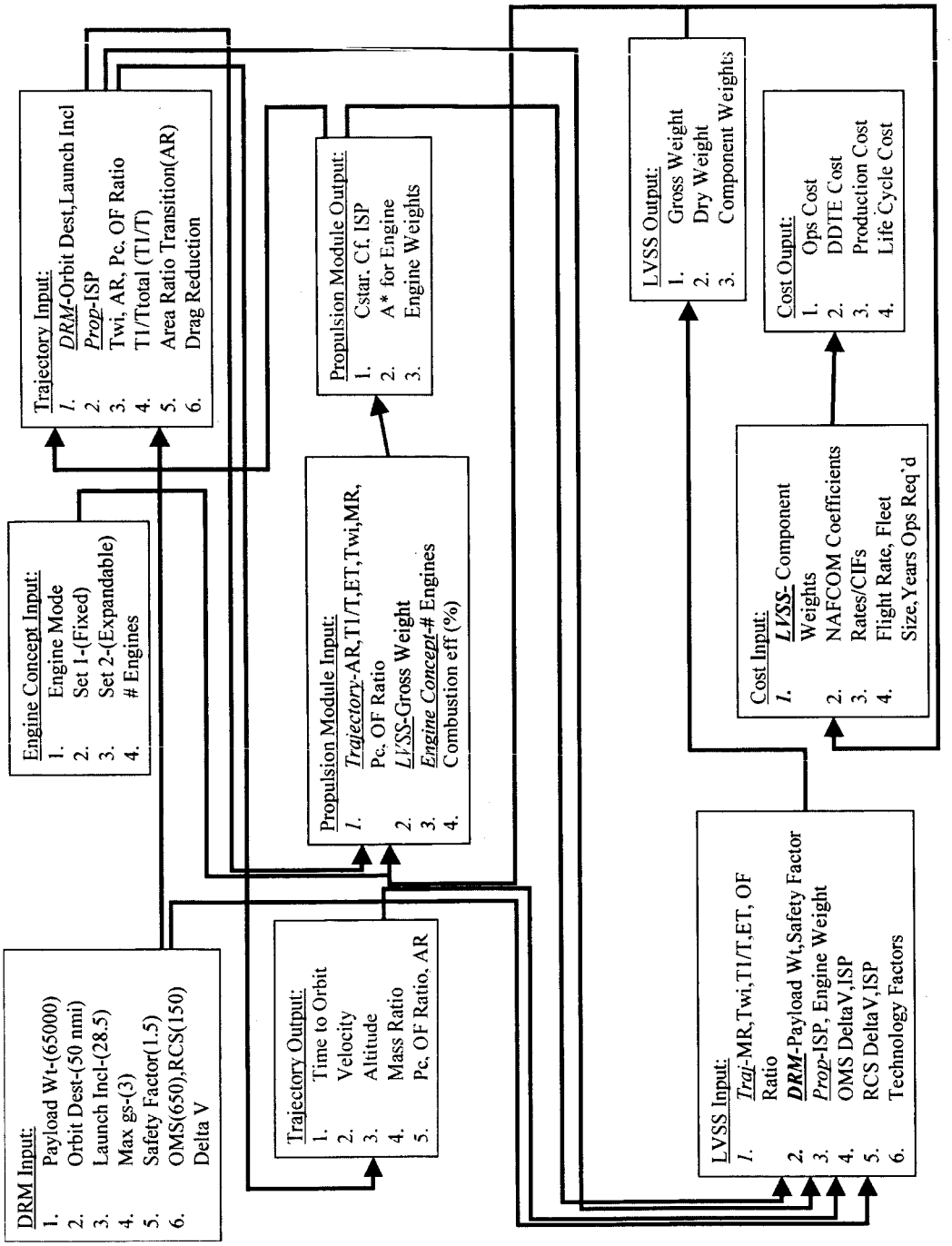

Figure 3.5 System Model Top-Level Schematic

3.1 Vehicle Concept Model

The first step in the model design was to develop a design for a rocket propelled SSTO vehicle concept in order to build the optimization model. The concept vehicle chosen requires the following specification parameters developed by Haefeli, Littler, Hurley, and Winter [1]: 1) Vertical Takeoff, 2) Dual-Engine Mode, 3) 500 Mission Lifetime, 4) 65,000 lb Payload, 5) 28.5 degree Launch Inclination from the NASA John F. Kennedy Space Center, 6) and 50 nmi Orbit. The concept vehicle is shown here in Figure 3.6.

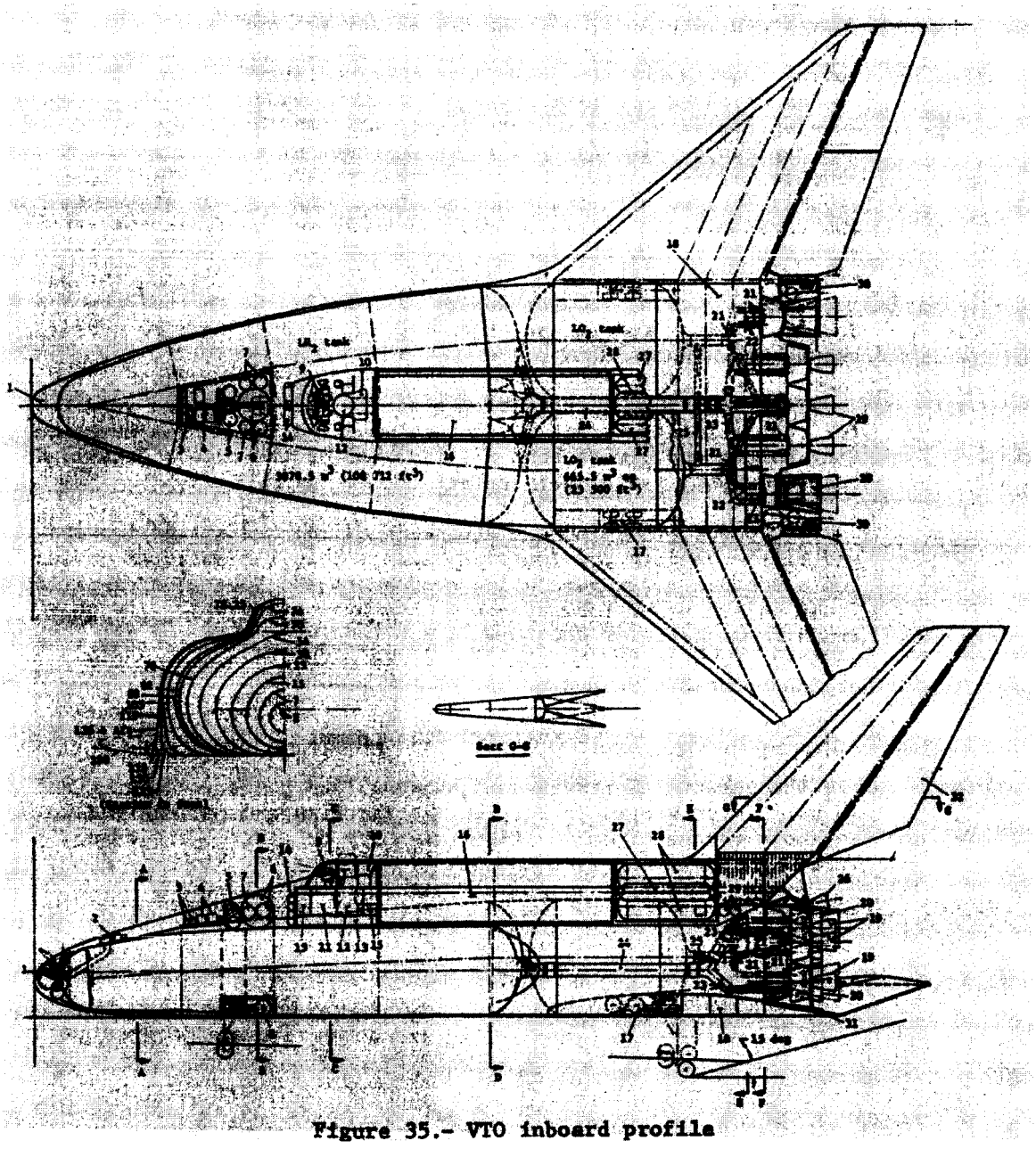

Figure 35.- VTO inboard profile

Figure 3.6 SSTO Concept Vehicle

The vehicle utilizes LOX as the oxidizer and LH2 fuel and uses fixed nozzle engines to propel the vehicle to orbit. The concept incorporates improved technologies for enhanced performance as well as using historical data to produce projections for

future technology upgrades in the areas of material science for composite and metal matrix composites, rocket engine efficiency, and lighter and more thermally resistant protection systems for the vehicle exterior. For the analysis of the launch vehicle and the launch vehicle propulsion system, a model of the entire system was developed using equations for rocket propulsion parameters, trajectory profiles, weights and sizing, cost and economics, and historical data.

The initial baseline engine system defined an adjustable nozzle extension for the second cluster of engines, and also allowed the system designer to adjust the percentage of thrust for the first cluster engines versus the second cluster. For the application of this model, the dual engine approach was modified to include only 1 set of identical engines. The approach required to model a system of fixed nozzle engines was significantly less difficult. The important aspects of this computer modeling approach are to show how the model can be developed and how the tools can be used to design, analyze and optimize the system, not how to define a complex system. Once the approach to the model is established, then it will be much easier to focus on a dual thrust and dual mode engine configuration.

3.1.1 Vehicle Weights and Sizing Model

The first phase of the model development addressed the building of a core weights and sizing model of the concept vehicle. This module utilizes a modified version of a Microsoft Excel model called Launch Vehicle Sizer and Synthesis (LVSS) from

Wilhite, Gholston, Farrington, and Swain [2]. The LVSS component is made up of a number of Microsoft Excel worksheets that share data together.

The initial inputs are dedicated to input variable definition for the vehicle *MR*, *Twi*, payload weight, delta-velocity requirements, engine *ISP*s, and *AR*s. The Propellant worksheet is used to formulate a propellant module for determining tank volumes and weights based upon inputs for density of fuel, payload volume and body volume. The Propulsion worksheet is used to determine the engine masses based upon the *ISP*, area ratio, engine compilation, and thrust level needed. The Weight Equations worksheet is dedicated to determining the vehicle component weights using historical data and technology factors defined for each component. The Sizing worksheet provides the outputs for the vehicle sizing based upon inputs from the previous sheets. The formats of the LVSS worksheets are defined in Appendix B. The values in Appendix B are shown for illustration purposes and are representative of the optimum design case for *GLOW*.

3.1.1.1 Vehicle Component Historical Data

The vehicle weights and sizing approach, in the LVSS model's 'Wt Eqns' worksheet, utilizes a database of actual flight weights for vehicle wings, tail, liquid hydrogen tanks, oxygen tanks, overall body, thrust structure, landing gear, hydraulics, and engine mass. In order to define each component weight, a measurable variable was used for each case and plotted on an x-y curve. Plotting the x-axis variable of component weight against the y-axis measured variable for the particular component provides the curves necessary to approximate each vehicle component weight. The y-axis measured

variables are shown in Table 3.2. The Alpha variable in Table 3.2 is defined as a multiple of the wing gross weight, load, safety factor times, and the span divided by the root chord.

Table 3.2 Vehicle Weight Component and Measured Variables

Component	**Measured Variable**	**Units**
Wing	Alpha	not applicable
Tail	Area	ft^2
Hydrogen Tanks	Volume	ft^3
Oxygen Tanks	Volume	ft^3
Overall Body	Surface Area	ft^2
Thrust Structure	Thrust Level	lbf
Landing Gear	Design Weight	lbm
Hydraulics	Surface Control Area	ft^2
Engine Mass	Thrust Level	lbf

The component historical data is shown here in Tables 3.3 to 3.11. The data list the historical vehicle or system by name, the measured variable, actual weights, predicted weight from the curve fit, and the delta % between the actual and predicted weight. The curve fits shown in Figures 3.7 to 3.15, utilize a power curve graph on an x-y logarithmic

scale axis. The results are shown linearly since a power curve overlaid on a logarithmic axis is represented by a linear fit.

Each graph defines a value for the 'correlation coefficient' that is defined as the sample coefficient of determination (R^2). These coefficients are calculated automatically as a Microsoft Excel function. Walpole correlation coefficient is the measure of the strength of relationship for the least squares fit and is calculated using the equation (3.1) defined by Walpole, Myers, Myers and Ye [5],

$$R^2 = \frac{S^2_{xy}}{S_{xx} S_{yy}}, \qquad (3.1)$$

where S is representing the standard deviation of the of the 'xy', 'xx', and 'yy' terms for each curve fit. The coefficient can be stated more simply as the 'measure of goodness' of the curve fit. A perfect correlation is represented by an R^2 value equal to 1.0. Any value that approaches 1.0 is considered a close fit; whereas any R^2 value that is less than 1.0 and trending toward zero (0), is not considered a close fit. The uncertainty of each vehicle component weight is directly linked to the accuracy of the curve fit when the actual weights are compared to the predicted weights. In subsequent sections, it is proven that as the R^2 value approaches 1.0, the uncertainty in the predicted output approaches zero.

The delta percentages or regression values are defined for each component as defined in Tables 3.3 to 3.11. The upper and lower bounds of the regression values measured will be used to determine the uncertainty values for the overall vehicle weight.

Table 3.3 Wing Component Historical Weight Data [2]

Vehicle	Alpha	Actual Weight, pounds force (lbf)	Predicted Weight	Delta, %
737	8.7	11135	10234	-8%
Shuttle	23.6	15646	17764	14%
727-200	20.4	18483	16400	-11%
H-33	37.5	19074	22962	20%
707	69.7	28576	32376	13%
NAR	47.2	31168	26107	-16%
DC-8	88.5	34821	36971	6%
L-1011	138.9	47284	47461	0%
C-5	417.2	81581	87345	7%
747	304.5	88523	73346	-17%

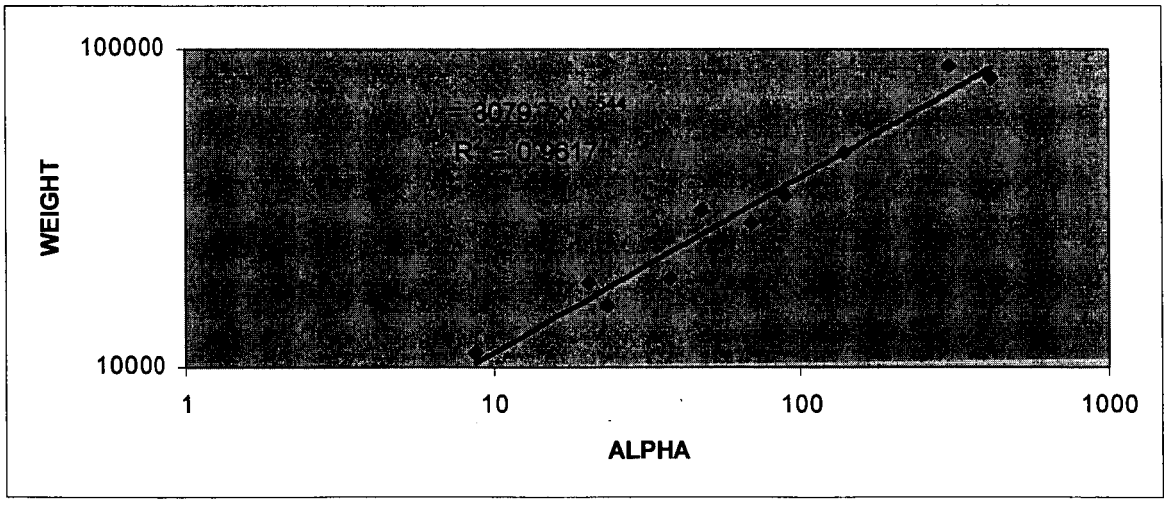

Figure 3.7 Wing Component Regression Curve Fit [2]

Table 3.4 Tail Component Historical Weight Data [2]

Vehicle	Area, ft^2	Actual Weight, lbf	Predicted Weight	Delta, %
F-111B	121	843	759	-10%
DC-9	161	1088	1009	-7%
737	224	1168	1403	20%
KC-135A	312	1761	1953	11%
Shuttle	375	2825	2347	-17%
727	384	2142	2403	12%
C-141A	417	2583	2603	1%
NA Orbiter	667	3965	4164	5%
C-5A	962	5540	6004	8%
B-9U	1502	13243	9362	-29%
Martin II SSTO	2212	11607	13781	19%

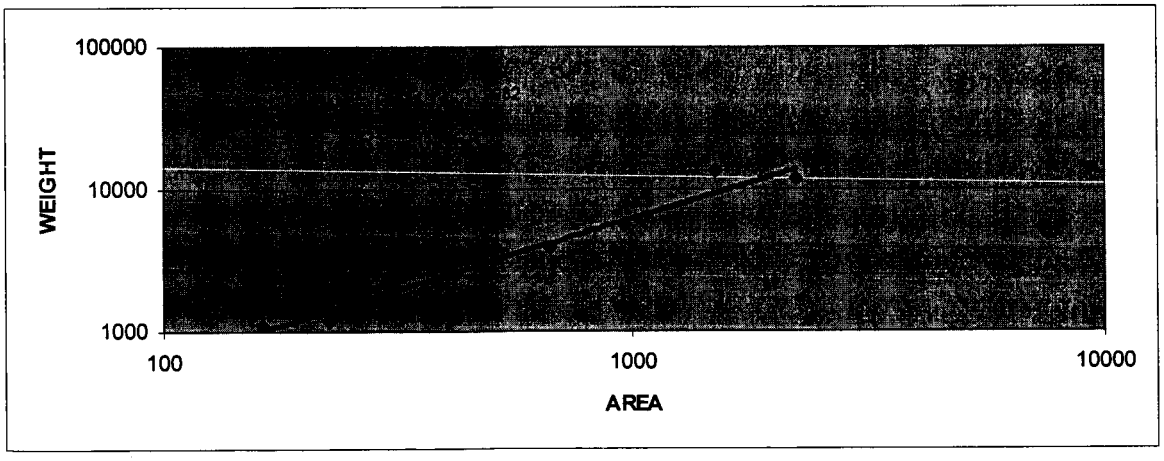

Figure 3.8 Tail Component Regression Curve Fit [2]

Table 3.5 Hydrogen Tank Historical Weight Data [2]

Vehicle	Volume, ft^3	Weight, lbf	Predicted Weight	Delta, %
Centaur	1271	560	601	7%
SIV	4520	2125	2207	4%
SIVB	10524	4987	5247	5%
MDC Orbiter	17058	9711	8607	-11%
NA Orbiter	18894	11704	9558	-18%
SII	38424	20529	19786	-4%
Shuttle	53646	27088	27856	3%
H33 Booster	72540	32789	37952	16%
MDC Canard Booster	98780	61511	52081	-15%
Martin TII	108739	40692	57470	41%
B9U	109799	67478	58044	-14%

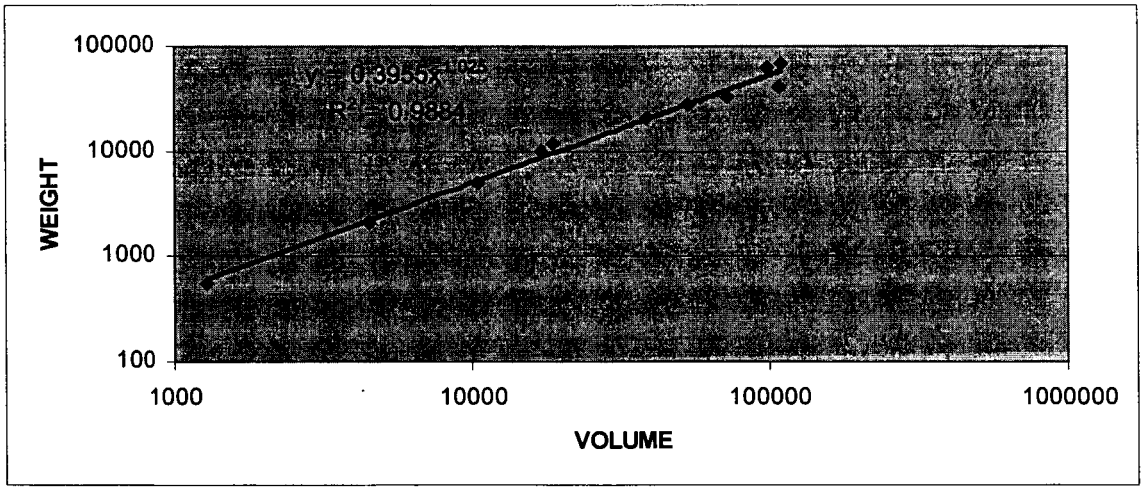

Figure 3.9 Hydrogen Tank Regression Curve Fit [2]

Table 3.6 Oxygen Tank Historical Weight Data [2]

Vehicle	Volume, ft^3	Weight, lbf	Predicted Weight	Delta, %
Shuttle ET	19632	12077	13260	10%
B9U	40826	17701	26356	49%
SII	12537	9550	8705	-9%
SIV	1261	842	1009	20%
SIVB	2903	2066	2206	7%
SI	9324	13448	6593	-51%
SIC	47250	37989	30229	-20%
H-33 Booster	27052	18195	17913	-2%
MDC Booster	36694	19720	23845	21%
MDC Orbiter	6322	6027	4579	-24%
Martin TII	47006	24041	30083	25%
Centaur	381	278	329	18%

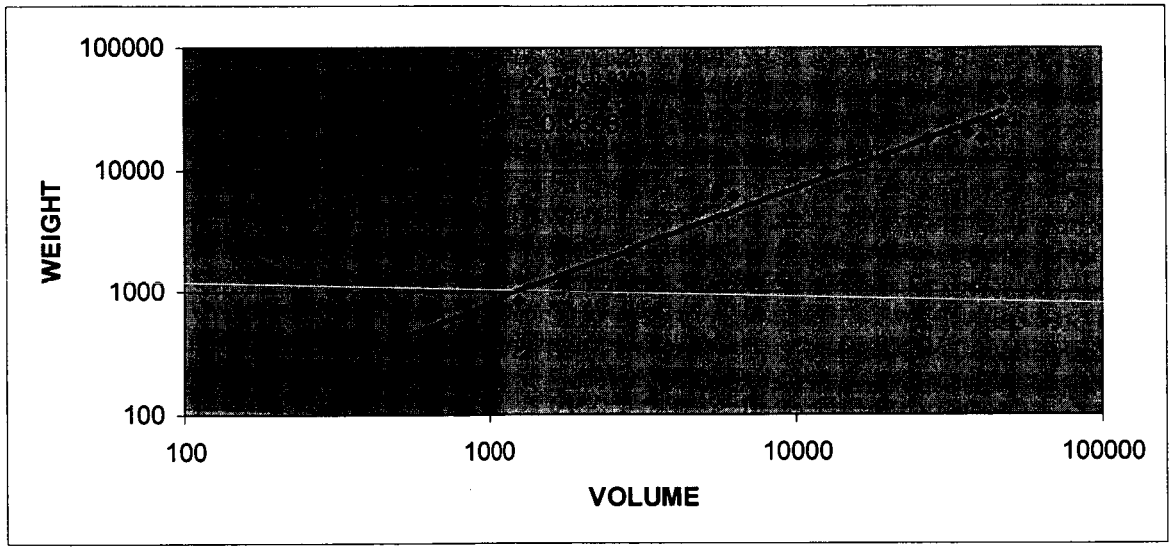

Figure 3.10 Oxygen Tank Regression Curve Fit [2]

Table 3.7 Overall Body Historical Weight Data [2]

Vehicle	Area, ft^2	Weight, lbf	Predicted Weight	Delta, %
Boeing HLLL (BS, AS, IT)	52066	225310	240492	7%
Shuttle (AS, N)	2820	11358	11776	4%
B9U (AS,N, IT)	8030	30937	34767	12%
C130A (Body)	3343	14010	14043	0%
Martin (AS, IT)	11634	31047	51021	64%
Shuttle (all)	6609	38900	28423	-27%
C-5A	16533	114934	73397	-36%
Martin (AS, IT)	7381	30513	31864	4%

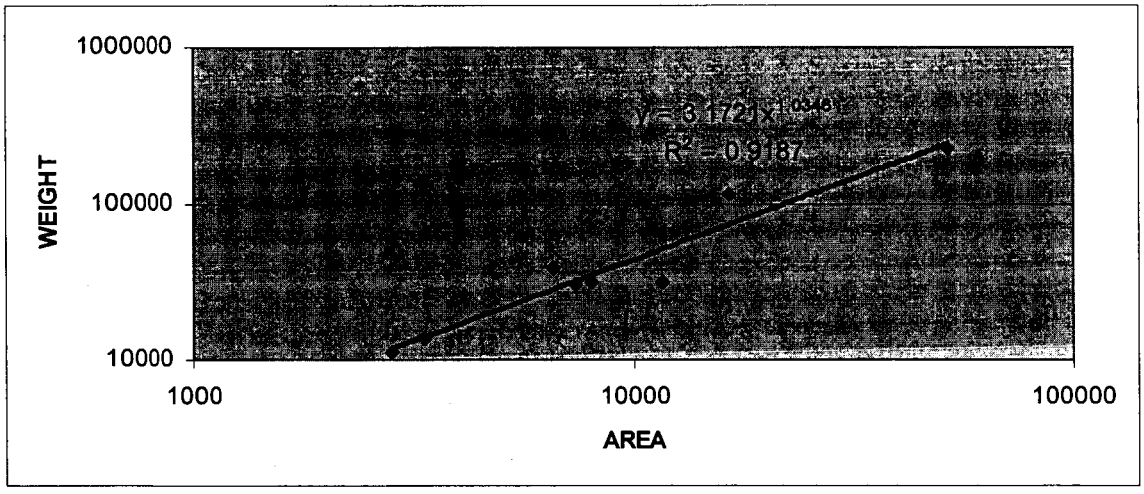

Figure 3.11 Overall Body Regression Curve Fit [2]

Table 3.8 Thrust Structure Historical Weight Data [2]

Vehicle	Thrust, lbf	Weight, lbf	Predicted Weight	Delta, %
Shuttle	1537920	3822	3675	-4%
HLLV SSTO	36045000	64374	86058	34%
Martin	6159690	16003	14714	-8%
Boeing SSTO	2088608	4389	4991	14%
B9U	7257060	14564	17335	19%
NAR	1265580	2773	3025	9%
Tita IIIST1	464400	784	1110	42%
11	105975	245	253	4%
SIVB	235350	510	563	10%
SII	1180350	6389	2821	-56%
S-IC	9230850	32368	22048	-32%
Martin TIV	3937500	8931	9407	5%

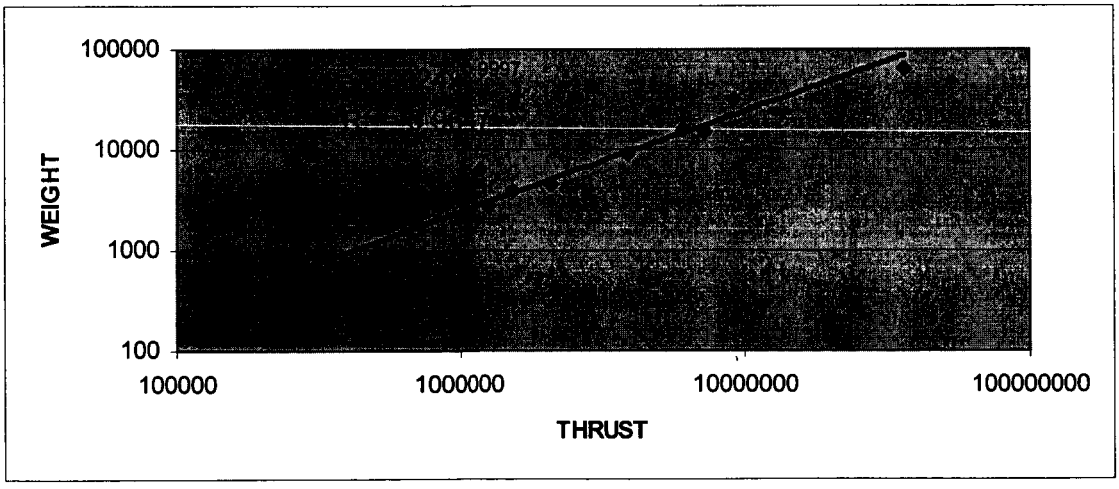

Figure 3.12 Thrust Structure Regression Curve Fit [2]

Table 3.9 Landing Gear Historical Weight Data [2]

Vehicle	Design Weight, lbf	Gear Weight, lbf	Predicted Weight	Delta, %
C-130E	341713	11193	12677	13%
KC-135A	606265	23585	23681	0%
C-133B	630516	24387	24716	1%
C-141A	696874	23212	27564	19%
C-5A	1604949	82955	68425	-18%
737	229278	8902	8206	-8%
727	354941	15970	13213	-17%
707	687835	24727	27174	10%
747	1708565	71032	73253	3%
Shuttle	411378	17436	15518	-11%
B9U	1485504	62736	62894	0%
NAR	638254	28296	25046	-11%
Martin TII	522774	16103	20150	25%

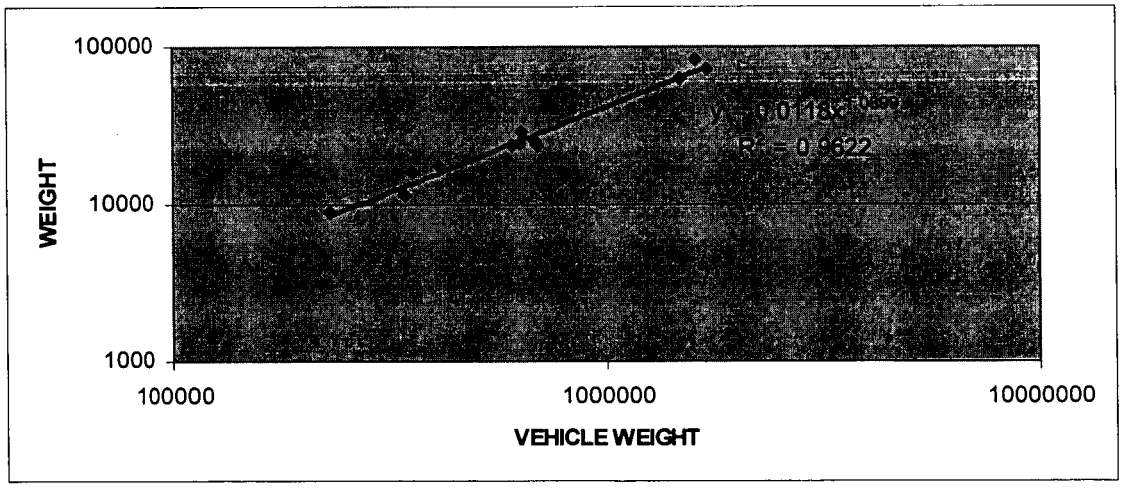

Figure 3.13 Landing Gear Regression Curve Fit [2]

Table 3.10 Hydraulics Historical Weight Data [2]

Vehicle	Surface Control Area, ft^2	Weight, lbf	Predicted Weight	Delta, %
Martin	29709	26164	19181	-27%
Shuttle	9031	10218	5349	-48%
B9U	36868	26061	24178	-7%
Boeing	20323	13448	12765	-5%
C-5A	40678	23084	26867	16%
C-141	18181	10917	11328	4%
747	40032	21310	26410	24%
727	12842	7888	7803	-1%
DC-9	6921	3351	4021	20%
NAR	8902	3177	5267	66%

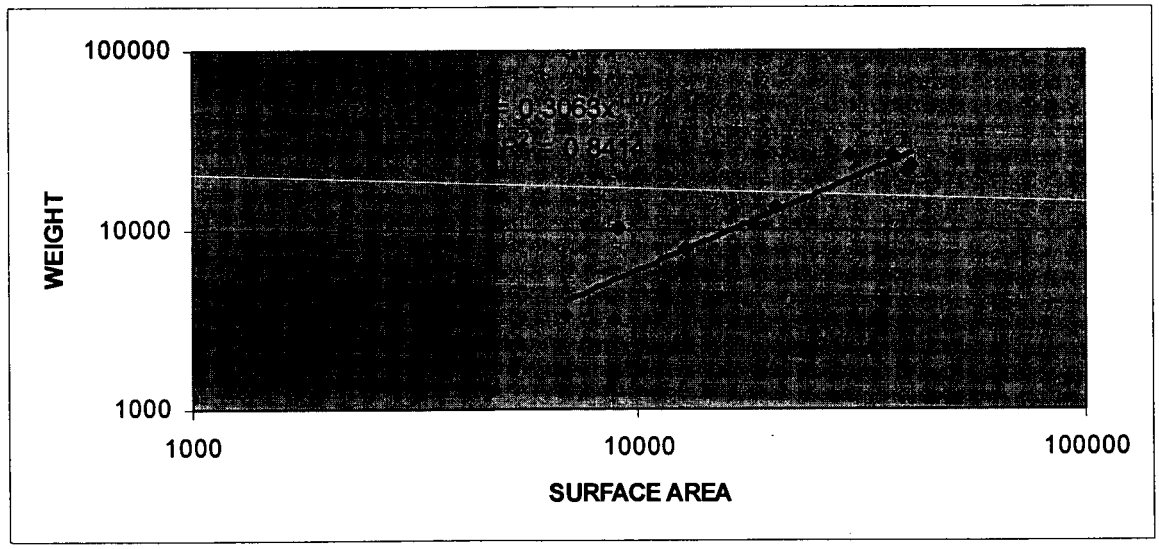

Figure 3.14 Hydraulics Regression Curve Fit [2]

Table 3.11 Engine Historical Weight Data

Engine	Avg Thrust, lbf	Actual Engine Mass, lbm	Predicted Engine Mass	Delta, %
SSME Block IA	395,707	7,445	7,424	0%
SSME Full Power Level	395,640	7,004	7,423	-6%
SSME Block II	395,546	7,813	7,421	5%
SSME Block IIA	394,191	7,607	7,394	3%
SSME Return to Flight	394,261	7,094	7,395	-4%
SSME Block I	393,626	7,445	7,383	1%
SSME 1st Flight	374,500	6,846	7,000	-2%
LE-7	190,000	3,440	3,391	1%
RS-68	650,000	14,560	12,614	15%
Vulcain 2	304,050	4,497	5,603	-20%
Vulcain	183,000	3,249	3,258	0%
J-2	156,400	3,170	2,755	15%

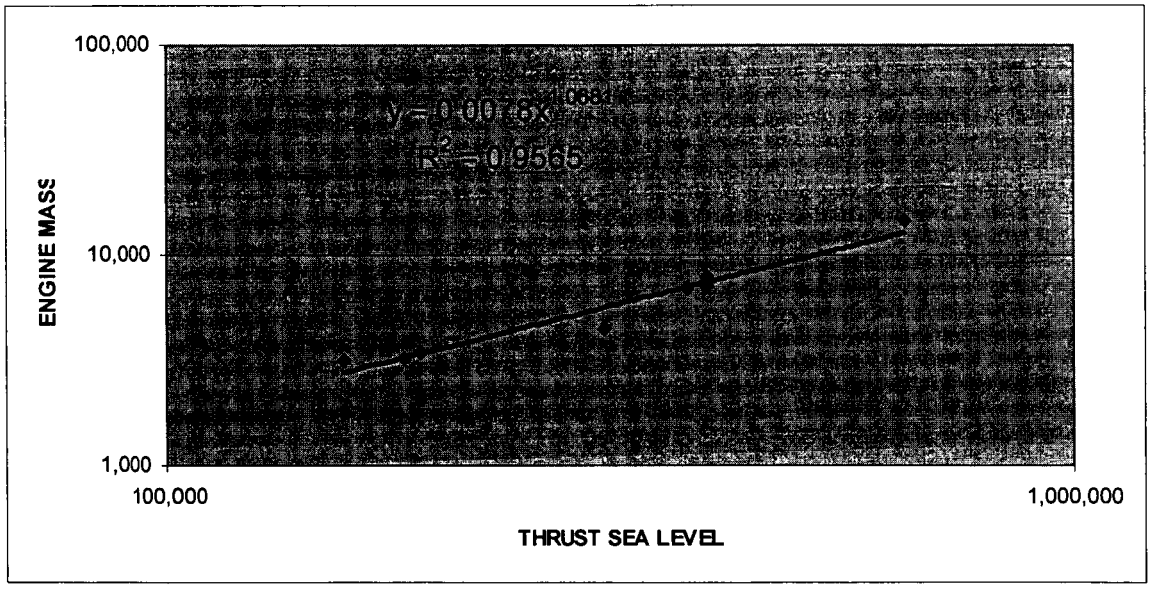

Figure 3.15 Engine Regression Curve Fit

3.1.1.2 Numerical Uncertainty in LVSS Model Dry Weight

The historical vehicle data is used to define linear regression curve fits for systems development. The curve fits formulate an equation to represent the relationship between a measured variable such as area, volume, etc., and the component weight. For each component weight, the regression of the curve is defined by the +/- value for the entire range of historical data. Uncertainty techniques were used to define the combined uncertainty for an entire system. The individual components, within the overall uncertainty, prove the mathematical and statistical fact that individual uncertainty components are not additive in equal measure to the total uncertainty. This means that the uncertainty band for each component will have a varying impact on the overall uncertainty of the system depending upon the magnification factor of the component. The magnification factor is the level by which a particular component effects the overall uncertainty calculation.

There are two methods used to determine the system uncertainty for the Dry Weight calculated using the LVSS model. The first is a numerical approximation to the general uncertainty analysis by assuming a delta *x* for the component weight in the weights and sizing model and return the results of the delta *x* on the overall impact on the vehicle dry weight. The next step is to subtract the difference in the old and new value and divide this result with the delta *x* value. Coleman and Steele [21] defined equations (3.2) and (3.3),

$$\left.\frac{\partial r}{\partial x}\right|_{X_2,\ldots X_J const} \approx \frac{\Delta r}{\Delta X_1} \tag{3.2}$$

and

$$\left.\frac{\partial r}{\partial x}\right|_{X_2,\ldots X_J const} \approx \frac{r_{X_1+\Delta X_1, X_2,\ldots X_J} - r_{X_1, X_2,\ldots X_J}}{\Delta X_1}. \qquad (3.3)$$

Each derivative is multiplied with the component uncertainty calculated from the regression curves. Coleman and Steele [21] show that all values are included in the finite difference approximation form of the Uncertainty equation as shown in equation (3.4),

$$U_r^{\,2} = \left(\frac{\Delta r}{\Delta X_1} U_{X_1}\right)^2 + \left(\frac{\Delta r}{\Delta X_2} U_{X_2}\right)^2 + \ldots\ldots + \left(\frac{\Delta r}{\Delta X_J} U_{X_J}\right)^2. \qquad (3.4)$$

The results are shown in Appendix A, Numerical Uncertainty Tables A.1 and A.2. Each component that adds to the overall vehicle dry weight is used to define the overall system uncertainty level. Tables 3.3 to 3.11 define the +/- regression level used in the numerical calculations. The regression levels are defined in Tables A.1 and A.2 within the column titled 'Table Data (U_X)'.

Log Normal Monte Carlo Uncertainty in LVSS Model

The weight uncertainty for the historical data curves for vehicle component weights is defined as power series regression curve-fits and is plotted on a logarithmic scale. The power series graph appears to be linear when using the logarithmic axes scale.

The uncertainty or error (E) is shown for the power series regression curves and given by equation (3.5) of form,

$$Y = aX^{b} * E. \tag{3.5}$$

In order to define uncertainty for the power series equations, the logarithmic form of the power series equation must be defined after taking the natural log of equation (3.6). The expanded form of the equation is given by equation (3.6),

$$\ln(y) = \ln(a) + b\ln(X) + \ln(E). \tag{3.6}$$

The resulting equation defines a new equation that is no longer in log space. The requirement for this step is mandated by the need to have variables and levels of uncertainty in non-log space in order to represent the values on a readable scale.

The vehicle data defined in Tables 3.3 to 3.11 is used to determine the standard error for each component. The standard error for a component (example: Vehicle Wing) is calculated by taking the summations of the differences between natural log (ln) of the actual weight and the ln of the predicted weight. This term is squared and then divided by the number of degrees of freedom in the calculation. The degrees of freedom are the 'n' number of examples subtracted by two. The Standard Error (SE) for the Wing is then calculated by taking the square root of the entire equation. This summation occurs for each of the 'n' examples of historical data defined for each component. This equation is applied to each of the sets of historical data tables defined from Table 3.3 to Table 3.11. Smart [4] showed that the SE equation, as defined here in equation (3.7), should be used for calculating each component SE,

$$SE = \sqrt{\frac{\sum((\ln(actual) - \ln(estimate))^2}{n-2}}. \qquad (3.7)$$

The standard deviation and mean for a given *SE* are defined for the wing, tail, tanks, body, thrust structure, landing gear, propulsion and TPS. Walpole, Myers, Myers and Ye [5] defined each component mean (μ) using equation (3.8),

$$\mu = e^{.5*SE}. \qquad (3.8)$$

Walpole, Myers, Myers and Ye [5] also defined the standard deviation using equation (3.9),

$$\sigma = \sqrt{e^{SE2} * (e^{SE2} - 1)}. \qquad (3.9)$$

For each case, the mean and standard is used with @Risk to define a lognormal distribution. The weight distribution is defined by taking the models calculated weight and multiplying it times the uncertainty from the lognormal distribution. Monte Carlo runs are used to allow an overall weight distribution to be formulated using the individual distributions. The higher the number of Monte Carlo runs, the better the accuracy of the overall weight distribution.

3.1.2 Trajectory Model

The trajectory model uses the rocket equation to formulate a *MR* for the vehicle system. This module also includes a pressure, temperature and density parameter calculation based upon altitude. The program uses input values for ΔV required, Orbit

Inclination, Orbit height, and Drag Reduction percentage. These values are set and determined based upon the DRM for a specified mission and will not change during the optimization of the design process. The module also takes *Twi*, *ARs*, P_c, *OF* Ratio, Delta *ISP*, A^*/T_{vac}, and Vacuum *ISP* (ISP_{vac}) and uses these values to determine a value for *MR* of the vehicle for the given DRM conditions. The *Twi*, *AR*, P_c, *OF* Ratio, Delta *ISP*, and A^*/T_{vac} are parameters input into the trajectory program by the user. The formats of the Trajectory worksheets are defined in Appendix C, Figures C.1 to C.3. The values in Appendix C are shown for illustration purposes and are not the final results.

The value(s) for ISP_{vac} are inputs from the Propulsion Module. The propulsion module will define a value for ISP_{vac} based upon the P_c, *AR*, and *OF* Ratio optimization outputs from the Trajectory Model. This relationship is described in more detail during the discussion of the Propulsion Model in Section 3.1.3. The Trajectory Model has the option for defining dual engine systems and the ability to specify the percentage of thrust being provided by engine set 1 versus the total (T1_T), and having an engine set 2 which allows for an expandable nozzle to be extended at some point during the trajectory. The value for this term is a percentage of the trajectory and is defined as the Area Ratio Transition (ART). The significance of the adjustable nozzle is to allow for greater area ratios later in flight without having the negative pressure benefits of atmospheric pressure that occurs earlier in the trajectory. Therefore, the ART will be later in the flight when atmospheric pressure is low. This is mentioned for illustration as a model capability. This system being described herein is not using dual engine and expandable nozzle functions.

The rocket equation is based upon the calculation of a ΔV by using the vehicles *ISP*, *MR*, Drag, Thrust, Weight (*W*), and launch angle (γ). When solving for ΔV, the form of the equation (3.10) is shown here,

$$\Delta V = g_o * ISP \ln(MR)(1 - Drag/Thrust - W/T \sin\gamma). \tag{3.10}$$

The Trajectory program solves for the vehicle *MR* as the primary output. The output also includes Time-to-Orbit, Final Velocity, Final Altitude. The output values of Final Velocity and Final Altitude must match the DRM inputs mentioned earlier. The rocket equation (3.11) is solved for *MR* and is shown in equation (3.11),

$$MR = \Delta V / (ISP * (1 - Drag/Thrust - W/Thrust * \sin\gamma). \tag{3.11}$$

The input parameters for *Twi*, *AR*, P_c and *OF* Ratio are modified during the analysis of the system by using the GA optimization Evolver Tool Software [3]. By choosing to minimize the Overall Vehicle Dry Weight, the program will define the best possible configuration for reduced weight by changing the input parameters above. The Weights and Sizing Model and the Propulsion Module use these parameters as inputs. The integration of these parameters is described in more detail in Section 3.2.

3.1.3 Propulsion Module

The Propulsion Module resides as a worksheet within the LVSS Vehicle Weights and Sizing Model. The Propulsion Module utilizes parameters calculated using Cequel from the Software and Engineering Associates, Inc. [18]. Cequel uses the minimization of Gibbs Free Energy and provides combustion process outputs based upon rocket inputs. Key propulsion parameter inputs to Cequel include P_c, AR, and OF Ratio. These three parameters are input into Cequel after having been optimized in the Trajectory Model and output values are defined for a range of thirty-one different output variables. This vehicle model uses only the sea level ISP (ISP_{sl}), ISP_{vac}, C_f, C_{star} outputs from Cequel. The outputs are integrated with the weights and sizing, and trajectory models to determine the overall vehicle weights and performance output. The Propulsion Module worksheet is defined in Appendix D, Figures D.1 and D.2. The values in Appendix D are shown for illustration purposes and are not the final results.

The launch vehicle's required sea level thrust (T_{sl}) is determined by multiplying the $GLOW$ times the Twi as shown in equation (3.12),

$$T_{sl} = GLOW * Twi . \tag{3.12}$$

The Launch Vehicle Model will utilize whatever Twi value it is given. The value for Twi is also used during the GA optimization techniques described earlier. The Propulsion Module utilizes T_{sl} and the value for ISP_{sl}, to calculate the W_{dot}. The value of W_{dot} is

defined as the rate of change in overall vehicle weight and varies with changes in *GLOW* and/or ISP_{sl}, as shown in equation (3.13),

$$W_{dot} = \frac{GLOW}{ISP_{sl}}. \tag{3.13}$$

The value for ISP_{sl} is an output from the Cequel code. Any change to the vehicle model that impacts the value of these two parameters (*GLOW* and ISP_{sl}) has an impact on the value of W_{dot}. This is an important point and should not be lost when understanding how propulsion model functions as a closed loop system. The significance lies in the understanding that when a parameter changes, it has impact to other values in the model. Understanding this relationship and how to model it is the most significant accomplishment of this problem.

The value for vacuum level thrust (T_{vac}) is defined based upon the W_{dot}, calculated in equation (3.13) above, multiplied times the Cequel output for ISP_{vac}. This relationship is shown here in equation (3.14) and gives the T_{vac} based upon thermo-chemical output,

$$T_{vac} = W_{dot} * ISP_{vac}. \tag{3.14}$$

This relationship between T_{vac} and T_{sl} is established using W_{dot} because the propellant flow rate is the same regardless whether the value is determined using sea level conditions or vacuum conditions.

The engine design parameter for Combustion Efficiency is 96%, and is based upon historical engine system and studies performed by the NASA-MSFC Transportation Directorate organization during the development of the NASA's Propulsion Sizing, Thermal Analysis and Weight Relationship (PSTAR) Model [15]. The efficiency level reduces the Cequel output for ISP_{vac} and ISP_{sl} by 4%. The user can modify the efficiency if level is deemed to high or low for a particular system. Any values for engine design parameters, including Trajectory Model optimization parameters, are using the reduced level of *ISP* due to efficiency. The *ISP* value is an important component in the Trajectory Model's determination of the vehicle *MR*, as shown in equation (3.11). An important integration step is to ensure that the value for *ISP* is actually resulting from the design inputs being used to size the system and define the propulsion system.

The Propulsion Module also provides the correlation of engine parameters to the engine weight. The engine weight is determined using a combined Rocketdyne Power Balance, U.S. Air Force, NASA Langley approach and using historical engine data to develop a curve that relates engine weight to the value found when multiplying *OF* Ratio, *AR* and P_c together. The four methods are averaged together to give an engine weight based upon these methods that are defined in Section 2.5. The Power Balance and U.S. Air Force methods make use of the nozzle geometry model in order to determine nozzle weight. The nozzle weight is determined using engine *AR*, A^* and coefficients for unit weights of the material used in the design of the nozzle.

The Cequel code requires only inputs for P_c, AR and OF Ratio. These inputs are entered into the model and are linked such that any changes to these values result in a change in the Cequel output. The output from the code is available for up to 32 unique parameters. Only Cequel outputs for C_{star}, C_f, ISP_{vac} and ISP_{sl} are used in this model. Although exit mach number and combustion temperature are defined within the Propulsion Module, they are not used in the optimized solution. The combined parameters, as shown in Figure 3.16, define other variables that are used to determine Engine Thrust required, A^* and m_{dot}. The equations (3.15) and (3.16) shows how Sutton [20] defined A^* and subsequently throat diameter (D^*) from the propulsion parameters,

$$A^* = \frac{T}{P_c * C_f} \tag{3.15}$$

and

$$D^* = \sqrt{\frac{4 * A^*}{\pi}} . \tag{3.16}$$

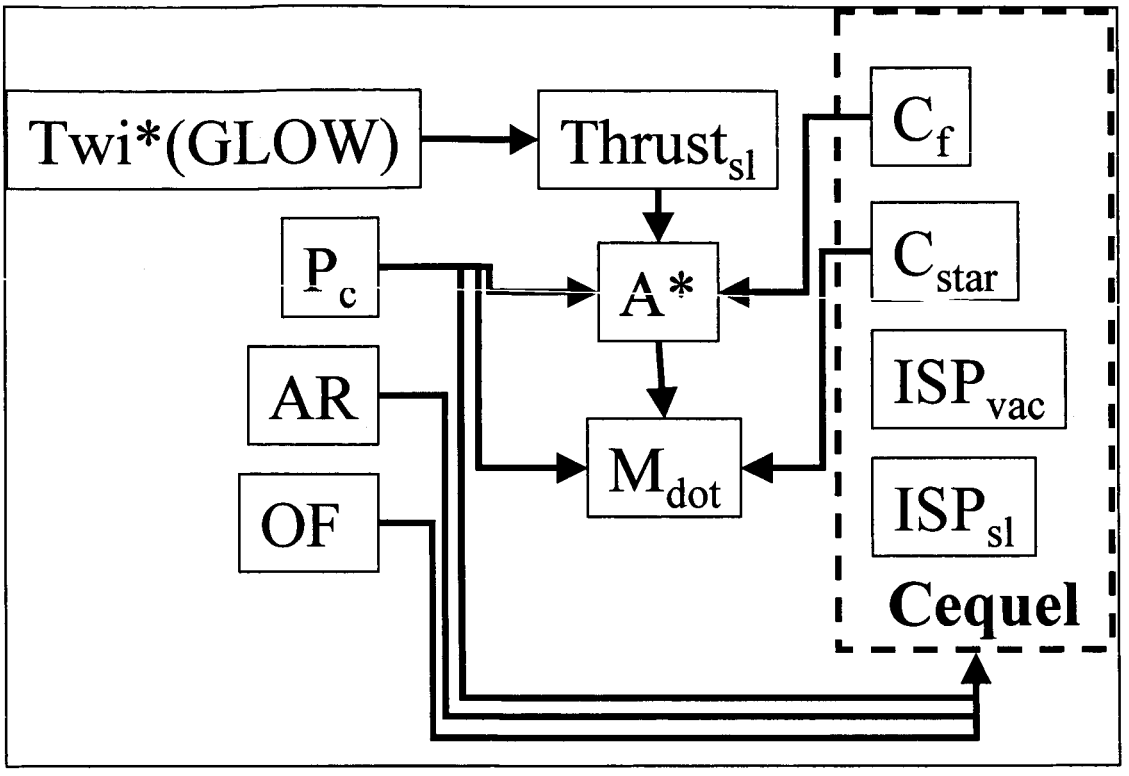

Figure 3.16 Cequel Output Functionality

The key to determining the engine geometry and weight is establishing the value for several secondary parameters. The value for mass flow rate (m_{dot}) of the engine is defined by Sutton [20] and is illustrated in equation (3.17),

$$m_{dot} = \frac{P_c * A^*}{C_{star}}, \tag{3.17}$$

where C_{star} is define in the thermo-chemical output calculation using Cequel. The results for m_{dot} will be used in the determination of the engine mass.

Engine mass is a function of the calculation techniques defined by Paulson, Burkhardt, Mysko, and Jenkins[13], Wilhite [12], Wells [14] and historical data curves for the relationship between *OF* Ratio*P_c*AR and engine mass. The engine mass approximation methods are described in Section 2.5. The resulting predicted engine mass is determined using the mass average of each of these four approaches. The engine mass relationship is important to the overall model because of the significance in the engine mass as a percentage of the overall *GLOW*. Equations (3.18) and (3.19) show which parameters are used to determine the nozzle mass and then overall engine mass. An important point is to note is that Cequel defines both C_f and C_{star} and provides a solution approach with the precision that only the thermo-chemical solution can provide.

$$NozzleMass = f(A^*, AR) \tag{3.18}$$

and

$$EngineMass = f(m_{dot}, C_f, AR, P_c, Thrust, OF, ISP). \tag{3.19}$$

3.1.4 Cost and Economics Model

The cost and economics model is derived based upon the NASA cost projection methodology. The model is developed using the component weights of previous systems, and plotting the cost of the component versus the weight of the component. The resulting regression curves are then used in order to project future cost for a particular system. The CIFs that result from using technology factors are also used to calculate the cost of a component DDTE. The technology factor (TF) will decrease the weight of the

component or increase the effectiveness of a component, but will almost always increase the cost of development. The factors, both TFs and CIFs, are model design and analysis parameters that will change as technology evolves and also as the ability to efficiently manufacture or develop a design is enhanced or minimized. A Boolean code is used to relate 1, 2 or 3 with the desired TF and CIF. Table 3.12 below shows which TFs and CIFs related to 1, 2 or 3 in each case. Table 3.12 data is shown for illustration purposes only.

Table 3.12 Technology and Cost Influence Factor Boolean Code

Parameter	Boolean Code	Factor	Material	Code 1	Code 2	Code 3
Wing Technology Factor	3	0.869	MMC	1.000	0.724	0.869
Tail Technology Factor	3	0.970	MMC	1.000	0.842	0.970
LH2 Tank Technology Factor	3	0.900	MMC	1.000	0.750	0.900
LOX Tank Technology Factor	2	0.700	Composite	1.000	0.700	0.840
Basic Structure Technology Factor	2	0.700	Composite	1.000	0.700	0.840
Thrust Structure Technology Factor	2	0.740	Composite	1.000	0.740	0.888
Gear Technology Factor	1	1.000	Aluminum	1.000	0.781	0.937
Engine Accessories technology Factor	1	1.000	Aluminum	1.000	0.891	1.070
Wing CIF (Cost influence Factor)	3	10.000	MMC	1.000	2.100	10.000
Tail CIF	3	10.000	MMC	1.000	2.100	10.000
LH2 tank CIF	3	10.000	MMC	1.000	2.100	10.000
LOX tank CIF	2	2.100	Composite	1.000	2.100	10.000
Body CIF	2	2.100	Composite	1.000	2.100	10.000
Basic structure CIF	2	2.100	Composite	1.000	2.100	10.000
Thrust Structure CIF	2	2.100	Composite	1.000	2.100	10.000
Landing Gear CIF	1	1.000	Aluminum	1.000	1.800	10.000

The uncertainty surrounding the DDTE cost is normally high due to the large number or data points used in fitting the historical data to a regression curve. Also, the approach described in the Log Normal Monte Carlo Uncertainty in Section 3.1.1.3, is the same approach used to determine the overall uncertainty in the DDTE cost. All of the subsystem components have *SE*'s that are used in determining the overall DDTE cost uncertainty value. In addition to the subsystems, the NAFCOM model also applies standard errors for the RCS, and OMS.

CHAPTER 4

RESULTS

The results show the optimal vehicle design, optimized propulsion parameters and parameter sensitivity, engine mass calculated, and uncertainty measurements for *GLOW*, Dry Weight and DDTE cost. The optimal vehicle design shown herein is determined based upon the optimization of key technical performance measures related to cost and weight. The results also show the impact of varying propulsion parameters on the overall vehicle performance measures, particularly on the weight of the vehicle.

4.1 Optimal Vehicle Design

The optimal vehicle design defined herein is based upon the minimization of the seven key FOMs referenced in Section 3.2. For each of the seven cases, the values of propulsion parameters are defined using the Palisades Evolver optimization tool. Secondary engine design parameters are defined as well in order that the engine system specification could be written from the model output. The range of TFs and corresponding CIFs are based upon the Boolean code for technologies 1, 2 or 3. Tables 4.1 and 4.2 show the results of the GA Evolver Tools for the optimal vehicle design. The three cases of weight minimization are shown in

Table 4.1: Minimum *GLOW*, Minimum Dry Weight, Minimum Dry Weight with Margin, and the four cases where cost is minimized are shown in Table 4.2: Minimum DDTE Cost, Minimum Production Cost, Minimum Operations Cost, and Minimum Life Cycle Cost (LLC).

The relationship between the weight components shows an absolute correspondence between the Dry Weight and the Dry Weight with Margin. The cost numbers were slightly different between the *GLOW* and Dry Weight, with the upfront cost (DDTE/Production) of the *GLOW* optimized solution being higher. The downstream cost of the *GLOW* optimized system was slightly lower that the Dry Weight optimized solution. The P_c and *AR* were nominally unchanged but the *OF* Ratio and *Twi* were significantly different between the Dry Weight and *GLOW* cases. The *OF* Ratio for Dry Weight optimization is focused on tank weight, while the *GLOW* optimized solution is focused on lower fuel weight. Flight Autonomy is the only TF that ever differed between the multiple runs of the 2 weight optimization cases. The Boolean code for the Flight Autonomy relates 1-Shuttle Like, 2-Semi Airplane Like, and 3-Airplane Like. The remaining TFs can be understood by referencing Table 3.12. The table explains the Boolean Code link to the material property for each, either 1, 2 or 3.

The optimization parameters for the cost cases are shown in Table 4.2. The propulsion parameters are closely tied together for each of the 4 cost optimization cases. The only exception is the *Twi* value. The *Twi* for the minimum DDTE and Production cost is lower than the *Twi* for the minimum Operations and LCC cost. The significant

difference for the cost cases is in the Boolean Codes (1, 2 or 3) for each of the 4 cases. This is logical because the TFs and more importantly the CIFs have a significant impact of cost due to the fact the CIFs are multiplying factors in the cost of each component.

Table 4.1 Optimized Vehicle Parameters for Weight Minimization

PARAMETER	GLOW Minimization Parameters	Dry Wt Minimization Parameters	Dry Wt w/ Margin Minimization Parameters
GLOW	4,635,904	4,848,013	4,848,013
Dry Weight	437,676	428,123	428,123
GLOW + Dry Wt	5,073,580	5,276,136	5,276,136
Dry Weight with margin	473,342	463,011	463,011
DDT&E	$39.866	$42.508	$42.508
Production Costs	$114.552	$125.177	$125.177
Operations Costs	$219.354	$195.913	$195.913
LCC	$373.772	$363.598	$363.598
Thrust to Weight Ratio	1.63	1.40	1.40
ENGINE			
Chamber Pressure	2712.8	2464.9	2464.9
OF Ratio	6.90	7.43	7.43
Area Ratio	95.1	87.5	87.5
Mass Ratio	7.6	8.0	8.0
Throat Diameter	13.5	13.4	13.4
Vacuum ISP	445.7	440.7	440.7
Sea Level ISP	429.4	422.7	422.7
Per Engine Vacuum Thrust	784,262.8	707,828.7	707,828.7
Per Engine Sea Level Thrust	755,445.1	679,062.9	679,062.9
Per Engine Weight	9,818.6	8,851.0	8,851.0
TECHNOLOGY			
Wing Technology Factor	2	2	2
Tail Technology Factor	2	2	2
LH2 Tank Technology Factor	2	2	2
LOX Tank Technology Factor	2	2	2
Basic Structure Technology Factor	2	2	2
Thrust Structure Technology Factor	2	2	2
TPS Technology Factor	2	2	2
Gear Technology Factor	2	2	2
Engine Accessories technology Factor	2	2	2
MPS Technology Factor	2	2	2
Engine Technology Factor	2	2	2
Flight Autonamoy	2	3	3

Table 4.2 Optimized Vehicle Parameters for Cost Minimization

PARAMETER	DDTE Cost Minimization Parameters	Production Cost Minimization Parameters	Ops Cost Minimization Parameters	LLC Minimization Parameters
GLOW	7,732,600	7,796,955	5,719,590	6,436,192
Dry Weight	733,872	735,936	542,143	608,671
GLOW + Dry Wt	8,466,471	8,532,891	6,261,733	7,044,862
Dry Weight with margin	793,675	795,907	586,323	658,271
DDT&E	$26.079	$30.972	$45.715	$39.900
Production Costs	$93.186	$56.713	$83.369	$70.855
Operations Costs	$287.301	$237.704	$171.223	$183.601
LCC	$406.566	$325.388	$300.307	$294.357
Thrust to Weight Ratio	1.43	1.41	1.67	1.53
ENGINE				
Chamber Pressure	3162.4	3167.3	3033.6	3044.6
OF Ratio	7.45	7.54	7.69	7.57
Area Ratio	101.5	103.8	99.7	98.4
Mass Ratio	7.9	7.9	7.7	7.8
Throat Diameter	15.0	15.0	14.3	14.5
Vacuum ISP	443.5	443.2	441.0	441.9
Sea Level ISP	426.4	425.9	423.2	424.4
Per Engine Vacuum Thrust	1,147,237.5	1,143,811.4	993,328.3	1,028,207.4
Per Engine Sea Level Thrust	1,102,959.3	1,099,370.6	953,234.3	987,353.1
Per Engine Weight	13,814.4	13,887.3	12,243.6	12,516.6
TECHNOLOGY				
Wing Technology Factor	1	2	2	2
Tail Technology Factor	1	1	2	1
LH2 Tank Technology Factor	1	1	2	2
LOX Tank Technology Factor	1	2	2	2
Basic Structure Technology Factor	1	1	2	2
Thrust Structure Technology Factor	1	1	2	2
TPS Technology Factor	2	3	3	3
Gear Technology Factor	1	2	2	2
Engine Accessories technology Factor	2	2	2	2
MPS Technology Factor	2	2	2	2
Engine Technology Factor	1	1	2	1
Flight Autonamoy	1	1	3	3

The most significant differences between the weight parameters and cost parameters in Tables 4.1 and 4.2 are the TFs and corresponding CIFs. For the weight minimization cases, the TFs are driven to a Boolean value of two (2) and the DDTE cost minimization case in general is equal to one (1). These results are expected because the weight savings for the Boolean value of two (2) represents a weight savings over current baseline technologies but represents a cost increase by a multiple of 2.1 times the cost for current technology for a Boolean value of one (1). The *GLOW*, Dry Weight and Dry Weight with Margin reflect near identical TFs based upon the fact that the technologies defined in the database by Boolean two (2) represent a multiple for component weights that is less than one. The production, operations and life cycle cost reflect a wider range of TF and CIF possibilities. This is true because the most significant cost impact for new technologies is absorbed by the DDTE cost and will in some cases result in cost savings during the other cost phases of the program. In essence, increased cost incurred during the DDTE phase results in cost savings for the vehicle production, operations and life cycle.

The propulsion design parameters shown in Tables 4.1 and 4.2 vary based upon the specific minimization case. The chamber pressure influence follows the same trend for the *GLOW*, Dry Weight with Margin and Dry Weight minimization cases. The chamber pressure is slightly higher for the *GLOW* minimization case. This is due to the fact that the *ISP* level is higher at increased chamber pressure and thus the vehicle requires less fuel. The Dry Weight minimization chamber pressure is lower due in great part to the sole focus on reducing engine mass. The lower the chamber pressure results in

smaller engine mass. At high chamber pressures the chamber size and weight, lines and valves, and support structure must be more robust and drive the engine mass up. The cost optimization cases define the chamber pressure level at approximately 3100 psi. This level is approximately the level for the current SSME block design.

The area ratio for the various cases follows a similar pattern to the chamber pressure described earlier. The area ratio is lowest for the Dry Weight minimization case because smaller area ratios result in a lighter engine nozzle. But the ratio must be high enough to enable the appropriate specific impulse. It is logical that the Dry Weight case does not consider the impacts of specific impulse, as does the *GLOW* minimization case. The *GLOW* case defines a slightly higher area ratio that is due in part to the increased specific impulse for the higher area ratio. The area ratio for the cost minimization cases is nearly identical and is slightly higher than the weight cases. The higher area ratio for the cost cases is driven by the increased specific impulse but is not impacted as severely by the magnitude of increased weight due to increasing the area ratio.

The optimized *OF* Ratio is defined for each of the 7 minimization cases. The value for *OF* Ratio is driven to an optimized solution for the *GLOW* case based upon decreased engine propellant mass. The *OF* Ratio for the Dry Weight minimization case is higher because this ratio impacts the propellant tank volume only and does not consider propellant mass. So in essence, the optimized value for the *OF* Ratio is driven by the propellant density and propellant volume. The *OF* Ratio for the cost minimization cases is in the range similar to the *GLOW* minimization case. The ratio value for the DDTE

cost minimization and the Dry Weight minimization cases are nearly identical due to the correlation between the component weight relationships within the DDTE cost estimates.

4.2 Optimization of Propulsion Parameters

The optimization cases, including propulsion parameters, are shown for *OF* Ratio, P_c and *AR*. *OF* Ratio has a significant impact on the overall weight of the vehicle and vehicle components due to the large percentage of the *GLOW* that is dedicated to fuel and oxidizer. The results from varying the P_c and *AR* prove that these parameters have a much lower impact on the *GLOW* and Dry Weight than the *OF* Ratio. The impacts of each of these parameters on the overall engine mass are shown for an incremental range of values. The results in subsequent sections show how each of the propulsion parameters will affect the vehicle and how the vehicle will be impacted when a propulsion parameter is changed to a value that is different than the optimum value.

4.2.1 *OF* Ratio

OF Ratio effects on vehicle Dry Weight, *GLOW*, ISP_{vac}, propellant volume, propellant weight, propellant density and engine mass are defined in Tables 4.3 to 4.6 and Figures 4.1 to 4.4. The program includes an Excel macro that increments the *OF* Ratio from 5.0 to 8.0 and shows the results on each parameter. The incremental values for the *OF* Ratio are run against overall vehicle optimization case for Dry Weight minimization. The data for the *OF* Ratio that corresponds to the minimum Dry Weight, minimum *GLOW*, maximum ISP_{vac}, minimum propellant volume, minimum propellant weight, and minimum engine mass are found using the Excel VLOOKUP function search. The

search returns the value for the *OF* Ratio that results in the minimum or maximum of the case being analyzed.

Figures 4.1 to 4.4 show the data plots for Dry Weight, *GLOW*, ISP_{vac}, propellant volume, propellant weight, and engine mass versus *OF* Ratio. By examining Figure 4.1, the *OF* Ratio value for minimum *GLOW* has a range from approximately 6.2 to 7.1 where there is little impact on the *GLOW*. The data in Table 4.4 shows that when the *OF* Ratio is varied within this range, the impact on the overall propellant weight is only .75% (*OF* Ratio = 6.2) to .82% (*OF* Ratio = 7.2) above the optimum *OF* Ratio. The results prove that for optimum *GLOW*, the best takeoff *OF* Ratio is in the range of 6.2 to 7.2, if the system is a LOX/H2 fixed bell nozzle engine configuration. The results for minimum engine mass in Figure 4.2, are also consistent with this range of values. An *OF* Ratio in the range of 6.2 to 7.2 is best for the initial phase of the trajectory when the vehicle propellant mass is most important.

The maximum ISP_{vac} is found at the *OF* Ratio of 5.2. These results are defined in Table 4.3. An *OF* Ratio of 5.0 (ISP_{vac} = 449.01) to 5.6 (ISP_{vac} = 448.81) would be best for the later phase of the trajectory profile, when higher *ISP* is important. The *ISP* value changes only slightly over this range of values for *OF* Ratio. These *OF* Ratio results are consistent with the early plans for the SSME that called for an adjustable *OF* Ratio. The preliminary plans for the SSME included a value for *OF* Ratio equal to 6.5 for the initial takeoff, with the ratio being modified to 5.5 later in flight when the higher *ISP* was more important.

Table 4.3 *OF* Ratio Effects

Avg O/F Ratio	Dry Wt	ISPvac	GLOW	Highest ISP Lowest Dry Wt Lowest GLOW Real ISPVac	OF Ratio 5.2 7.4 6.7 Avg O/F Ratio
5	489127.19	467.72	5233755.06	449.01	5
5.2	477888.84	467.81	5124935.50	449.09	5.2
5.3	472910.05	467.79	5078174.77	449.08	5.3
5.4	468311.13	467.73	5035988.93	449.02	5.4
5.6	459711.70	467.51	4956864.78	448.81	5.6
5.8	452788.36	467.15	4900207.51	448.46	5.8
6	446943.55	466.65	4856986.13	447.98	6
6.2	442063.04	466.02	4826036.43	447.38	6.2
6.3	439569.59	465.65	4808149.82	447.03	6.3
6.4	437633.71	465.26	4799041.62	446.64	6.4
6.5	435950.65	464.82	4793523.62	446.23	6.5
6.6	434514.46	464.36	4791569.01	445.78	6.6
6.7	432805.26	463.86	4784020.75	445.30	6.7
6.8	431766.91	463.32	4787619.00	444.79	6.8
6.9	430454.66	462.75	4785680.10	444.24	6.9
7	429809.75	462.14	4795009.56	443.66	7
7.1	428904.22	461.49	4799042.49	443.03	7.1
7.2	428626.75	460.80	4813822.31	442.37	7.2
7.3	428572.15	460.05	4832113.17	441.65	7.3
7.4	428390.92	459.26	4847536.30	440.89	7.4
7.5	428845.60	458.40	4874089.23	440.07	7.5
7.6	429240.88	457.47	4899006.82	439.17	7.6
7.7	429962.83	456.45	4929405.06	438.19	7.7
7.8	431237.48	455.31	4969403.19	437.10	7.8
7.9	433316.65	453.95	5023712.15	435.79	7.9
8	436514.41	452.28	5099080.18	434.18	8

Table 4.4 *OF* Ratio Versus Propellant Density and Weight

OF Ratio	Density	LOX Wt	H2 Wt	Total Wt	Wt %
5	20.15	3796740.26	759,348	4,556,088	9.14%
5.2	20.62	3741565.39	719,532	4,461,097	6.86%
5.3	20.86	3718788.98	701,658	4,420,447	5.89%
5.4	21.09	3698911.64	684,984	4,383,895	5.01%
5.6	21.55	3661473.71	653,835	4,315,308	3.37%
5.8	22.00	3639550.61	627,509	4,267,059	2.21%
6	22.44	3626474.80	604,412	4,230,887	1.35%
6.2	22.88	3621634.47	584,135	4,205,769	0.75%
6.3	23.09	3616790.18	574,094	4,190,884	0.39%
6.4	23.30	3618642.15	565,413	4,184,055	0.23%
6.5	23.51	3623093.96	557,399	4,180,493	0.14%
6.6	23.72	3630154.76	550,023	4,180,178	0.13%
6.7	**23.93**	**3632476.44**	**542,161**	**4,174,637**	**0.00%**
6.8	24.13	3643551.15	535,816	4,179,367	0.11%
6.9	24.34	3649950.20	528,978	4,178,928	0.10%
7	24.54	3665274.81	523,611	4,188,885	0.34%
7.1	24.74	3676131.24	517,765	4,193,896	0.46%
7.2	24.94	3695559.14	513,272	4,208,831	0.82%
7.3	25.13	3717712.94	509,276	4,226,989	1.25%
7.4	25.33	3737397.92	505,054	4,242,452	1.62%
7.5	25.52	3766066.81	502,142	4,268,209	2.24%
7.6	25.71	3793297.36	499,118	4,292,415	2.82%
7.7	25.90	3824931.48	496,744	4,321,676	3.52%
7.8	26.09	3864377.71	495,433	4,359,811	4.44%
7.9	26.28	3915556.92	495,640	4,411,197	5.67%
8	26.46	3984139.55	498,017	4,482,157	7.37%

Table 4.5 *OF* Ratio Versus Propellant Density and Volume

OF Ratio	Density	Real ISPvac	LOX Vol	H2 Vol	Total Vol	Vol %
5	20.15	449.01	53,551	172,579	226,130	35.53%
5.2	20.62	449.09	52,772	163,530	216,302	29.64%
5.3	20.86	449.08	52,451	159,468	211,919	27.02%
5.4	21.09	449.02	52,171	155,678	207,849	24.58%
5.6	21.55	448.81	51,643	148,599	200,242	20.02%
5.8	22.00	448.46	51,334	142,616	193,949	16.25%
6	22.44	447.98	51,149	137,366	188,516	12.99%
6.2	22.88	447.38	51,081	132,758	183,839	10.19%
6.3	23.09	447.03	51,013	130,476	181,488	8.78%
6.4	23.30	446.64	51,039	128,503	179,542	7.61%
6.5	23.51	446.23	51,101	126,682	177,783	6.56%
6.6	23.72	445.78	51,201	125,005	176,206	5.61%
6.7	23.93	445.30	51,234	123,218	174,452	4.56%
6.8	24.13	444.79	51,390	121,776	173,166	3.79%
6.9	24.34	444.24	51,480	120,222	171,703	2.91%
7	24.54	443.66	51,696	119,002	170,699	2.31%
7.1	24.74	443.03	51,850	117,674	169,523	1.61%
7.2	24.94	442.37	52,124	116,653	168,776	1.16%
7.3	25.13	441.65	52,436	115,744	168,180	0.80%
7.4	25.33	440.89	52,714	114,785	167,499	0.39%
7.5	25.52	440.07	53,118	114,123	167,241	0.24%
7.6	25.71	439.17	53,502	113,436	166,938	0.06%
7.7	**25.90**	**438.19**	**53,948**	**112,896**	**166,845**	**0.00%**
7.8	26.09	437.10	54,505	112,598	167,103	0.15%
7.9	26.28	435.79	55,226	112,645	167,872	0.62%
8	26.46	434.18	56,194	113,186	169,380	1.52%

Table 4.6 *OF* Ratio Versus Engine Mass

	Minimum Engine Mass (OF Ratio) for Min Dry Weight Optimization		
	6.4		
Per Engine Mass	Engine Mass	OF Ratio	% Opt Engine Mass
9226	92,259	5	6.762%
9060	90,596	5.2	4.837%
8990	89,902	5.3	4.034%
8929	89,288	5.4	3.324%
8817	88,171	5.6	2.032%
8743	87,431	5.8	1.175%
8692	86,923	6	0.587%
8663	86,625	6.2	0.243%
8645	86,453	6.3	0.043%
8642	86,415	6.4	0.000%
8644	86,436	6.5	0.025%
8652	86,516	6.6	0.116%
8652	86,520	6.7	0.122%
8670	86,696	6.8	0.324%
8679	86,795	6.9	0.439%
8707	87,066	7	0.754%
8727	87,268	7.1	0.987%
8763	87,633	7.2	1.410%
8806	88,058	7.3	1.902%
8845	88,453	7.4	2.358%
8902	89,018	7.5	3.012%
8958	89,575	7.6	3.657%
9023	90,227	7.7	4.411%
9104	91,043	7.8	5.355%
9210	92,097	7.9	6.575%
9346	93,457	8	8.149%

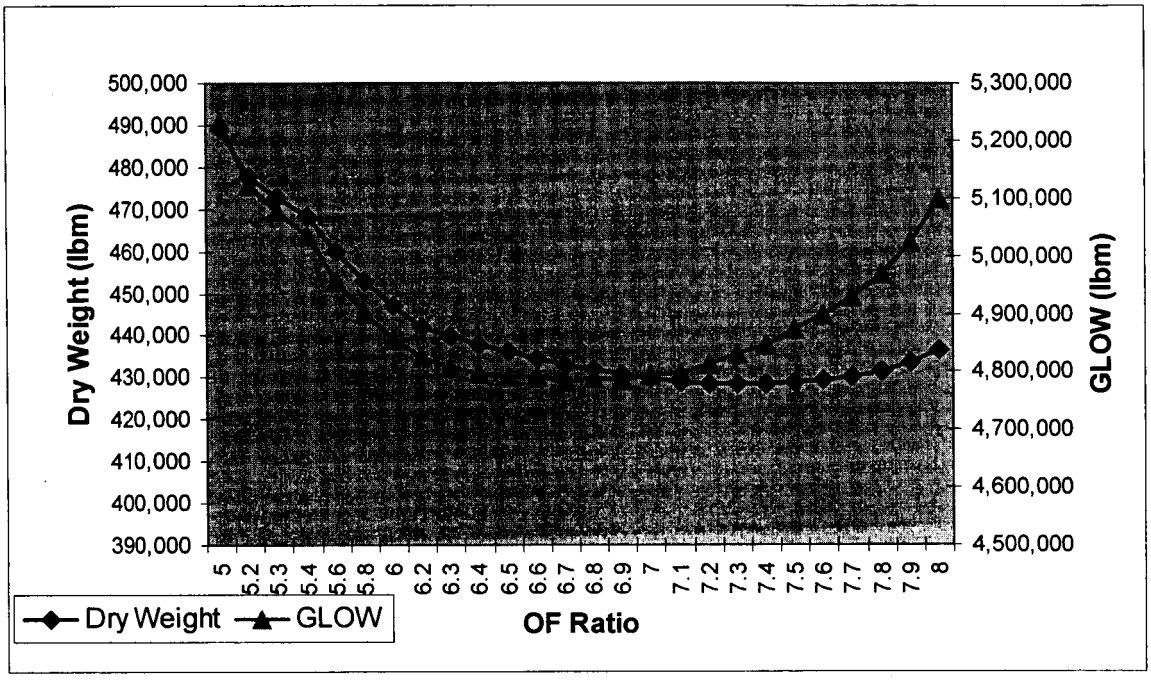

Figure 4.1 *OF* Ratio Versus *GLOW*/Dry Weight [case 2]

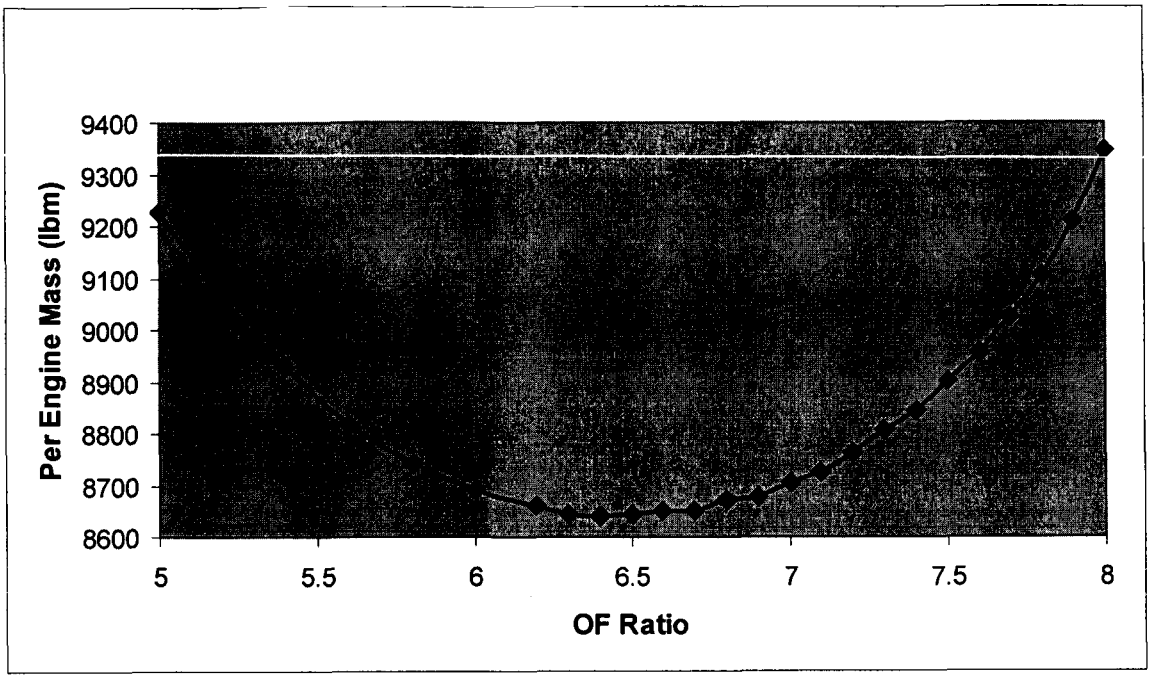

Figure 4.2 *OF* Ratio Versus Engine Mass [case 2]

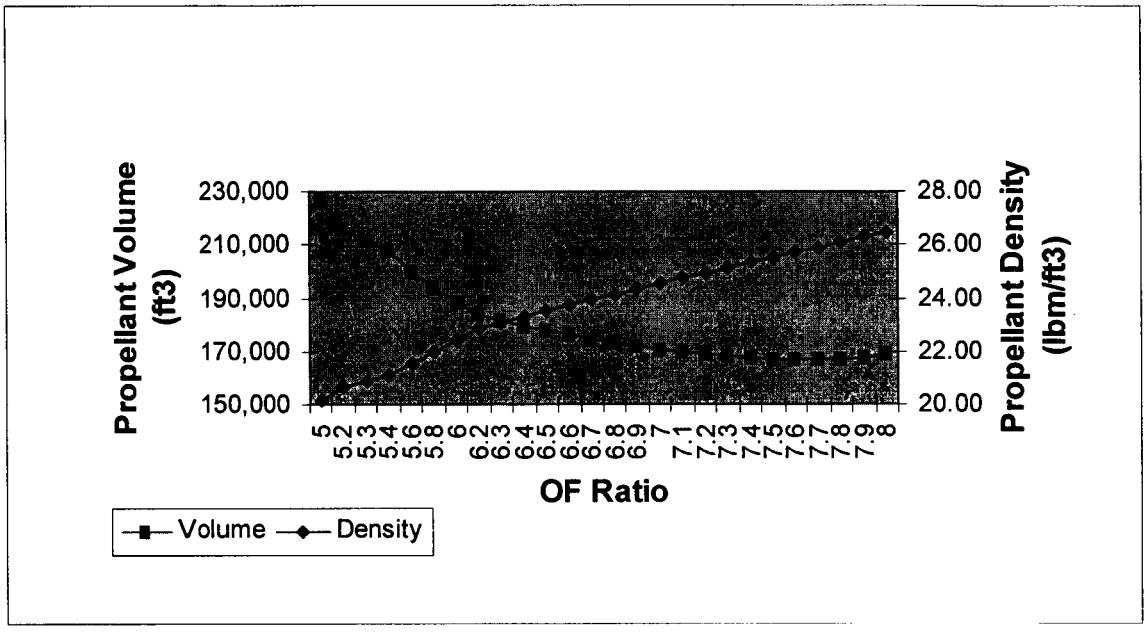

Figure 4.3 *OF* Ratio Versus Fuel Volume/Fuel Weight [case 2]

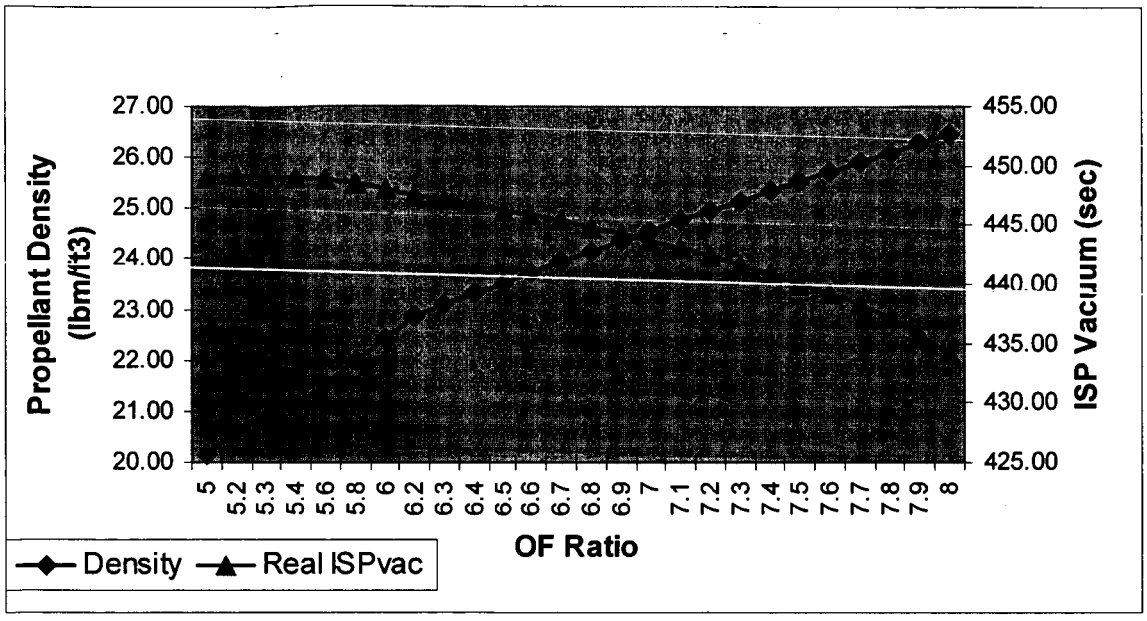

Figure 4.4 *OF* Ratio Versus Fuel Density/*ISP* Vacuum [case 2]

4.1.2 Chamber Pressure

The Dry Weight and *GLOW*, for the range of P_c from 2000 to 3700 psi, increased only slightly above the minimum weights for the optimized P_c. The incremental changes in vehicle Dry Weight, *GLOW* and ISP_{vac} are defined in Table 4.7 and the values for Dry Weight and *GLOW* are shown in Figure 4.5. The optimum value for lowest Dry Weight and engine mass correlated to a P_c value near 2400 psi. The value for the lowest *GLOW* is near 2700 psi. Table 4.7 and Figure 4.6 illustrate that the ISP_{vac} increases as P_c increases. This is a logical conclusion because higher pressures translate into higher *ISP* values. The data defined in Table 4.8 and Figure 4.7 shows a significant increase in the engine mass as the P_c approaches 3700 psi or as the P_c value increases. The increased engine mass is due to the thickness and design of the thrust chamber, increased robust

design for valves, ducts and lines needed at the higher pressures. The overall engine mass increase is at such a rate that the improved weight of the nozzle mass does not offset the core engine mass increase.

Table 4.7 Chamber Pressure Effects

Pc	Dry Wt	ISPvac	GLOW	Real ISPVac	Pc
2000	429,787	458.64	4877360.444	440.29	2000
2200	428,872	458.81	4863788.464	440.46	2200
2400	428,512	458.97	4856206.496	440.61	2400
2500	428,500	459.04	4854220.258	440.68	2500
2600	428,583	459.11	4853264.717	440.74	2600
2700	428,746	459.18	4853180.878	440.81	2700
2800	428,982	459.24	4853893.199	440.87	2800
2900	429,286	459.30	4855342.516	440.93	2900
3000	429,649	459.36	4857432.658	440.98	3000
3100	430,062	459.41	4860078.07	441.04	3100
3200	430,526	459.47	4863272.381	441.09	3200
3300	430,987	459.52	4866110.563	441.14	3300
3500	432,161	459.62	4875546.027	441.23	3500
3700	433,421	459.71	4885610.092	441.32	3700

Table 4.8 Chamber Pressure Versus Engine Mass

Engine Mass	Pc	% Opt Engine Mass	Per Engine Mass
88,992	2000	0.490%	8899
88,595	2200	0.042%	8859
88,558	2400	0.000%	8856
88,647	2500	0.101%	8865
88,798	2600	0.271%	8880
89,000	2700	0.499%	8900
89,249	2800	0.780%	8925
89,541	2900	1.110%	8954
89,871	3000	1.482%	8987
90,232	3100	1.891%	9023
90,626	3200	2.335%	9063
91,036	3300	2.798%	9104
91,962	3500	3.844%	9196
92,961	3700	4.972%	9296

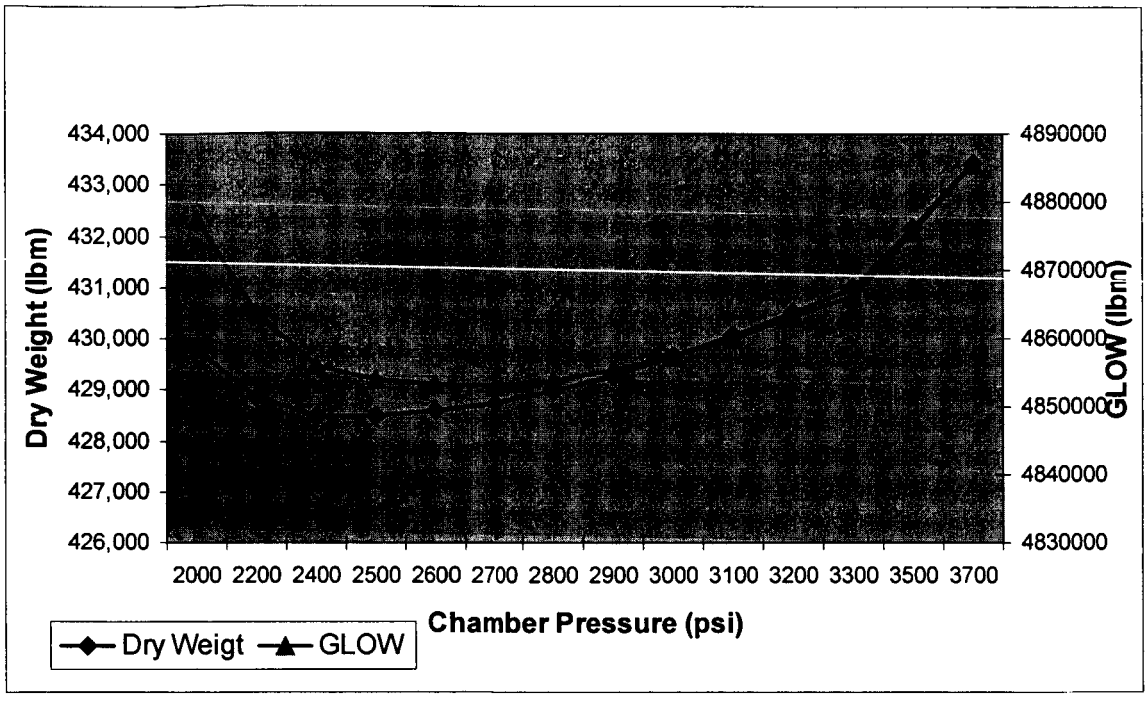

Figure 4.5 Chamber Pressure Versus *GLOW*/Dry Weight [case 2]

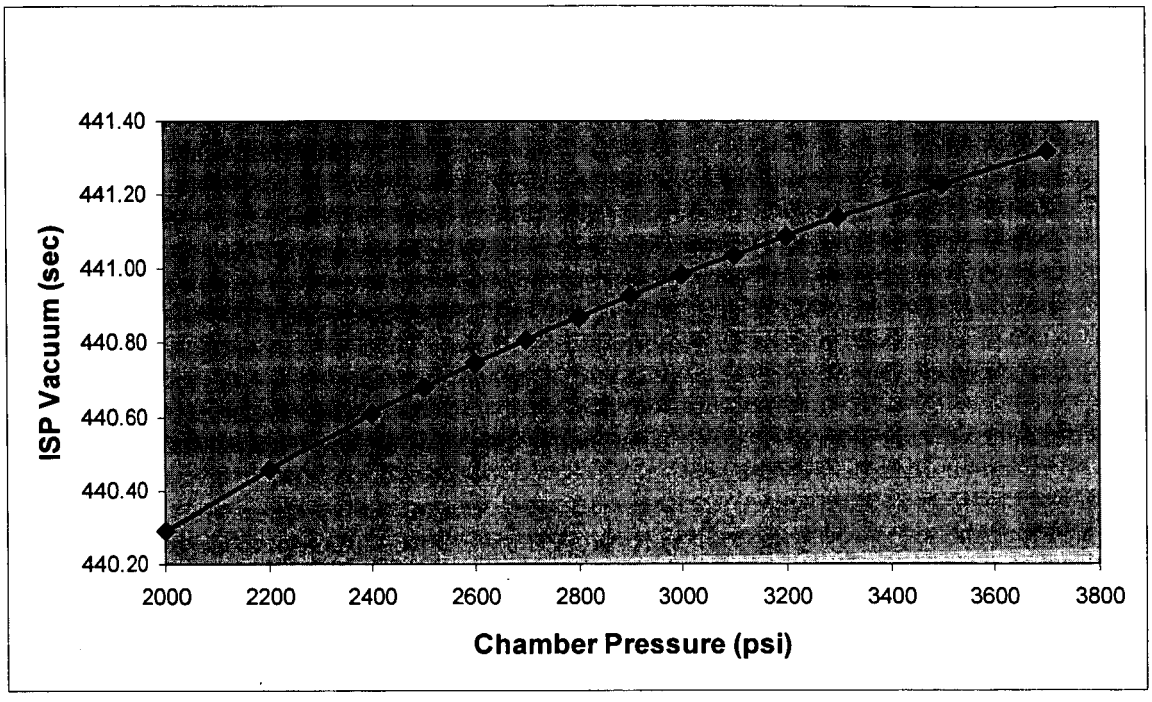

Figure 4.6 Chamber Pressure Versus *ISP* Vacuum [case 2]

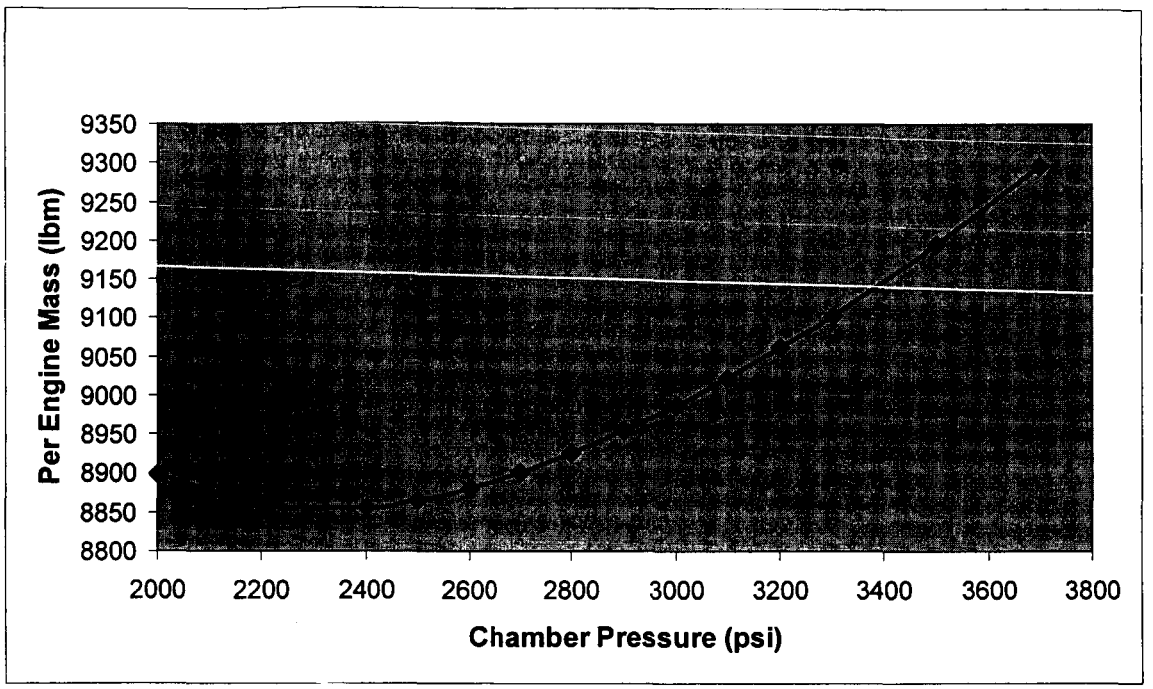

Figure 4.7 Chamber Pressure Versus Engine Mass [case 2]

4.1.3 Area Ratio

The Dry Weight and *GLOW* change very little over the range of *AR* from 50 to 120. The incremental changes in vehicle Dry Weight, *GLOW* and ISP_{vac} are defined in Table 4.9 and the values for Dry Weight and *GLOW* are shown in Figure 4.8. The optimum value for lowest Dry Weight correlated to an *AR* value in the range of 70 to 105 for a SSTO vehicle. Historically, the *AR* range for engines of multi-stage vehicles is from 45 to 60. The *AR* range, for engines used to complete the entire trajectory from launch to orbit, is 69 to 85. This is for the SSME (*AR* = 69 to 77.5) and the Russian made RD-0120 (*AR* = 85).

Table 4.10 and Figure 4.10 show that the lower the *AR*, the lower the engine mass. This is understandable due to the nozzle mass required for an *AR* equal to 50 versus an *AR* equal to 120. An *AR* of 50 corresponds to a much smaller exit area than the exit area for and engine with *AR* equal to higher values. Figure 4.9 shows that ISP_{vac} increases with the larger values for *AR*. This does not take into account the possibility of shocks in the nozzle due to over-expansion.

Table 4.9 Area Ratio Effects

AR	Dry Wt	ISPvac	GLOW	Real ISPVac	AR
50	442,417	447.71	5,273,320	429.81	50
55	438,251	449.76	5,175,356	431.77	55
60	435,127	451.59	5,096,505	433.52	60
65	432,656	453.23	5,029,557	435.10	65
70	430,864	454.71	4,975,013	436.53	70
75	429,477	456.07	4,927,795	437.83	75
80	428,913	457.31	4,895,612	439.02	80
85	428,523	458.46	4,866,512	440.13	85
90	428,443	459.53	4,842,964	441.15	90
95	428,851	460.52	4,828,247	442.10	95
100	429,386	461.45	4,815,742	443.00	100
105	430,430	462.32	4,812,388	443.83	105
110	431,139	463.14	4,802,837	444.62	110
115	432,725	463.92	4,809,080	445.36	115
120	434,311	464.65	4,815,197	446.06	120

Table 4.10 Area Ratio Versus Engine Mass

Engine Mass	AR	% Opt Engine Mass	Per Engine Mass
83,587	50	0.000%	8359
83,634	55	0.057%	8363
83,948	60	0.432%	8395
84,475	65	1.063%	8448
85,043	70	1.742%	8504
85,950	75	2.827%	8595
86,950	80	4.023%	8695
88,012	85	5.294%	8801
89,145	90	6.649%	8914
90,439	95	8.197%	9044
91,757	100	9.775%	9176
93,104	105	11.386%	9310
94,603	110	13.180%	9460
96,200	115	15.090%	9620
97,841	120	17.053%	9784

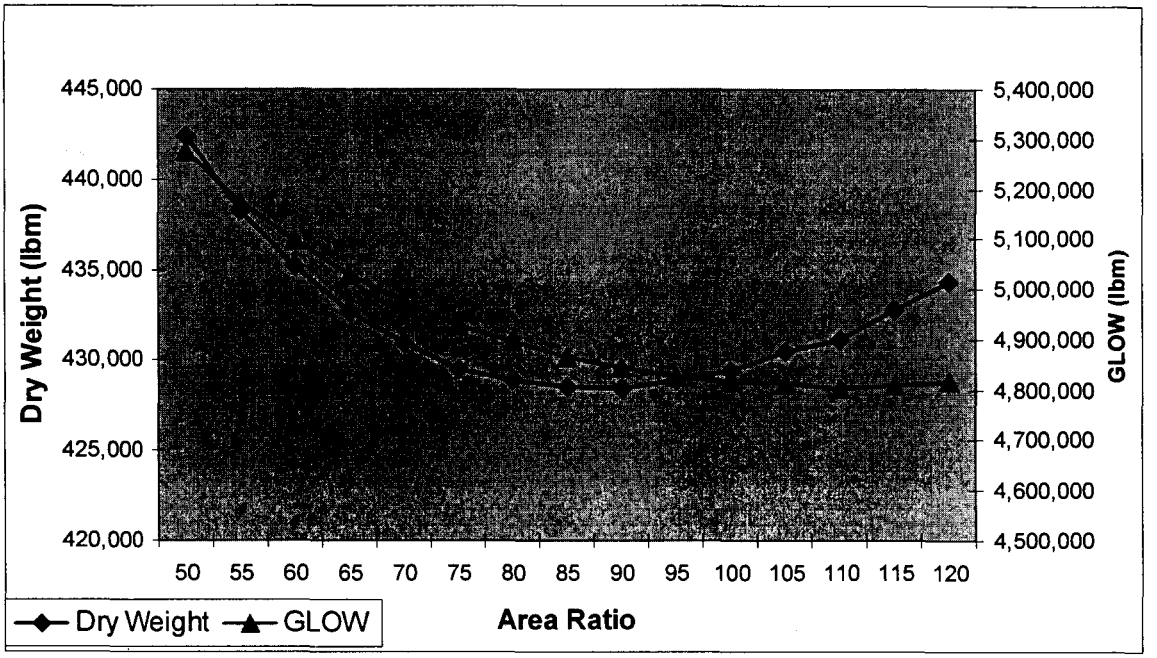

Figure 4.8 Area Ratio Versus *GLOW*/Dry Weight [case 2]

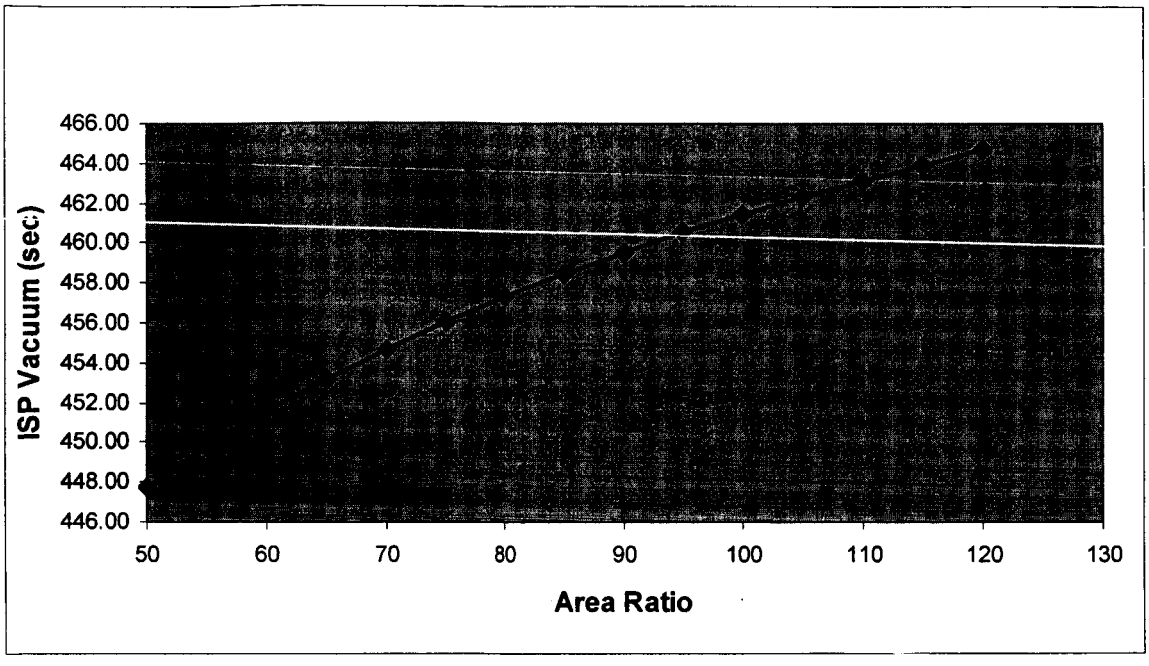

Figure 4.9 Area Ratio Versus *ISP* Vacuum [case 2]

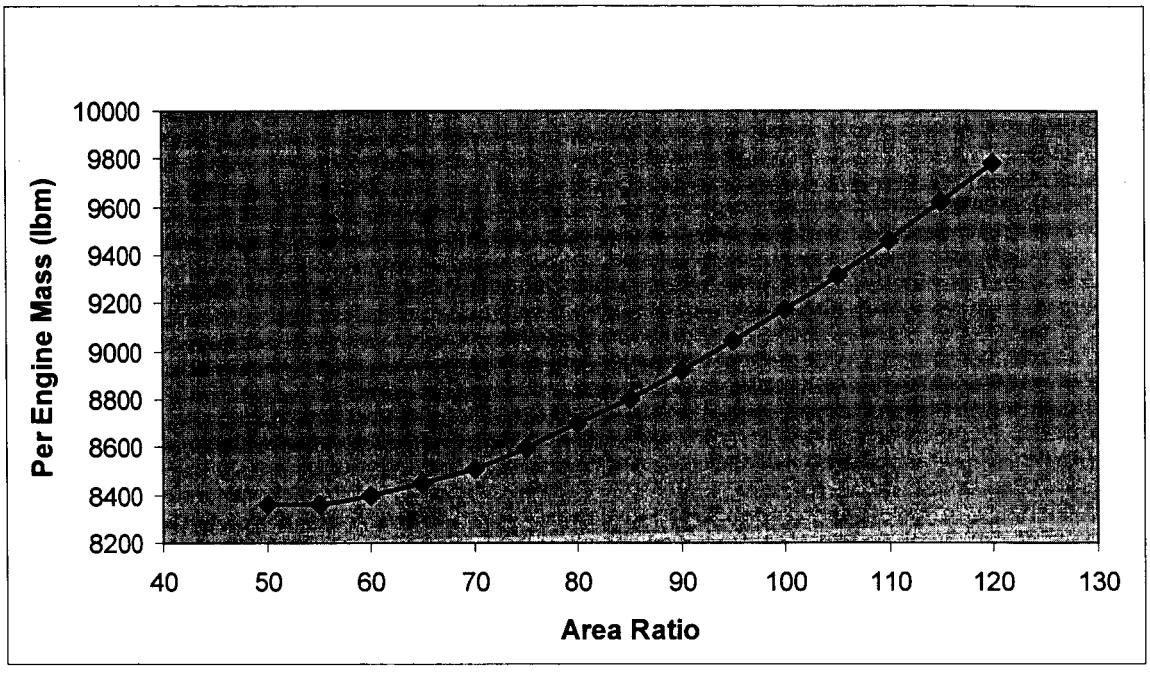

Figure 4.10 Area Ratio Versus Engine Mass [case 2]

4.2 SSME Comparison Case

The SSME comparison case involves optimization where the total thrust level is in the SSME range of T_{vac} equal to 500,000 lbf. The optimized cases are shown below in Tables 4.11 to 4.13. The tables relate the *OF* Ratio, *AR*, and P_c that correspond the SSTO case where the SSME thrust level is used. The error percentages are given for the *GLOW* minimization using an engine T_{vac} of 500,000 lbf as compared to the SSME design case.

The key comparison focuses on how the models optimum values for P_c, *AR* and *OF* Ratio differ from the actual design values for the SSME. The optimizer defined P_c is 2250 psi, where the SSME is designed to 3141 psi. This also manifests itself in a higher

throat area due to the direct correlation between P_c and A* in calculating the engine thrust level. The *OF* Ratio and *AR* are approximately 10% higher than the SSME case leading to the conclusion that the *OF* Ratio should be higher to achieve optimum *GLOW* minimization. The optimum engine *OF* Ratio is equal to 6.63. This value is consistent with the historical desire to have the shuttle system initial *OF* Ratio set to 6.5, instead of the 6.0 to which it is currently designed. The engine should also be designed to an area ratio of 86.7, which is more in the range of the RD-0120's *AR* of 85.7.

Table 4.11 SSME Comparison Results

PARAMETER	GLOW with SSME Thrust Level Minimization Parameters	GLOW Minimization SSME Thrust, Pc,OF,AR	GLOW Cases % Difference
GLOW	4,798,118	4,933,651	2.7%
Dry Weight	450,979	473,894	4.8%
GLOW + Dry Wt	5,249,097	5,407,545	2.9%
Dry Weight with margin	487,730	512,511	4.8%
DDT&E	$41.475	$41.355	-0.3%
Production Costs	$128.648	$131.461	2.1%
Operations Costs	$230.634	$250.427	7.9%
LCC	$400.757	$423.242	5.3%
Thrust to Weight Ratio	1.57	1.63	
ENGINE			
Chamber Pressure	2243.0	3141.0	28.6%
OF Ratio	6.63	6.00	-10.4%
Area Ratio	86.7	77.0	-12.6%
Mass Ratio	7.6	7.5	-1.5%
Throat Diameter	12.2	10.1	-20.5%
Vacuum ISP	445	446	0.2%
Per Engine Vacuum Thrust	520,340	491,460	-5.9%
Per Engine Weight	10,238	10,929	6.3%
Number of Engines	15	17	11.8%
TECHNOLOGY			
Wing Technology Factor	2	1	
Tail Technology Factor	2	2	
LH2 Tank Technology Factor	2	2	
LOX Tank Technology Factor	2	2	
Basic Structure Technology Factor	2	2	
Thrust Structure Technology Factor	2	2	
TPS Technology Factor	2	2	
Gear Technology Factor	2	2	
Engine Accessories technology Factor	2	2	
MPS Technology Factor	2	2	
Engine Technology Factor	2	2	
Flight Autonamoy	2	1	

Table 4.12 *OF* Ratio Effects for SSME Optimization

Avg O/F Ratio	Dry Wt	ISPvac	GLOW	Highest ISP Lowest Dry Wt Lowest GLOW Real ISPVac	OF Ratio 5.2 7.2 6.7 Avg O/F Ratio
5	508717.49	467.56	5251002.53	448.86	5
5.2	495339.35	467.63	5126176.74	448.93	5.2
5.3	490518.07	467.61	5082446.99	448.91	5.3
5.4	486074.98	467.55	5043130.23	448.85	5.4
5.6	478218.01	467.32	4976567.44	448.62	5.6
5.8	471156.79	466.94	4917536.97	448.26	5.8
6	466052.58	466.43	4885831.63	447.77	6
6.2	461072.87	465.78	4852151.39	447.15	6.2
6.3	459131.70	465.41	4843051.71	446.79	6.3
6.4	457407.15	465.00	4836725.08	446.40	6.4
6.5	455893.40	464.56	4833139.12	445.98	6.5
6.6	454580.48	464.09	4832226.70	445.52	6.6
6.7	453073.48	463.58	4827268.40	445.04	6.7
6.8	452118.45	463.04	4831006.76	444.51	6.8
6.9	451463.54	462.45	4839260.69	443.96	6.9
7	450517.23	461.83	4841894.09	443.36	7
7.1	450225.76	461.17	4855226.65	442.73	7.1
7.2	450204.27	460.47	4872687.20	442.05	7.2
7.3	450312.53	459.71	4891911.22	441.33	7.3
7.4	450329.37	458.91	4908993.51	440.55	7.4
7.5	451020.41	458.04	4937388.20	439.72	7.5
7.6	452033.40	457.10	4970993.60	438.81	7.6
7.7	453049.01	456.06	5004065.98	437.82	7.7
7.8	454990.62	454.91	5053042.01	436.71	7.8
7.9	460652.21	453.54	5141410.65	435.40	7.9
8	464125.13	451.86	5217232.24	433.79	8

Table 4.13 *OF* Ratio Versus Propellant Density and Weight for SSME Case

OF Ratio	Density	LOX Wt	H2 Wt	Total Wt	Wt %
5	20.15	3792557.24	758,511	4,551,069	8.50%
5.2	20.62	3726096.94	716,557	4,442,654	5.91%
5.3	20.86	3705646.64	699,179	4,404,825	5.01%
5.4	21.09	3687977.31	682,959	4,370,936	4.20%
5.6	21.55	3660312.40	653,627	4,313,940	2.85%
5.8	22.00	3636513.15	626,985	4,263,498	1.64%
6	22.44	3632472.47	605,412	4,237,885	1.03%
6.2	22.88	3625429.96	584,747	4,210,177	0.37%
6.3	23.09	3627559.19	575,803	4,203,362	0.21%
6.4	23.30	3631608.26	567,439	4,199,047	0.11%
6.5	23.51	3637578.27	559,627	4,197,206	0.06%
6.6	23.72	3645443.14	552,340	4,197,783	0.08%
6.7	**23.93**	**3649826.15**	**544,750**	**4,194,576**	**0.00%**
6.8	24.13	3660973.01	538,378	4,199,351	0.11%
6.9	24.34	3675565.01	532,691	4,208,256	0.33%
7	24.54	3685436.70	526,491	4,211,928	0.41%
7.1	24.74	3703786.57	521,660	4,225,447	0.74%
7.2	24.94	3725337.34	517,408	4,242,745	1.15%
7.3	25.13	3748191.48	513,451	4,261,642	1.60%
7.4	25.33	3769175.54	509,348	4,278,524	2.00%
7.5	25.52	3799267.61	506,569	4,305,837	2.65%
7.6	25.71	3833530.06	504,412	4,337,942	3.42%
7.7	25.90	3867273.58	502,243	4,369,517	4.17%
7.8	26.09	3913988.75	501,793	4,415,782	5.27%
7.9	26.28	3991565.36	505,261	4,496,827	7.21%
8	26.46	4060378.04	507,547	4,567,925	8.90%

4.3 Vehicle Model Uncertainty

There are two areas that uncertainty values apply in the model. The first is the DDTE cost uncertainty and the second is the uncertainty in the vehicle weight. The DDTE cost uncertainty is approached in two parts. The first is the weight of the components that directly feeds the NAFCOM regression curves and the other are the NAFCOM regression curves. The component weight distributions will be used for both the uncertainty in weight and uncertainty in the DDTE cost since weight is the basis for the cost curves.

4.3.2 DDTE Cost Uncertainty

Weight regression curves were used to define the *SE*, μ, and σ for the vehicle components shown in Table 4.14. This data is based upon historical data gathered from previously designed systems and is not linked to any of the NAFCOM Cost model data. The high and low values for the power series regression curve fits are defined along with the corresponding Lognormal parameters necessary to formulate the distributions. The table data reflects the parameters used in the @Risk tool runs that exercise the Monte Carlo simulations.

The weight only portion of the overall DDTE cost uncertainty represents the first part of the total uncertainty in cost. This portion is dedicated to the uncertainty in the weight of the vehicle components. Figures in Appendix D show the @Risk outputs for the Lognormal distributions for each component weight. The second component of the uncertainty due to the regression errors is defined using the NAFCOM historical

data/curve fits. The SEs for the NAFCOM regression fits are not shown herein but are combined with the data from the weight distribution curves to define a total uncertainty distribution for the projected cost of the vehicle.

Table 4.14 Numerical Uncertainty for Vehicle Dry Weight

	(Weight Regression)		SE	Mean	Sigma	LogNor
Wing	-0.17	0.2	0.14256	1.07388	0.14475	1.07388
Tail	-0.29	0.2	0.17237	1.09001	0.17625	1.09001
LH2 Tank	-0.18	0.41	0.16922	1.08829	0.17289	1.08829
LOX Tank	-0.51	0.49	0.31036	1.16787	0.33368	1.16787
Overall Body	-0.36	0.64	0.30752	1.16621	0.33018	1.16621
Thrust Stucture	-0.56	0.42	0.33138	1.18020	0.35991	1.18020
Landing Gear	-0.18	0.25	0.13930	1.07213	0.14134	1.07213
Propulsion	-0.056	0.29	0.33225	1.18072	0.36102	1.18072
TPS	-0.25	0.25	0.19875	1.10448	0.20473	1.10448

The uncertainty in the DDTE cost is computed by taking each of the component cost equations and multiplying the weight by the uncertainty in weight and the overall cost equation by the uncertainty in the NAFCOM regression curve. Equations (4.1) to (4.3) below are an explanation of the DDTE cost uncertainty and show how the Lognormal distributions for weight uncertainty (Wt_{unc}) and NAFCOM uncertainty ($NAFCOM_{unc}$) will be exercised as a multiplier of the terms in order to determine the total uncertainty in the cost number for a specified component (Wing, Tail, Tanks, etc.),

$$Wing_{unc} = CIF * CompFactor * A * Wt_{wing}^{\ B}, \qquad (4.1)$$

$$Wt_{wing} = Wt * Wt_{unc}, \qquad (4.2)$$

and

$$A * Wt_{wing}^{\ B} = A * Wt^{B} * NAFCOM_{unc}. \qquad (4.3)$$

The total DDTE cost uncertainty was defined by operating 10,000 Monte Carlo runs in @Risk using the distributions defined in Appendix D, along with the NAFCOM Lognormal distributions that result from the SE's of the components that make up the vehicle. The total uncertainty is defined in the range shown here in Figure 4.11. The sensitivity of the individual components that make up the total uncertainty is shown in Figure 4.12. The maximum and minimum values for uncertainty are presented here based upon the 95th percentile case. The absolute minimum and maximum values are decidedly outside the bounds of acceptable engineering estimates. This is the benefit of using the 95th percentile case to describe the bounds of the DDTE cost uncertainty. The total cost distribution is shown in Table 4.15. The data in Table 4.15 defines and lower and upper values of uncertainty at –45% to 76% of the mean value of DDTE cost, which is 37.22 $B. The results show that there is a significant level of uncertainty in the cost based upon the uncertainty in component weights and upon the NAFCOM uncertainty.

Table 4.15 Total DDTE Cost Uncertainty

Parameter	Low Range (5%)	High Range (95%)
DDTE Cost ($B)	22.92785	76.9315

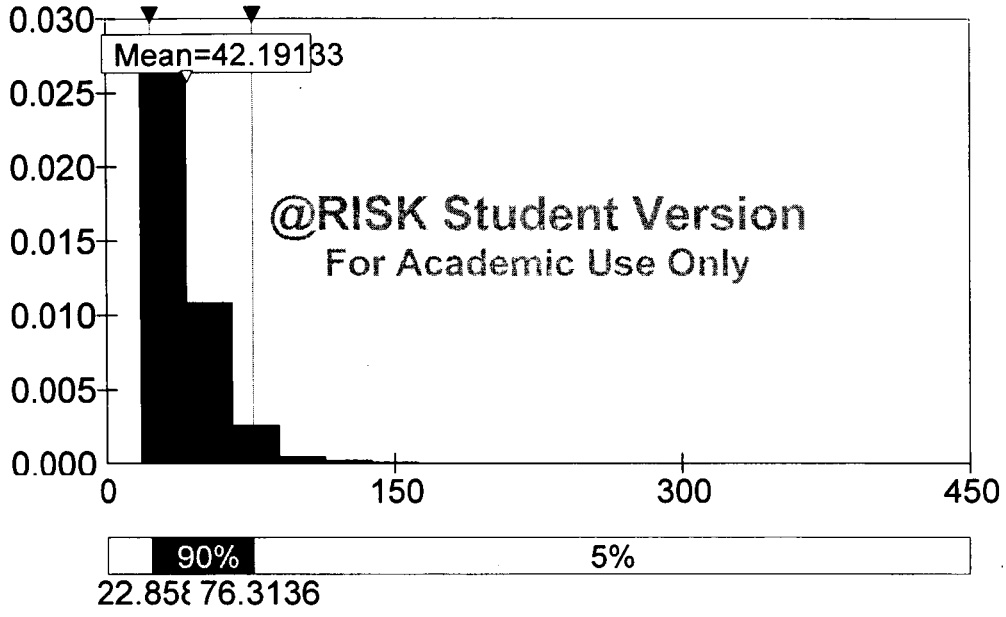

Figure 4.11 DDTE Cost Distribution

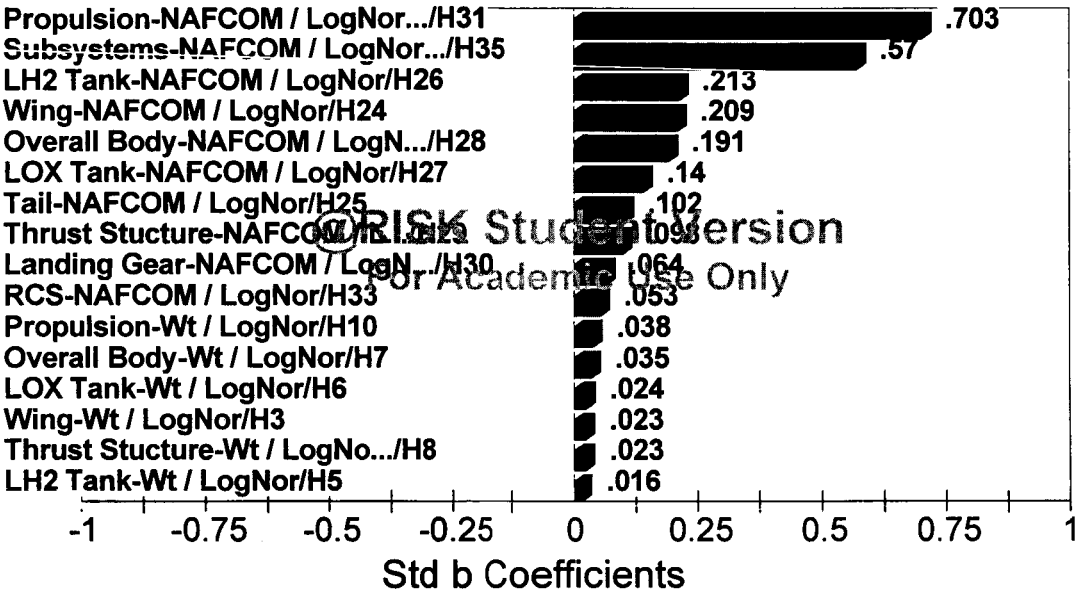

Figure 4.12 Cost Regression Sensitivity

4.3.3 Vehicle Weight Uncertainty

The vehicle Dry Weight and *GLOW* uncertainty is determined using the lognormal distributions defined in Appendix D. In a similar manner as defined in the previous section, the distributions are developed for each of the components in Table 4.1. The SE is calculated using the power series regression curves defined in Figures 3.7 to 3.15 and applying equation (3.8). The μ, and σ are measured using the relationships defined in equations (3.9 and 3.10).

Taking each of the component weights and multiplying the weight by the uncertainty in weight computes the uncertainty vehicle weight. Equation (4.4) below is an example of the component weight uncertainty and will be used in order to determine the total uncertainty in the weight for a specified component (Wing, Tail, Tanks, etc.),

$$Wing_{unc} = Wt_{wing} * Wt_{unc}. \tag{4.4}$$

The uncertainty in Dry Weight and *GLOW* was defined by operating 10000 Monte Carlo runs in @Risk using the distributions defined in Appendix D. The total uncertainty is defined in the range shown here in Figure 4.13 for the Dry Weight and Figure 4.14 for the *GLOW*. The sensitivity of the individual components that make up the total uncertainty is shown in Figure 4.15 for Dry Weight and Figure 4.16 for *GLOW*. The maximum and minimum values for uncertainty are presented here based upon the 95^{th} percentile case. The absolute minimum and maximum values are decidedly outside the bounds of acceptable engineering estimates. This is the benefit of using the

95th percentile case to describe the bounds of the uncertainty. The total weight distribution is shown in Table 4.16. The data in Table 4.16 defines and lower and upper values of uncertainty for Dry Weight and *GLOW*. The results show that there is a significant level of uncertainty based upon the uncertainty in component weights.

Table 4.16 Total Weight Uncertainty

Parameter	Low Range (5%)	High Range (95%)
Dry Weight (lbm)	404,623	814,943
GLOW (lbn)	4,623,785	8,684,903

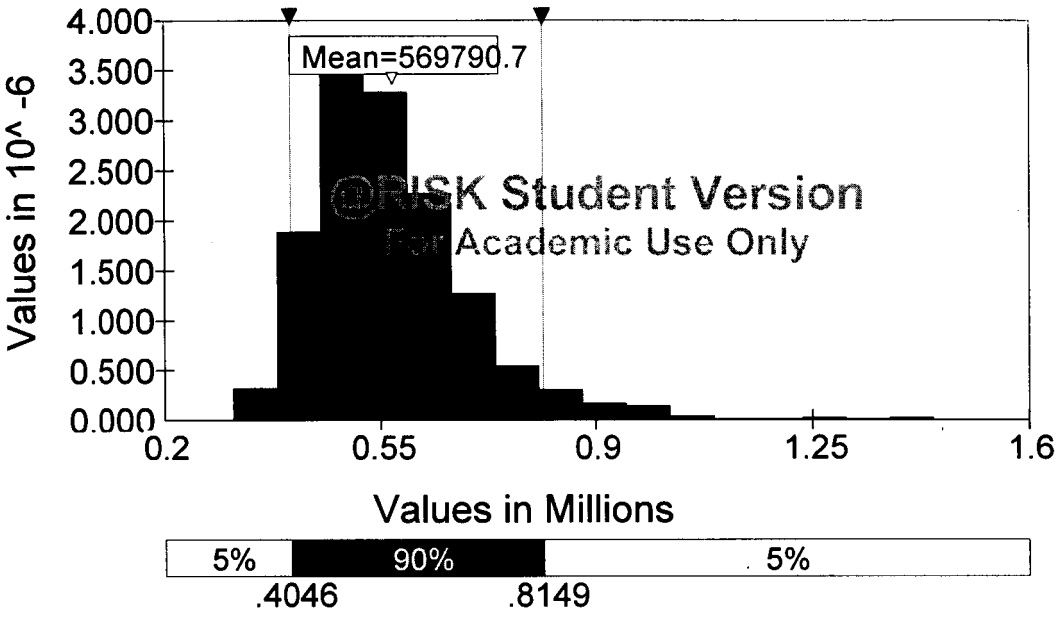

Figure 4.13 Dry Weight Distribution

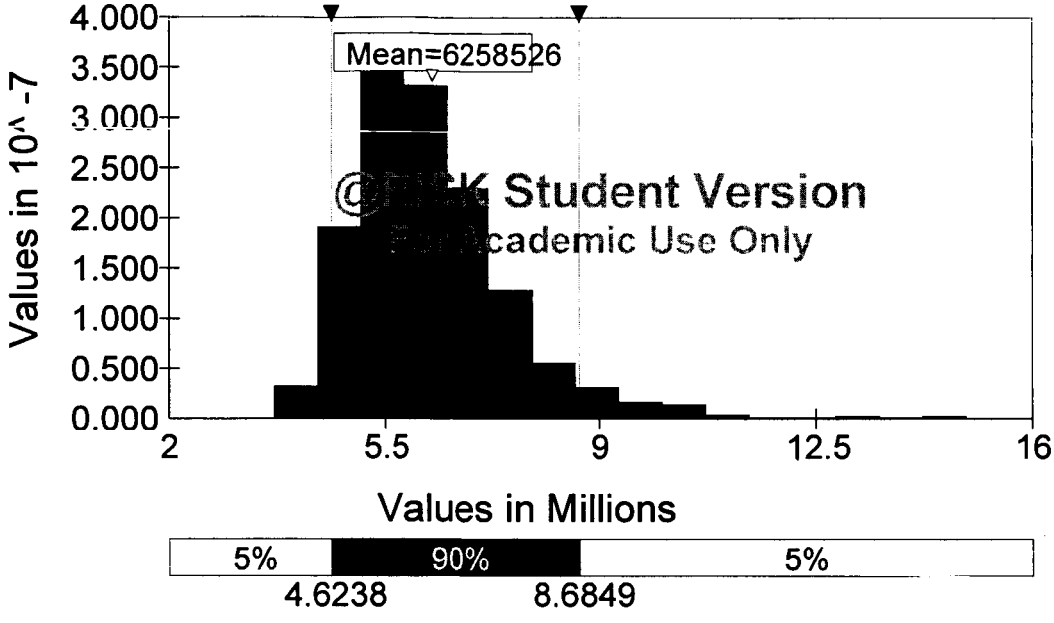

Figure 4.14 *GLOW* Distribution

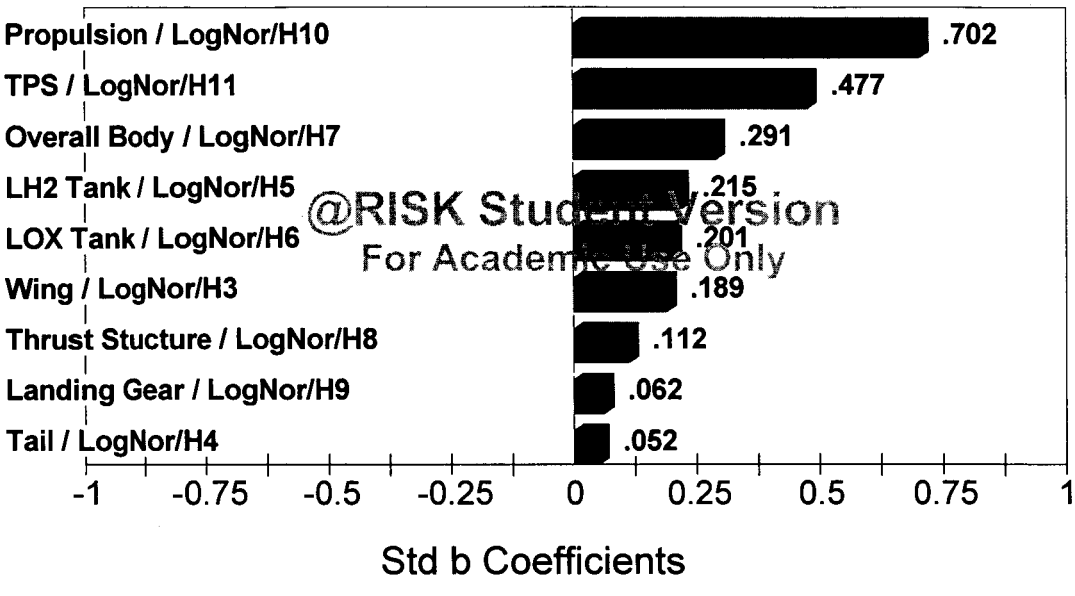

Figure 4.15 Dry Weight Regression Sensitivity

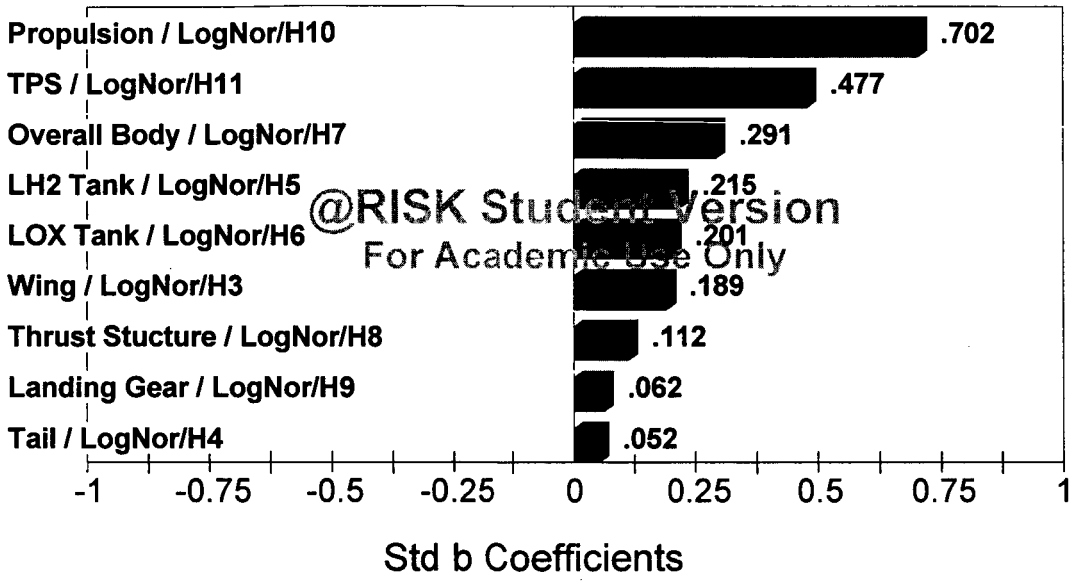

Figure 4.16 *GLOW* Regression Sensitivity

CHAPTER 5

CONCLUSIONS

Using the Cequel code for thermo-chemical outputs, by inputting P_c, AR and OF Ratio, provided a methodology that has not been used in previously designed tools attempting to optimize a closed loop system. The Cequel output and input structure designed in the cell linkages proved that a true closed loop system produces the results in a significantly more efficient way. The alternatives to integrating thermo-chemical results into the model are to use databases and extrapolate the results for a given input condition.

A key aspect of the model was the method to determine engine mass based upon parameters of the system or propulsion variables produced in the design process. Design synthesis of the proposed propulsion parameters and the goodness of the engine mass models led to the optimum design being chosen that closely matches the theoretical optimum vehicle. The engine mass modeling approach is open to updates based upon any new and/or improved methods to estimate the mass using design parameters. The ability to have the engine mass, parameters used to determine engine mass, and the vehicle weight and cost integrated together in an optimized fashion is the essence of CLO. The model outputs are only as good as the data being used to formulate the model. This point must not be overlooked and an emphasis must be made toward higher fidelity modeling in future efforts where CLO is attempted.

The integrated model output defined that the *GLOW* and Dry Weight was 67% higher for the DDTE cost minimization case when compared to the weights determined from the minimization of *GLOW* case. This is driven by the nature of the parameters tendency toward making the optimized value in each case as small as possible. In a likewise manner, the DDTE cost was 53% higher using the *GLOW* minimization case when compared to the case for minimization of the DDTE cost. Again, this was an expected result due to the higher cost for the case where weight is being optimized. These variables provide valuable insight into program management trades where cost and vehicle weight are involved.

The uncertainty of the model results is defined using the Lognormal distributions based upon the power series regression curves and SE values for each component weight and SE values for the NAFCOM regression curves. By using the Lognormal distributions, the data being used in the Monte Carlo runs was significantly more accurate than a Triangular distribution or Normal distribution. This was true because the Lognormal curves represent the log space distribution of the power curve data that is plotted on logarithmic scale axis. The model output for DDTE cost uncertainty was approximately 76% for the 95^{th} percentile upper limit. According to feedback from NASA and Academia experts, this closely matches the 80% value used for program planning purposes. The Dry Weight uncertainty output reflected a 95^{th} percentile uncertainty upper range that was +90.2% above the model output for Dry Weight minimization (428,123 lbs). Likewise, the *GLOW* uncertainty output had a value of 81.3% above the model output for *GLOW* minimization (4,635,904 lbs).

The model output for the core propulsion parameters was a significant result of the optimization effort. The chamber pressures for the best *GLOW* and Dry Weight are 2712.8 and 2464.9 psi respectively that compares to 2994 psi for the Block II SSME. The likelihood of these optimized values being the true optimized value can be clarified by further efforts in engine mass studies and engine reliability studies. Engine reliability is an important aspect of the engine modeling approach but was not included in this optimization approach.

The *AR* for optimum engine design, for the minimization of Dry Weight [case 2], was 86.7 and is almost identical to the Russian RD-0120 engine *AR* value of 85.7. These results, along with the fact of close correlation with the SSME and RD-0120, show that the model's optimum value for *AR* was close to the true optimum value. The conclusion can be drawn that the *AR* for SSTO systems should be slightly higher than the SSME and significantly higher than the 1st stage engines used in expendable launch vehicles.

The *OF* Ratio was the most sensitive component of the propulsion parameters due to its overwhelming impact on the propellant weight and tank volume. This was due to propellant mass, which was significant to the *GLOW,* and the propellant volume, which was significant to the Dry Weight. The optimum *OF* Ratio for *GLOW* minimization was found by considering the *GLOW* for the launch vehicle. The *GLOW* was most impacted by the propellant weight. Another driving force behind the *OF* Ratio was that the maximum specific impulse occurs at the ratio of 5.2. Using these driving factors, the

optimum *OF* Ratio for fuel weight was defined 6.87 for the *GLOW* optimization case involving the engine with T_{vac} equal to 800,000. The optimum *OF* Ratio for the SSME thrust level of 500,000 lbf was defined at 6.63.

The importance of the TFs and CIFs cannot be underestimated in determining the optimum system with respect to cost and weight. The base technology represented by the Boolean code one (1) does not improve the optimum system weight but does make the system cheaper to design and test. The technology improvements and weight savings represented by Boolean codes two (2) and three (3) are significant weight reducers but do increase the overall DDTE cost. The interesting result is the variability amongst the TFs for the optimum production, operations and life cycle cost cases. The CIFs have no direct impact on these cost cases. Their only influence is with the input weights and DDTE cost provided by the model components. A comparison of the optimization cases shows that system tradeoffs can be made to improve the cost of the system at the expense of vehicle weight. This was also true for the reverse. The improvement in overall vehicle weight resulted in significant increases in the cost of the system. The key component of trading cost and weight proved to be the technology and cost influence factors resulting from the inclusion of new technologies. The engine design parameters have some impact on the overall system optimization, but the effects are minimal in comparison to the technology factors.

4.3 Recommendations for Future Work

The *OF* Ratio, at the initial phase of flight, should be increased to a higher level than current engines are designed for. As a result, future work should be done to understand the incremental impacts of adjustable *OF* Ratio on the system. For the Shuttle–like system, the *OF* Ratio should be around 6.63 at the beginning of flight and should be reduced to a lower level at some point later in flight to a level near 5.2.

The parametric data used to develop the weights and cost models should be continually updated to add more fidelity in these areas. The model accuracy will increase significantly as the uncertainty in these regressions curve fits is defined and minimized. Also efforts to improve the extrapolation of technology factors onto future systems will enable the concept model to have improved minimization multiples for weight savings and cost influence factors that result from the technology funding required to develop a new material or method within the program.

APPENDICES

APPENDIX A

NUMERICAL UNCERTAINTY TABLES

Table A.1 Numerical Uncertainty for Vehicle Dry Weight

	Dry Wt 393,321 lbs			[Gross Wt (x+dx)-Gross Wt(x)]/dx					
	Baseline Weight (lbs)	Baseline + 10 lbs	New LVSS Wt 10	dWt/dx 10	dWt/dx^2	Table Data (Ux)	Ux*(x lbs)	Ux*(x lbs)^2	Component Uncertainty
Wing	49,764	49,774	393,342	2.003	4.011	0.2	9953	99059007	397303268
Tail	10,959	10,969	393,344	2.293	5.259	0.29	3178	10101162	53126223
LH Tank	38,303	38,313	393,342	2.012	4.050	0.41	15704	246520487	998814982
LOX Tank	18,064	18,074	393,343	2.182	4.762	0.51	9213	84872984	404167519
Body	45,082	45,092	393,346	2.405	5.782	0.64	28852	832462061	4813257116
Gear	15,390	15,400	393,344	2.220	4.928	0.28	4309	18568892	91514260
Thrust Structure	9,838	9,848	393,344	2.266	5.132	0.56	5509	30349693	155769781
TPS	82,074	82,084	393,340	1.810	3.274	0.5	41037	1684049285	5514277348
Propulsion	86,141	86,151	393,339	1.710	2.924	0.5	43071	1855079534	5425023386
Subsystems	32,473	32,483	393,345	2.382	5.673	0.5	16237	263623932	1495447845

Total Uncertainty	139,100	lbs
% Uncertainty	35.37%	
High	532,421	lbs
Median	393,321	lbs
Low	254,222	lbs

Table A.2 Numerical Uncertainty for Vehicle Dry Weight (Factors =1)

	Dry Wt (lbs) 339,302.18 lbs Baseline Weight (lbs)	Baseline + 10 lbs	New LVSS Wt 10		[Gross Wt (x+dx)-Gross Wt(x)]/dx dWt/dx 10	dWt/dx^2	Table Data (Ux)	Ux*(x lbs)	(Ux*x lbs)^2	Component Uncertainty
Wing	22,031	22,041	339,323		2.04	4.15	0.20	4,406	19,415,306	80,536,607
Tail	10,628	10,638	339,324		2.14	4.57	0.29	3,082	9,499,855	43,439,286
LH Tank	34,780	34,790	339,321		1.85	3.43	0.41	14,260	203,337,859	697,966,325
LOX Tank	16,048	16,058	339,323		2.05	4.19	0.51	8,184	66,984,748	280,693,261
Body	44,331	44,341	339,324		2.22	4.92	0.64	28,372	804,944,565	3,956,794,995
Gear	13,431	13,441	339,323		2.05	4.21	0.28	3,761	14,143,485	59,608,275
Thrust Structure	8,672	8,682	339,323		2.12	4.48	0.56	4,856	23,584,910	105,590,784
TPS	75,793	75,803	339,320		1.76	3.08	0.50	37,896	1,436,141,899	4,424,964,088
Propulsion	76,502	76,512	339,324		2.22	4.92	0.50	38,251	1,463,141,027	7,192,200,368
Subsystems	32,473	32,483	339,324		2.22	4.92	0.50	16,237	263,623,932	1,295,872,909

Total Uncertainty	134676	lbs
% Uncertainty	39.69%	
High	473978	lbs
Median	339302	lbs
Low	204626	lbs

APPENDIX B

DRY WEIGHT MINIMIZATION WORKSHEET LAYOUTS FOR MODEL COMPONENTS

	B	C	D
2	**Input Variables**		**Input**
3	Mass Ratio	MassRatio	8.0161
4	Liftoff Thrust to Weight	TWi	1.4007
5	Area Ratio of Fixed Bell Nozzle	AreaRatio1	87.5325
6	Initial Area Ratio of Extendable Bell Nozzle	AreaRatio2Init	87.5325
7	Final Area Ratio of Extendable Bell Nozzle	AreaRatio2Final	87.5325
8	Ratio of Total Thrust provided by Fixed Nozzles	ThrustRatio	1.0000
9	Payload Weight	PayloadWt	65,000
10	OMS Maneuvers Delta-V	OMSDeltaV	650
11	RCS Maneuvers Delta V	RCSDeltaV	100
12	OMS Isp	OMSIsp	440
13	RCS Isp	RCSIsp	390
14	Wing Technology Factor	WingTF	0.724
15	Tail Technology Factor	TailTF	0.842
16	LH2 Tank Technology Factor	LH2_TF	0.750
17	LOX Tank Technology Factor	LOX_TF	0.700
18	Basic Structure Technology Factor	BasicStructTF	0.700
19	Thrust Structure Technology Factor	ThrStructTF	0.740
20	TPS Technology Factor	TPS_TF	0.667
21	Gear Technology Factor	GearTF	0.781
22	Engine Accessories technology Factor	EngAccTF	0.891
23	MPS Technology Factor	MPS_TF	0.510
24	Engine Technology Factor	Eng_TF	0.782
25	RCS Technology Factor	RCS_TF	0.497
26	OMS Technology Factor	OMS_TF	0.346
27	Number of Engines 1	No_Engine1	10.000
28	Number of Engines 2	No_Engine2	0.000
29	Number of Engines Total	No_Engine	10.000
30	Chamber Pressure	Pc	2464.887
31	O/F Ratio	OF	7.429
32	Time to Orbit	Time	315.500

Figure B.1 LVSS Input Variables (Dry Weight Minimization Case)

Outputs:		Value
Vehicle Gross Weight	GLOW	4,848,013
Vehicle Dry Weight (no margin)	DryWt	428,123
Vehicle Dry Weight with Margin	DryWtWithMargin	463,011
Vehicle Ascent LOX Weight	LOXWt	3,739,830
Vehicle Ascent LH2 Weight	LH2Wt	503,395
Vehicle OMS/RCS Propellant	OMSRCSPropWt	30,529
1.0 Wing	WingWt	53,728
2.0 Tail	TailWt	12,446
3.0 Body	BodyWt	125,955
Basic structure	BasicWt	45,082
LH2 tank	LHTankWt	45,407
LO2 tank	LOTankWt	23,463
Thrust Structure	ThrustStrWt	12,003
4.0 Induced environment protection	TPSWt	93,226
5.0 Undercarriage and aux. systems	GearWt	16,679
Engine accessories	EngineAccWt	4,796
Propellant System	PropSysWt	13,958
7.0 Propulsion, reaction control (RCS)	RCSWt	3,288
8.0 Propulsion, orbital maneuver (OMS)	OMSWt	2,350
9.0 Prime power	PowerWt	3,690
10.0 Electric conversion and distr.	ElecWt	6,560
11.0 Hydraulic conversion and distr.	HydWt	6,400
12.0 Control surface actuation	ActuationWt	5,458
13.0 Avionics	AvionicsWt	4,622
14.0 Environmental control	EnvirWt	4,048
15.0 Personnel provisions	PersonnelWt	1,100
18.0 Payload provisions	PayloadProvWt	595
6.3 Engines	EngineWt	69,224
Engine Weight 1	Engine1Wt	88,510
Engine Weight 2	Engine2Wt	0
Vehicle Landed Weight	LandWt	540,083
Vehicle LOX	LOXWt	3,739,830
Vehicle LH	LHWt	503,395
Maximum Length	MaxLength	271
Maximum Width	MaxWidth	213
Wing Wetted Area	WingWetArea	13,759
Tail Wetted Area	TailWetArea	4,935
Body Wetted Area	BodyWetArea	30,424
Fixed Nozzle Isp vacuum	Isp1vac	440.7
Initial Extendable Nozzle Isp vacuum	Isp2Initvac	440.7
Final Extendable Nozzle Isp vacuum	Isp2Finalvac	440.7
Throat Area	D*	13.4
ISPsl	ISPsl	422.7
Vac Thrust per engine	Vac Thrust per engine	707828.7
SL Thrust per engine	SL Thrust per engine	679062.9

Figure B.2 LVSS Output Variables (Dry Weight Minimization Case)

Propellant Model		Drawn		Sized			
Body Volume	256,782		231227	256782.1072			
Payload Volume	10603						
Tank efficiency factor	0.7000						
Tank Volume	172326						
Ullage Volume Fraction	0.03						
Fluid volume	167156	check		check		6	20
LH2 Volume	114408		213739	1.46105153	121802.2002	74583.72612	
LOX Volume	52748						
LH2 Weight	503395						
LOX Weight	3739830						
Total Propellant Weight	4243225						
Ascent LH2	503395						
Ascent LOX	3739830						
Ascent LH2 + LOX weight	4243225						
Propellants							
Fuel	LH2		SOA	Ref			
LH2 density (lb./cu. ft.)	4.4		4.4	4.8			
LOX density (lb./cu. ft.)	70.9		70.9	81.57			
LOX/LH2 mixture ratio	7.4292167		6	7			
Propellant Density	25.38						

Figure B.3 LVSS Propellant Model (Dry Weight Minimization Case)

Rubber Engine Assumption	Engine 1
Astar = Anozzle/Athroat	87.5324806
Thrust sl	6790629.2
Thrust, vacuum	7078287.4
Isp, vacuum	440.7
Wdot	16063.1
Wnozzle-ext	3075.904489
Wnozzle-act	1291.371336
Wb	75978.60667
Wpr,fd	9477.246946
Wtotal	98408.71222
Per Engine	9840.871222
Tv/W	719.3
Ts/W	690.0
Number of Engines	10

Gross Wt
4,848,013
Dry Weight
428,123

Figure B.4 LVSS Engine Weight Page 1 (Dry Weight Minimization Case)

ENGINE WEIGHT ESTIMATORS

	Air Force
	Engine 1
Nozzle Assembly	2610.59
Turbomachinery	3055.34
Preburner	84.61
Lines,Valves,Ducts	3801.14
Total	9551.69
Set 1 &2	95516.87
Total Eng Wt	**95,516.9**

	Thrust Level/Weight
Engine 1	11922.57775
Engine 2	#DIV/0!
Set 1	119225.7775
Set 2	#DIV/0!
Total Eng Wt	**119,225.8**

	Power Balance
Engine 1	8027.94
Engine 2	#DIV/0!
Set 1	80279.43
Set 2	#DIV/0!
Total Eng Wt	**80,279.4**

	Pc*OF*AR
	1602910.707
Engine Weight 1	7983.578544
Set Weight	**79,835.8**

	Langley Total
Set Weight	**98,408.7**

	Combined Approach
Engine Weight	**88,510.2**

Figure B.5 LVSS Engine Weight Page 2 (Dry Weight Minimization Case)

Chamber Pressure 2464.887303	O/F Ratio 7.429216694	Chamber Pressure **2464.887303**	O/F Ratio **7.42921669**
Temp (deg R)	2906.02	2906.02	2906.02
Me	4.41	4.41	4.41
Aratio	87.53	87.53	87.53
Cstar (ft/sec)	7259	7259	7259
Cf	1.9519	1.9519	1.9519
ISPvac (sec)	459.01	459.01	459.01
ISP (sec)	440.36	440.36	440.36
$Thrust_{sl}$ (lbs)	679,062.92	#DIV/0!	#DIV/0!
$Thrust_{vacuum}$ (lbs)	707,828.74	#DIV/0!	#DIV/0!
Real ISP_{vacuum} (sec)	440.65	440.65	440.65
Real ISP_{sl} (sec)	422.75	422.75	422.75
%eff ISP	96.00%	96.00%	96.00%
Throat $Area_{sl}$ (in2)	141.14	#DIV/0!	#DIV/0!
Throat $Diameter_{sl}$(in)	13.41	#DIV/0!	#DIV/0!
$Area_{Exit}$ (in2)	12,354.29	#DIV/0!	#DIV/0!
$Diameter_{Exit}$ (in)	125.45	#DIV/0!	#DIV/0!

Figure B.6 LVSS Propulsion Module (Dry Weight Minimization Case)

Component Weights				
			Max Length	271.32
Old Gross		4848013	Max Width	213.29
			structural span (one side)	124.50
			exposed wing area	6615.01
			landing weight w/payload	540083
			load factor	2.5
			Safety factor	1.5
			root thickness	5.362
			alpha	311.0879
			Wing Technology factor	0.7240
1.0 Wing	53,728			
			tail area	2372
			Tail Technology factor	0.8422
2.0 Tail	12,446			
			LH2 tank volume	114408
			LH2 Technology factor	0.7500
LH2 tank		45407		
			LOX tank volume	52748
			LOX Technology factor	0.7000
LO2 tank		23463		
			Structural wetted area	14567
			Basic Technology factor	0.7000
Basic structure		45082		
			Total Thrust	6790629
			Thrust Str. Technology fact	0.7400
Thrust Structure		12003		
3.0 Body	125,955			
			Body Wetted Area	30424
			Wing wetted area	13759
			Tail Wetted Area	4935
			TPS integrated unit weight	2.85
			TPS Technology factor	0.6670
4.0 Induced environment protection	93,226			
			Max Landed weight	540083
			L. Gear Technology factor	0.7811
5.0 Undercarriage and aux. systems	16,679			

Figure B.7 LVSS Vehicle Weight Equations Page 1 (Dry Weight Case)

6.1 Engine accessories		4796		
			Total thrust lb	6790629
			Isp, sec	423
			Propellant density flow rate,	16063
			MPS Technology factor	0.5096
6.2 Propellant System		13958		
			Engine 1	88510
			Engine 2	0
			Engine Technology Factor 1	0.7821
			Engine Technology Factor 2	0.7821
			Engine Weight 1	69224
			Engine Weight 2	0
6.3 Engines		69224		
6.0 Propulsion, main	87,978			
			Landing weight with payloac	540083.4
			Technology Factor	0.4965291
7.0 Propulsion, reaction control (RCS)	3,288			
			Landing weight with payloac	540083.4
			Technology Factor	0.3464797
8.0 Propulsion, orbital maneuver (OMS)	2,350			
9.0 Prime power	3,690			
10.0 Electric conversion and distr.	6,560			
11.0 Hydraulic conversion and distr.	6,400			
12.0 Control surface actuation	5,458			
13.0 Avionics	4,622			
14.0 Environmental control	4,048			
15.0 Personnel provisions	1,100			
18.0 Payload provisions	595			
Dry Weight	428,123			
			growth allowance fraction	0.08149
19.0 Growth allowance	34,888			
Total dry weight w/margin	463,011			
20.0 Personnel	2,644			
			Fraction of propellant	0.00222
23.0 Residual and unusable fluids	9,429			
Landing Weight	475,083			

Figure B.8 LVSS Vehicle Weight Equations Page 2 (Dry Weight Case)

22.0 Payload	65,000		
Landing Weight w/payload	540,083		
		Fraction of propellant	0.00413
23.0 Residual and unusable fluids	17,541		
		Fraction of propellant	0.00295
25.0 Reserve fluids	12,515		
		Fraction of propellant	0.00097
26.0 Inflight losses	4,119		
		LH2	503395
		LO2	3739830
27.0 Ascent Propellant	4,243,225		
		vac. specific impulse averag	390
		delta v req. orbit + entry	100
		gravity const (ft/sec2)	32.174
28.0 Propellant, reaction control	4,730	4,730	
		vac. specific impulse averag	440
		delta v req. orbit + entry	650
		gravity const (ft/sec2)	32.174
29.0 Propellant, orbital maneuver	25,798	25,798	
GROSS	4,848,013		

Figure B.9 LVSS Vehicle Weight Equations Page 3 (Dry Weight Case)

Payload Sizing

4,848,013	Pre launch
4,848,013	Gross
4,243,225	Ascent Propellant
8.016	Current Mass Ratio
8.016	Mass Ratio Required
0	Payload Sizing--->>Delta P/L

Photographic Sizing

Check if weight eauations have converged

TRUE	Weight Convergence

If false do not scale current vehicle

If true and Isize=2 then scale vehicle based on body volume requirements

TRUE	Scale if weight converged and isize=2
1.11052	Old Volume scale
4848013	Prelaunch gross
0	Startup propellant
4848013	Gross = Prelaunch gross - startup propellant
4243225	Ascent propellant
8.0161	Current Mass ratio
8.0161	Required Mass ratio
4,848,013	New Gross = Prelaunch gross- startup propellant
4,243,225	New Ascent Propellant
0	New Prelaunch propellant
4,243,225	New total propellant
4,848,013	New Prelaunch gross
167,156	New fluid volume
172,326	New tank volume
256,782	Body Volume required
1.1105	Volume scaling factor
1.0724	Area scaling factor
1.0356	Length scaling factor

Figure B.10 LVSS Vehicle Sizing (Dry Weight Minimization Case)

Nozzle Weight Calc Engine 1

uses surface area

data in red coming from weight tables worksheet:

Expansion Ratio	87.53			
Throat Area	141.14	in2		
Exit Area	12354.29	in2		
Radius Throat	6.703	in.		
Theta	15.0	deg,	0.262	rad
Alpha	30.0	deg,	0.524	rad
Reference Cone Length	80.0%			
R1	2.56	in.		
Xn	1.280	in.		
Rn	7.046	in.		
Exit Radius	62.710	in.		
Exit Length	167.486	in.		
Exit Divergence Angle	13.271	deg.		
Integration step size	1.658	in.		
Raa 'C' Coefficient	0.0225			
Rao 'B' Coefficient	1.415			
Rao 'A' Coefficient	-9.8051			
Total Surface Area	42106.23	in2		
Total Contour Length	177.10	in.		
Regen. Cooled Region	100.0%			
Film-Cooled Region	0.0%			
Ablative Region	0.0%			
Regen. Cooled Unit Weight	0.062	lbs/in2		
Film-Cooled Unit Weight	0.025	lbs/in2		
Ablative Unit Weight	0.082	lbs/in2		
Regen. Cooled TRF	1.00			
Film-Cooled TRF	1.00			
Ablative TRF	1.00			
Regen. Region Weight	2610.59	lbs.		
Film-Cooled Weight	0.00	lbs.		
Ablative Weight	0.00	lbs.		
Total Nozzle Weight	**2610.59**	**lbs.**		

Figure B.11 LVSS Nozzle Weight Page 1 (Dry Weight Minimization Case)

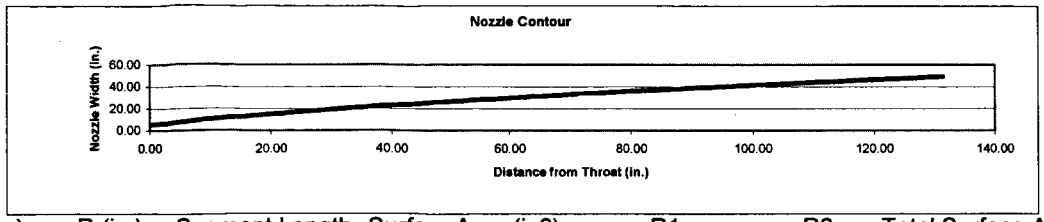

X (in.)	R (in.)	Segment Length	Surface Area (in2)	R1	R2	Total Surface Area
0.00	6.70					
1.66	7.26	1.75	73.72	7.31	7.26	73.72
3.32	8.20	1.91	87.01	#NUM!	8.20	160.73
4.97	9:12	1.90	97.72	#NUM!	9.12	258.45
6.63	10.02	1.89	108.10	#NUM!	10.02	366.55
8.29	10.90	1.88	118.18	#NUM!	10.90	484.74
9.95	11.76	1.87	127.98	#NUM!	11.76	612.72
11.61	12.61	1.86	137.53	#NUM!	12.61	750.25
13.27	13.43	1.85	146.83	#NUM!	13.43	897.08
14.92	14.25	1.85	155.92	#NUM!	14.25	1053.00
16.58	15.05	1.84	164.81	#NUM!	15.05	1217.81
18.24	15.83	1.84	173.50	#NUM!	15.83	1391.31
19.90	16.61	1.83	182.02	#NUM!	16.61	1573.33
21.56	17.37	1.82	190.37	#NUM!	17.37	1763.70
23.22	18.12	1.82	198.56	#NUM!	18.12	1962.26
24.87	18.85	1.82	206.60	#NUM!	18.85	2168.86
26.53	19.58	1.81	214.51	#NUM!	19.58	2383.36
28.19	20.30	1.81	222.28	#NUM!	20.30	2605.64
29.85	21.01	1.80	229.92	#NUM!	21.01	2835.56
31.51	21.70	1.80	237.45	#NUM!	21.70	3073.01
33.17	22.39	1.80	244.86	#NUM!	22.39	3317.87
34.82	23.07	1.79	252.16	#NUM!	23.07	3570.03
36.48	23.74	1.79	259.36	#NUM!	23.74	3829.39
38.14	24.41	1.79	266.46	#NUM!	24.41	4095.85
39.80	25.06	1.78	273.46	#NUM!	25.06	4369.31
41.46	25.71	1.78	280.38	#NUM!	25.71	4649.69
43.12	26.35	1.78	287.20	#NUM!	26.35	4936.89
44.77	26.99	1.78	293.94	#NUM!	26.99	5230.83
46.43	27.61	1.77	300.60	#NUM!	27.61	5531.44
48.09	28.23	1.77	307.19	#NUM!	28.23	5838.62
49.75	28.85	1.77	313.69	#NUM!	28.85	6152.32
51.41	29.46	1.77	320.13	#NUM!	29.46	6472.44
53.06	30.06	1.76	326.49	#NUM!	30.06	6798.94
54.72	30.65	1.76	332.79	#NUM!	30.65	7131.73
56.38	31.24	1.76	339.02	#NUM!	31.24	7470.75
58.04	31.83	1.76	345.19	#NUM!	31.83	7815.94
59.70	32.41	1.76	351.30	#NUM!	32.41	8167.23
61.36	32.98	1.75	357.34	#NUM!	32.98	8524.58
63.01	33.55	1.75	363.33	#NUM!	33.55	8887.91
64.67	34.12	1.75	369.27	#NUM!	34.12	9257.17
66.33	34.68	1.75	375.14	#NUM!	34.68	9632.32
67.99	35.23	1.75	380.97	#NUM!	35.23	10013.29
69.65	35.78	1.75	386.74	#NUM!	35.78	10400.03

Figure B.12 LVSS Nozzle Weight Page 2 (Dry Weight Minimization Case)

Input Variables		Input
Orbit Insertion	OrbitInsert	50.000
Launch Inclination	Inclination	28.500
Drag Reduction	DragRed	0.000%
Main Propulsion Delta Isp	MainIspDelta	0.973
Main Engine Nozzle efficiency	AstarOverTvac	0.000001131
ISP 1_Vacuum		441
ISP 2i_Vacuum		441
ISP 2f_Vacuum		441
Thrust to Weight Ratio (Twi)	Twi	1.40
Chamber Pressure (Pc)	Pc	2465
OF Ratio	OF	7.43
Nozzle Area Ratio	AR	87.53

Figure B.13 Trajectory Input Variables (Dry Weight Minimization Case)

Outputs:		Value
Time	TrajTime	316
Final Velocity	VelFinal	24,429
Final Altitude	AltFinal	303,433
Mass Ratio	MassRatio	8.016
T/W initial	ThrWtInitial	1.401
Area Ratio of Fixed Bell Nozzle	AreaRatio1	87.532
Initial Area Ratio of Extendable Bell Nozzle	AreaRatio2Init	87.532
Final Area Ratio of Extendable Bell Nozzle	AreaRatio2Final	87.532
Ratio of Total Thrust provided by Fixed Nozzles	ThrustRatio	1.000
Engine 2 Transition	NozzleTransition	1.000
OF Ratio	OF	7.429
Chamber Pressure	Pc	2464.887

Figure B.14 Trajectory Output Variables (Dry Weight Minimization Case)

UAH Trajectory

Trajectory Input

T/Wi	Orbit, n.mi.	Launch Inclination, deg	Vorbit, fps	Vinitial, fps
1.385120372			25765	1338

Aerodynamic Input

Drag Reduction

Propulsion Input

Area Ratio 1	Area Ratio 2 initial	Area Ratio 2 final	Thrust 1/Thrust total	Fraction of total trajectory time to transition from all engines burning to just engine 2 burn.	Fraction of total trajectory time to transition from initial area ratio of engine 2 to final area ratio.	Chamber Pressure	O/F Ratio
91.5451955	119.8656148	199.9105773	0.300059839	0.300059839	0.085193927	3900	6.9

Isp 1,vac	Isp 2 initial,vac	Isp 2 final, vac	Delta Isp	Astar/Tvac
3*LN(A14) + 381.7*(16.973*LN(B14) +D17*(16.973*LN(C14)+381.3627)/0.972)				

Trajectory Output

Time s	Final Velocity fps	Final Altitude ft	Mass Ratio	Mass Ratio	RSM Mass Ratio	%MR Error
315.5	24429	303433	8.0161	7.4947	8.2519	0.0000%

Figure B.15 Trajectory Program Sheet (Dry Weight Minimization Case)

Input Variables		Input
Vehicle DDTE	DDTE	$42.508
System TFU	SystemTFU	$7.594
Operations Cost per year	OpsCost	$19.591
Turnaround Time	TurnTime	164
Flights per year	FlightsPerYr	50
Years Operational	OpYears	10

Figure B.16 LCC Input Variables (Dry Weight Minimization Case)

Outputs:		Value
Vehicle DDTE	DDTECost	$43
Production Costs	ProductionCost	$88
Operations Cost	OpsCost	$196
Life Cycle Costs	LCCost	$326

Figure B.17 LCC Output Variables (Dry Weight Minimization Case)

Flts per Year per vehicle	2.23		DDT&E	$42.508
Number of units (fraction)	22.47		Production	$87.532
Number of units needed	23		Operations	$195.913
Learning curve slope	0.90		Total Life Cycle	$325.954
B	-0.1520			
Learning factor	0.62			
TFU Cost for first unit	$7.594			
Fleet Production Cost	87.5			
Ops Cost per Year	$19.591			
Number of Op Years	10			
Total Ops Cost	$195.913			
	0.90	7.6		
	1	7.6	$7.594	
	2	6.8	$14.429	
	3	6.4	$20.855	
	4	6.2	$27.006	
	5	5.9	$32.953	
	6	5.8	$38.736	
	7	5.6	$44.386	
	8	5.5	$49.922	
	9	5.4	$55.360	
	10	5.4	$60.711	
	11	5.3	$65.986	
	12	5.2	$71.191	
	13	5.1	$76.333	
	14	5.1	$81.418	
	15	5.0	$86.450	

Figure B.18 Lifecycle Cost Worksheet (Dry Weight Minimization Case)

Input Variables		Input
1.0 Wing	WingWt	53,728
2.0 Tail	TailWt	12,446
3.0 Body	BodyWt	125,955
Basic structure	BasicWt	45,082
LH2 tank	LHTankWt	45,407
LO2 tank	LOTankWt	23,463
Thrust Structure	ThrustStrWt	12,003
4.0 Induced environment protection	TPSWt	93,226
5.0 Undercarriage and aux. systems	GearWt	16,679
Engine accessories	EngineAccWt	4,796
Propellant System	PropSysWt	13,958
7.0 Propulsion, reaction control (RCS)	RCSWt	3,288
8.0 Propulsion, orbital maneuver (OMS)	OMSWt	2,350
9.0 Prime power	PowerWt	3,690
10.0 Electric conversion and distr.	ElecWt	6,560
11.0 Hydraulic conversion and distr.	HydWt	6,400
12.0 Control surface actuation	ActuationWt	5,458
13.0 Avionics	AvionicsWt	4,622
14.0 Environmental control	EnvirWt	4,048
15.0 Personnel provisions	PersonnelWt	1,100
18.0 Payload provisions	PayloadProvWt	595
6.3 Engines	EngineWt	69,224
Engine Weight 1	Engine1Wt	88,510
Engine Weight 2	Engine2Wt	0
1.0 Wing CIF (Cost influence Factor)	WingCIF	2.100
2.0 Tail CIF	TailCIF	2.100
3.0 Body CIF	BodyCIF	2.100
Basic structure CIF	BasicCIF	2.100
LH2 tank CIF	LHTankCIF	2.100
LO2 tank CIF	LOTankCIF	2.100
Thrust Structure CIF	ThrustStrCIF	2.100
4.0 Induced environment protection CIF	TPSCIF	1.000
5.0 Undercarriage and aux. systems CIF	GearCIF	1.800
Engine accessories CIF	EngineACCCIF	1.000
Propellant System CIF	PropSysCIF	1.000
7.0 Propulsion, reaction control (RCS) CIF	RCSCIF	1.000
8.0 Propulsion, orbital maneuver (OMS) CIF	OMSCIF	1.000
9.0 Prime power CIF	PowerCIF	1.000
10.0 Electric conversion and distr. CIF	ElecCIF	1.000
11.0 Hydraulic conversion and distr. CIF	HydCIF	1.000
12.0 Control surface actuation CIF	ActuationCIF	1.000
13.0 Avionics CIF	AvionicsCIF	4.000
14.0 Environmental control CIF	EnvirCIF	1.000
15.0 Personnel provisions CIF	PersonnelCIF	1.000
18.0 Payload provisions CIF	PayloadProvCIF	1.000
6.3 Engines CIF	EngineCIF	1.000
Engine Weight 1 CIF	Engine1CIF	1.000
Engine Weight 2 CIF	Engine2CIF	1.000

Figure B.19 DDTE Cost Input Variables (Dry Weight Minimization Case)

Outputs:		Value
Vehicle DDTE	DDTE	$42.508
System TFU	SystemTFU	$7.594
Propulstion TFU	Propulstion TFU	$0.763
Vehicle TFU	Vehicle TFU	$4.564

Figure B.20 DDTE Cost Output Variables (Dry Weight Minimization Case)

Input Variables		Input
Labor Cost per hour	LaborCostpHr	$75
Hardware LRUs / STS LRUs	HwReplace	100%
Flights per year	FlightsPerYr	50
Maximum Length	MaxLength	271
Maximum Width	MaxWidth	213
Wing Wetted Area	WingWetArea	13,759
Tail Wetted Area	TailWetArea	4,935
Body Wetted Area	BodyWetArea	30,424
Vehicle Landed Weight	LandWt	540,083
Vehicle TFU	VehicleTFU	4.564
Propulsion TFU	PropTFU	0.763
System TFU	SystemTFU	7.594
Number of Main Engines	NEng	10
Vehicle LOX	LOXWt	3,739,830
Vehicle LH	LHWt	503,395
Flight autonomy 1-AC to 0-Shuttle	FltAuto	80%
1.00 Wing Grp 0-STS 1-AC	WingProPct	0%
2.00 Tail Grp 0-STS 1-AC	TailProPct	0%
3.00 Body Grp 0-STS 1-AC	BodyProPct	0%
4.10 IEP-TPS 0-STS 1-AC	TPSProPct	20%
4.20 IEP-TCS 0-STS 1-AC	TCSProPct	0%
4.30 IEP-PVD 0-STS 1-AC	PVDProPct	0%
5.00 Landing Gear 0-STS 1-AC	GearProPct	0%
6.00 Prop-Main 0-STS 1-AC	MainEngProPct	0%
6.10 Prop-MPS 0-STS 1-AC	MPSProPct	0%
7.00 Prop-RCS 0-STS 1-AC	RCSProPct	0%
8.00 Prop-OMS 0-STS 1-AC	OMSProPct	0%
9.10 Pwr-APU 0-STS 1-AC	APUProPct	0%
9.30 Fuel Cell 0-STS 1-AC	FCellProPct	0%
10.00 Electrical 0-STS 1-AC	ElectProPct	0%
11.00 Hydraulics 0-STS 1-AC	HydrlProPct	0%
12.00 Aero SurfAct 0-STS 1-AC	AeroSurfProPct	0%
13.10 Avionics-GN&C 0-STS 1-AC	AvionicsProPct	80%
13.30 Comm 0-STS 1-AC	CommProPct	0%
13.40 Displays 0-STS 1-AC	DisplayProPct	0%
13.50 Instrumnt 0-STS 1-AC	InstruProPct	0%
13.60 Data Procc 0-STS 1-AC	DataProcProPct	0%
14.10 Envrn Cntrl 0-STS 1-AC	EnvContProPct	0%
14.20 ECS-LifeSpt 0-STS 1-AC	ECSProPct	0%
15.00 Pers Prov 0-STS 1-AC	PersProvProPct	0%

Figure B.21 Operations Cost Input Variables (Dry Weight Minimization Case)

Outputs:		Value
Operations Cost per year	OpsCost	$19.591
Turnaround Time	TurnTime	164

Figure B.22 Operations Cost Output Variables (Dry Weight Minimization Case)

APPENDIX C

ENGINE HISTORICAL DATA

Table C.1 Historical Engine Data

Engine	Oxidizer/Fuel	Engine Cycle	Chamber Pressure (psia)	Engine Mass (lb)	Avg Thrust-Vacuum (lbf)	Mixture Ratio	ISP Sea Level (sec)	ISP Vacuum (sec)	Nozzle Area Ratio
SSME Block IA	LOX/LH2	Staged Combustion	3141	7,445	489,985	6.032	363	453.4	76.79
SSME Full Power Level	LOX/LH2	Staged Combustion	3126	7,004	489,910	6	363	452.59	77.01
SSME Block II	LOX/LH2	Staged Combustion	2857	7,813	488,470	6.032	363	452.18	68.80
SSME Block IIA	LOX/LH2	Staged Combustion	2857	7,607	488,468	6.032	363	452.18	68.80
SSME Return to Flight	LOX/LH2	Staged Combustion	3126	7,094	488,369	6.011	363	452.86	77.02
SSME Block I	LOX/LH2	Staged Combustion	3126	7,445	487,903	6.011	363	452.09	76.79
SSME 1st Flight	LOX/LH2	Staged Combustion	3012	6,846	468,760	6	363	452.66	77.43
RD-0120	LOX/LH2	Staged Combustion	3162	7,606	440,925	6	359	455	85.70
LE-7A	LOX/LH2	Staged Combustion	1750	3,750	246,915	5.9	338	440	52.00
LE-7	LOX/LH2	Staged Combustion	2090	3,440	243,000	6	349	449	60.00
Vulcain 2	LOX/LH2	Gas Generator	1668	4,497	292,251	6.1	318	434	58.50
Vulcain	LOX/LH2	Gas Generator	1540	3,249	241,669	5.25	326	431.5	45.00
J-2	LOX/LH2	Gas Generator	702	3,170	225,000	5.5	293.81	423.8	28.00

APPENDIX D

LOGNORMAL UNCERTAINTY CURVES

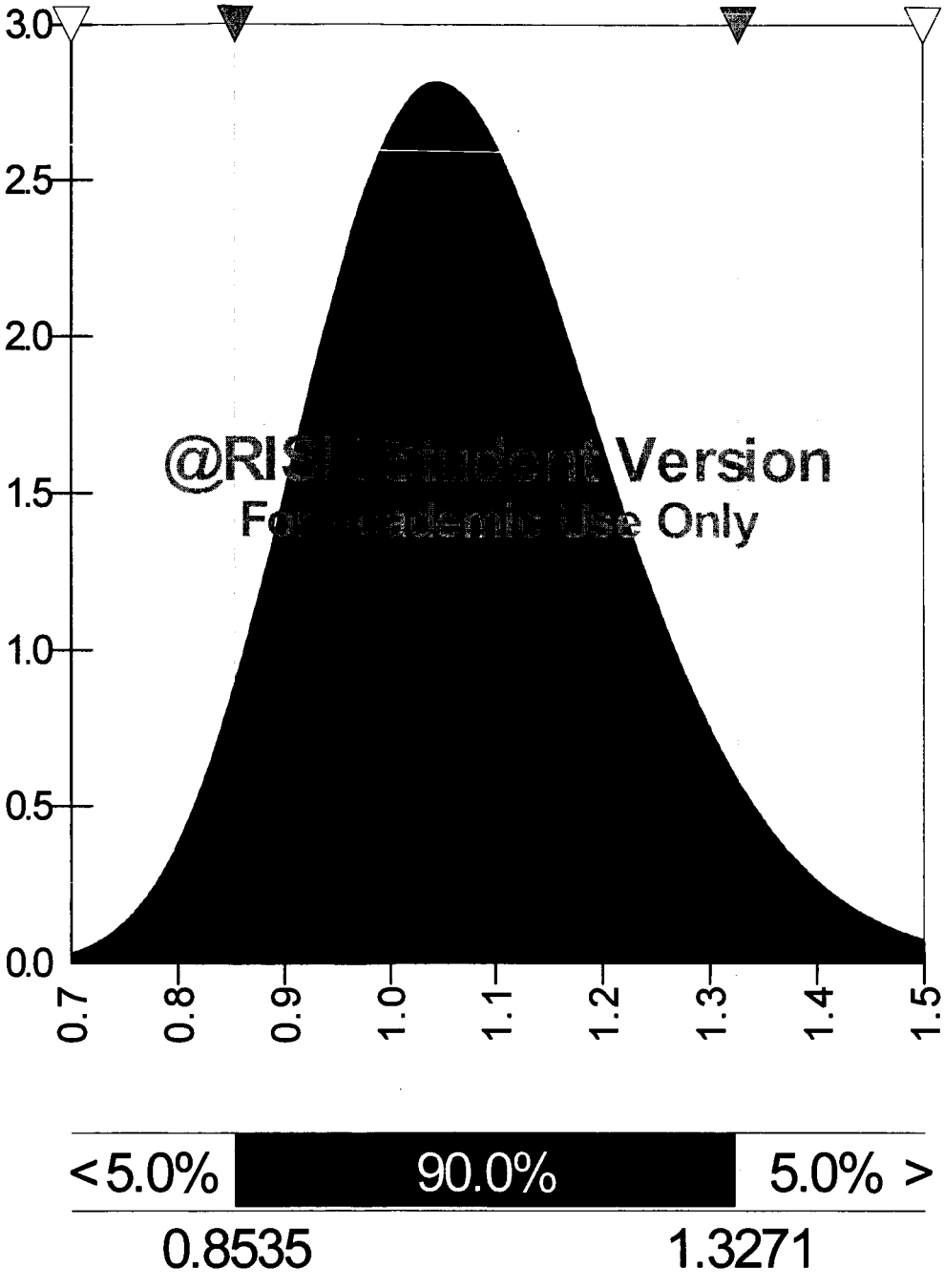

Figure D.1 Wing Lognormal Distribution

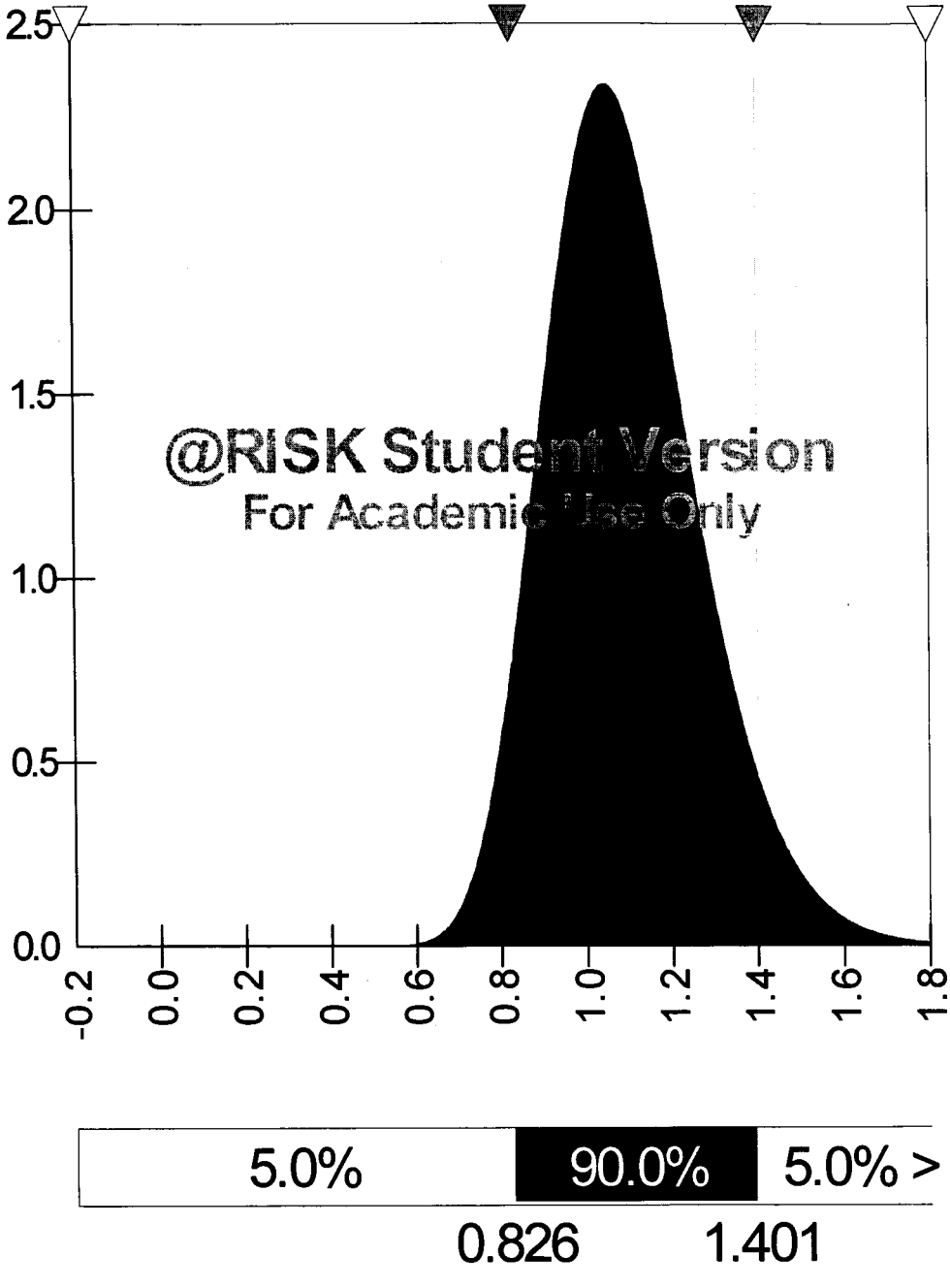

Figure D.2 Tail Lognormal Distribution

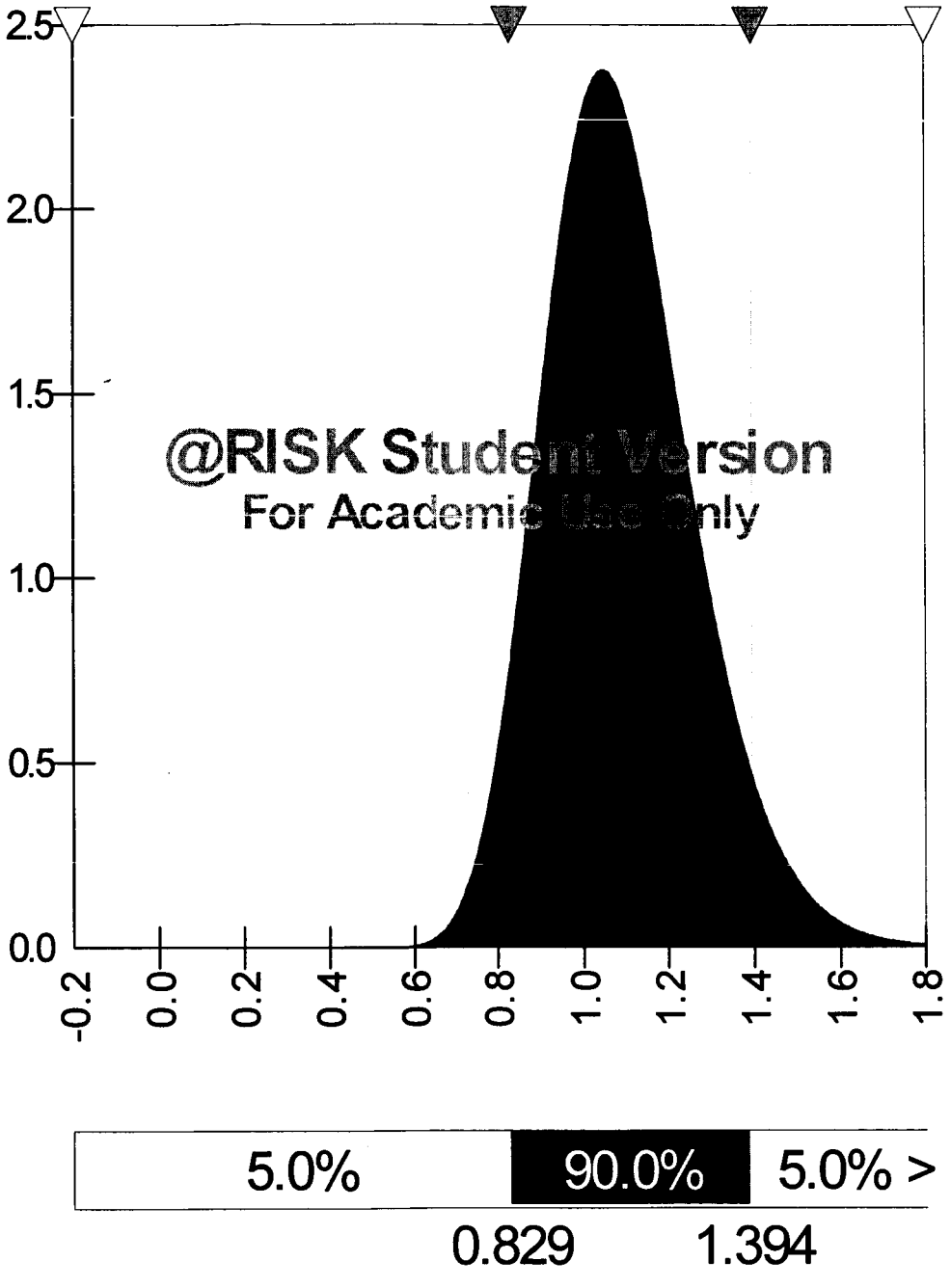

Figure D.3 LH2 Tank Lognormal Distribution

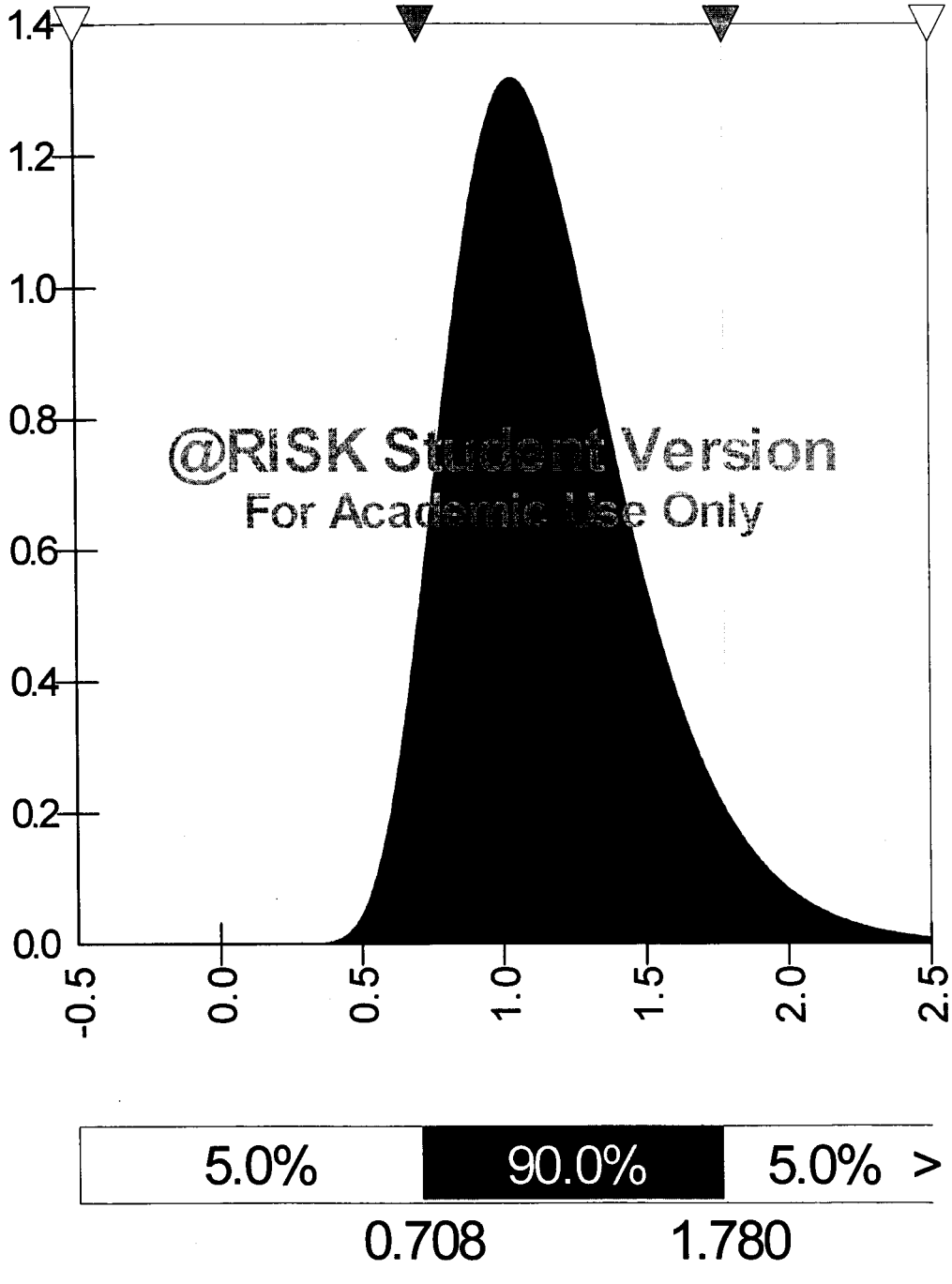

Figure D.4 LOX Tank Lognormal Distribution

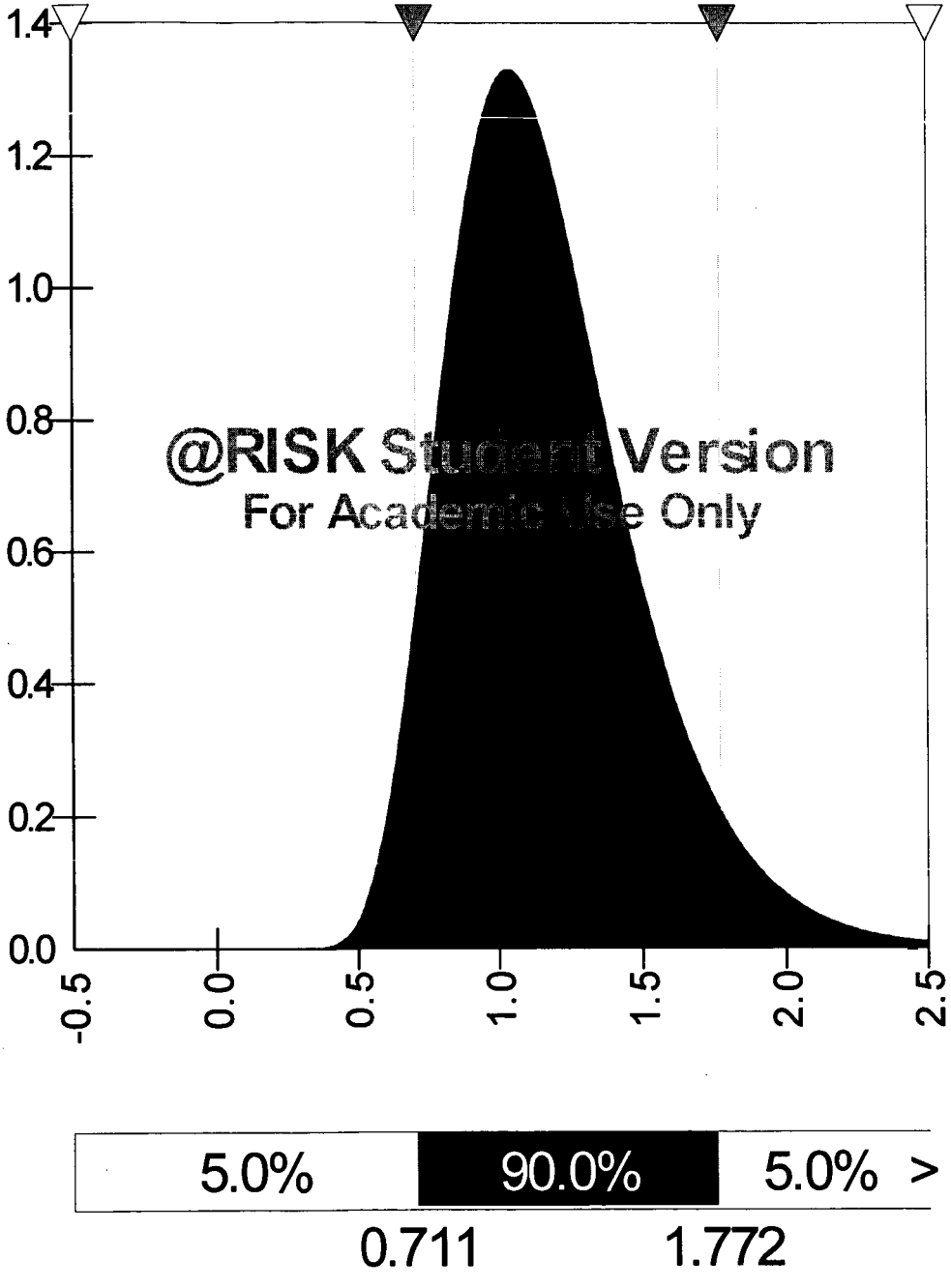

Figure D.5 Overall Body Lognormal Distribution

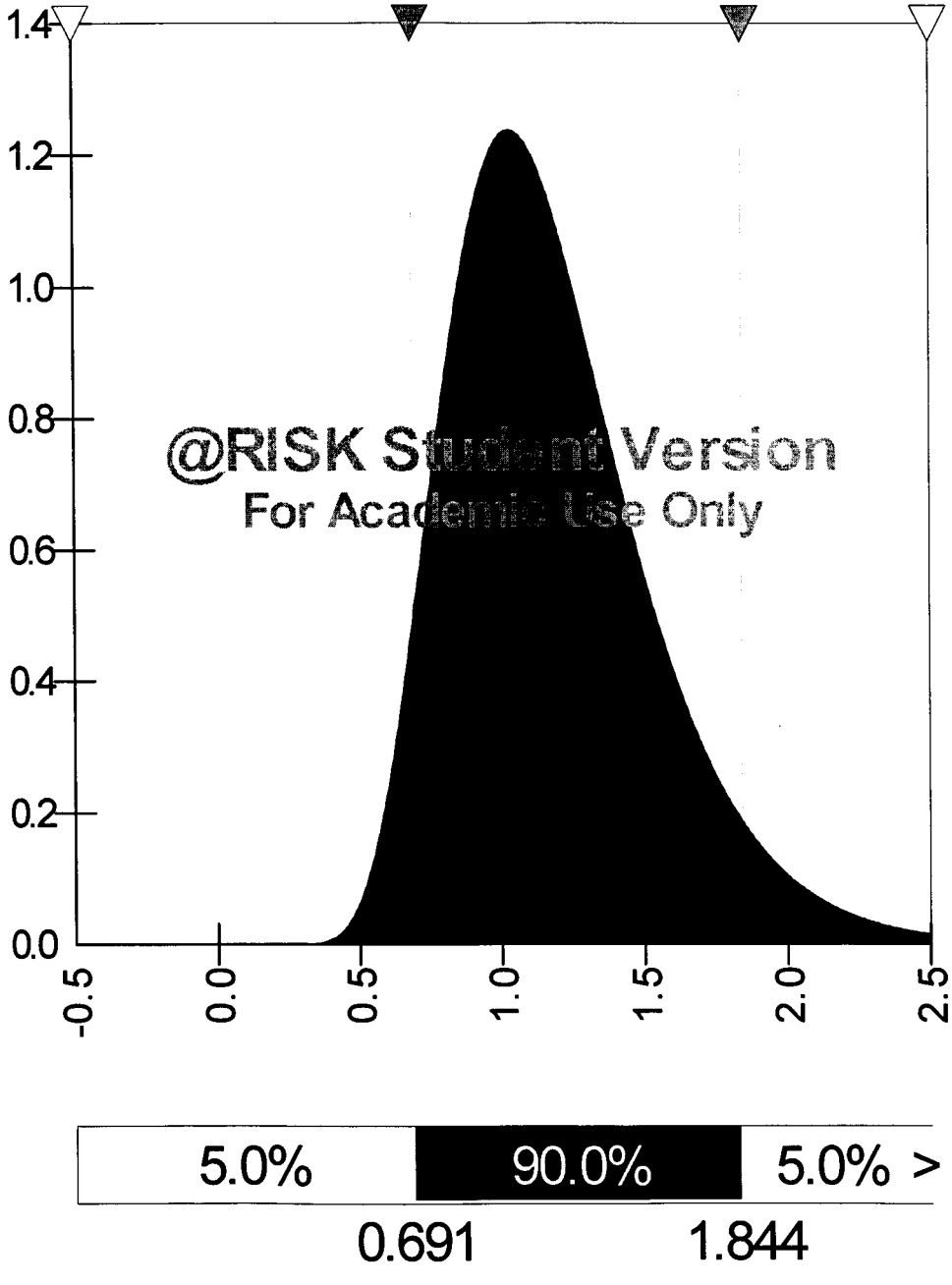

Figure D.6 Thrust Structure Lognormal Distribution

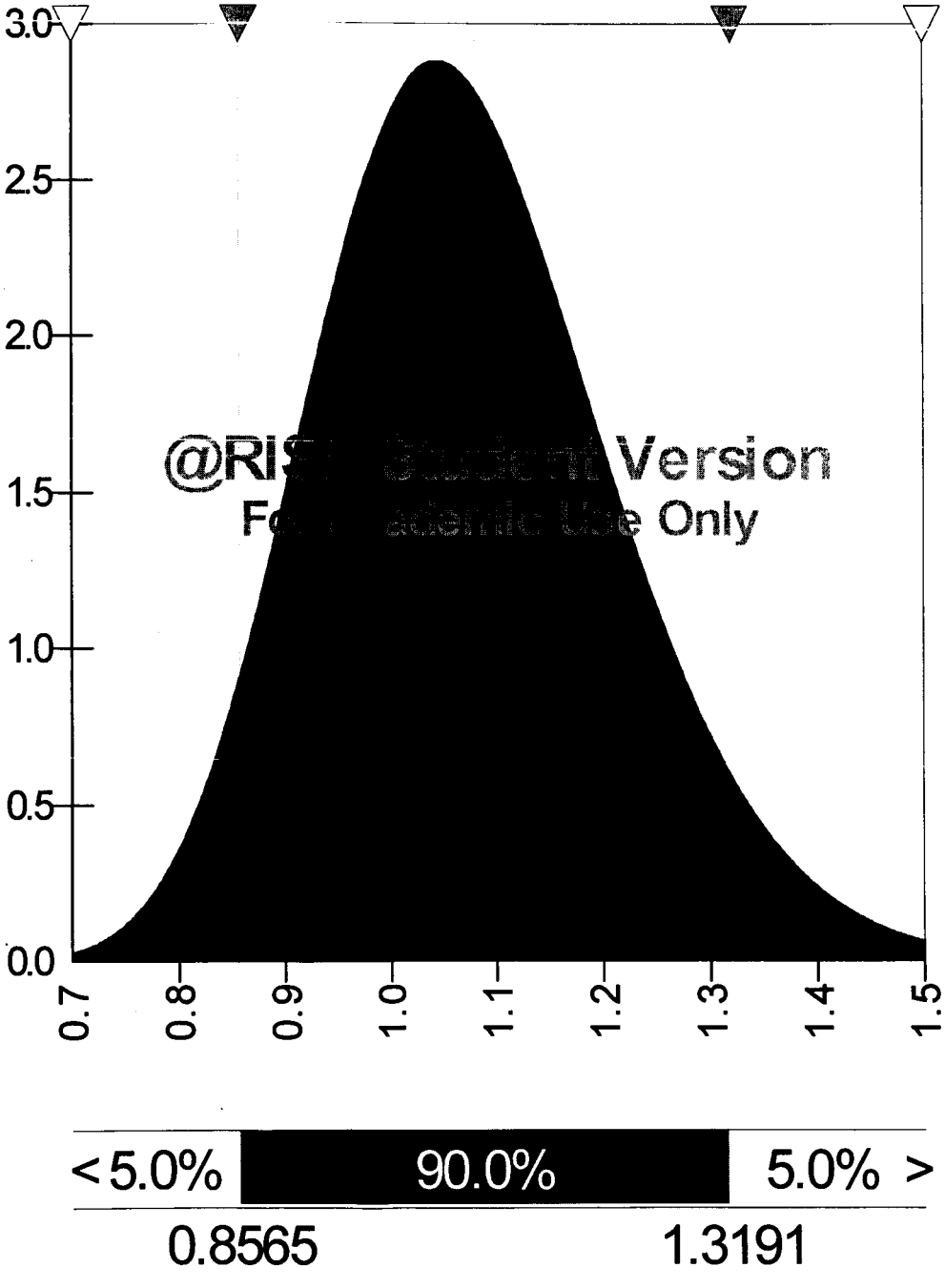

Figure D.7 Landing Gear Lognormal Distribution

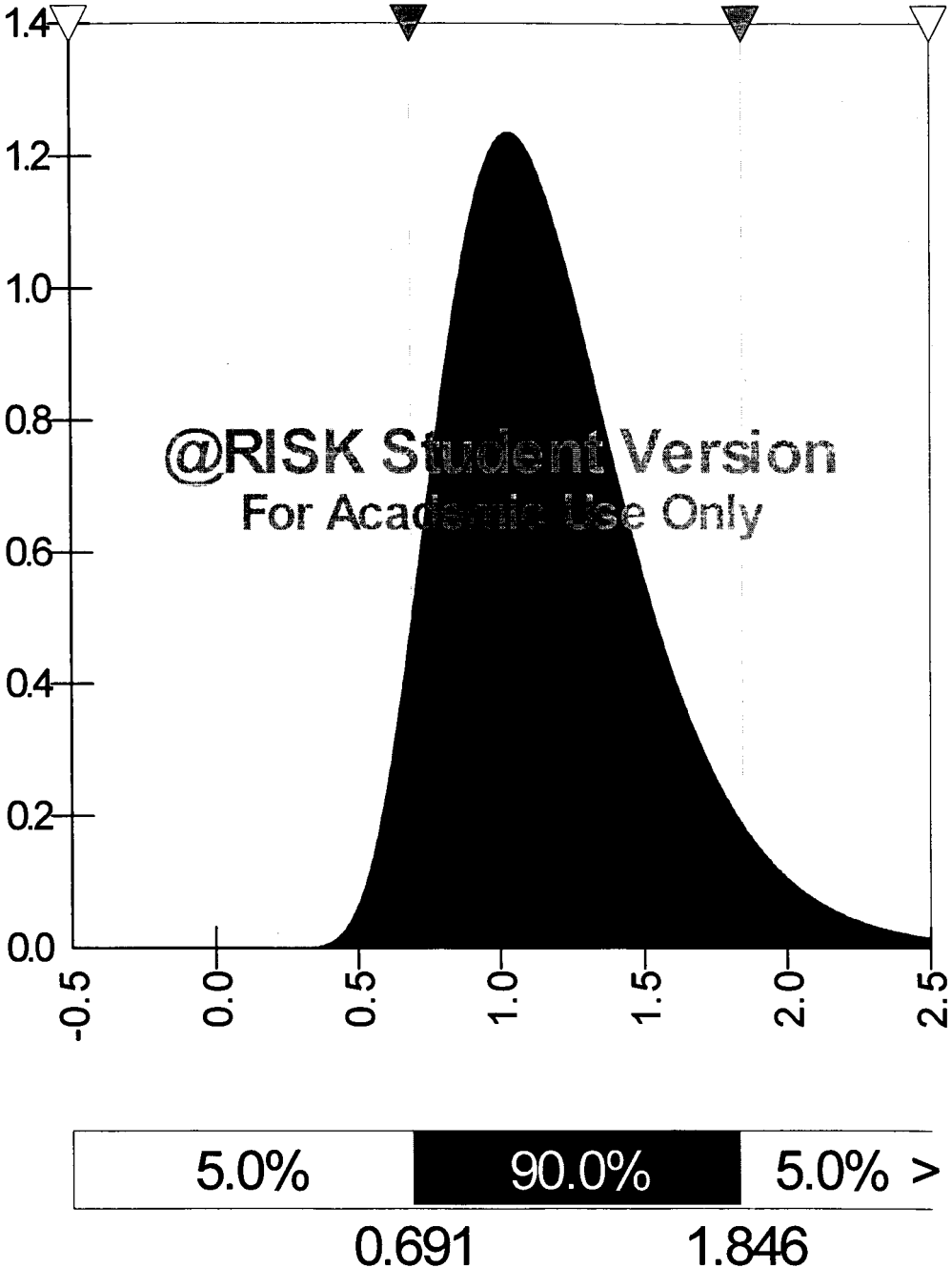

Figure D.8 Propulsion Lognormal Distribution

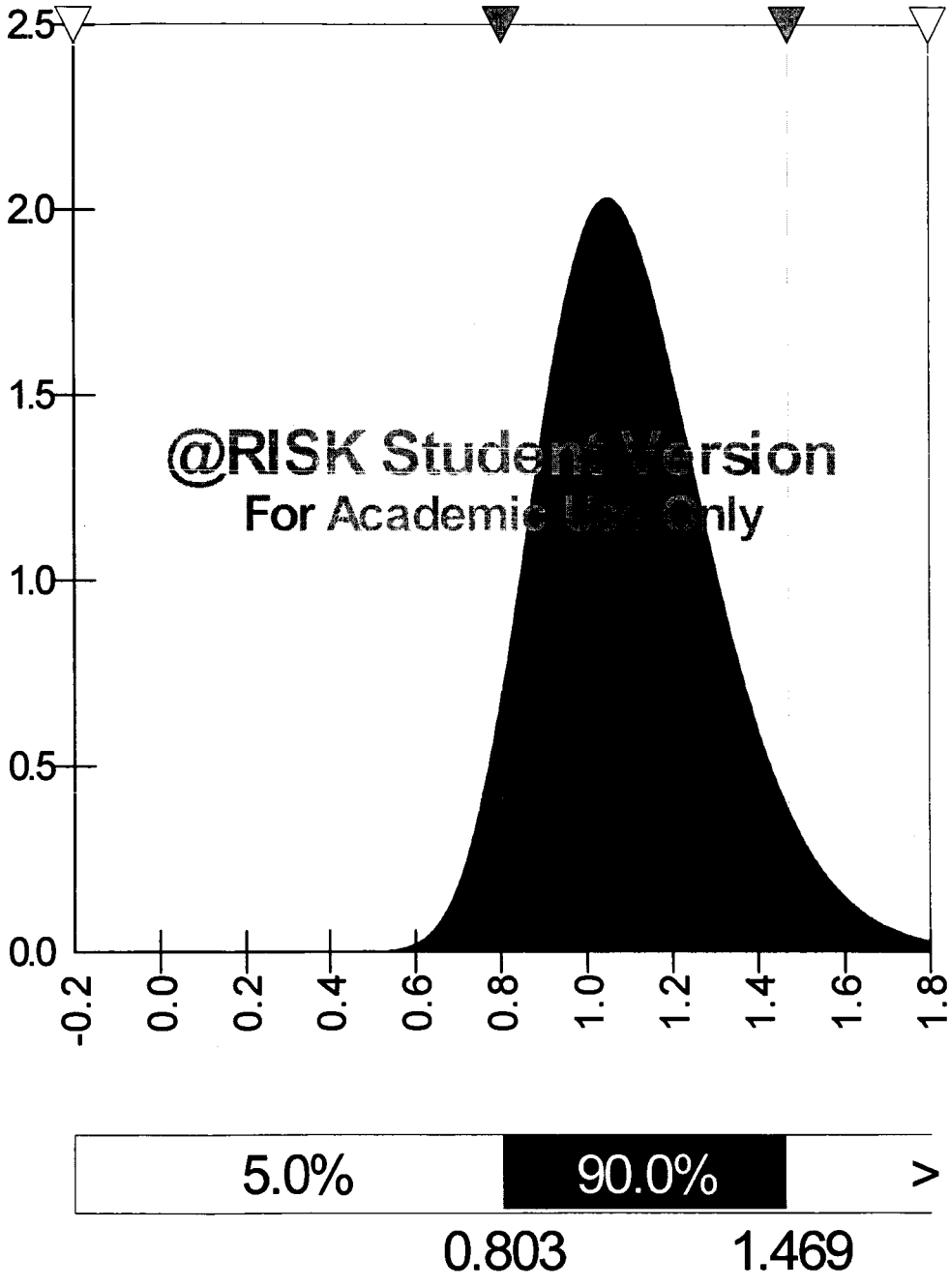

Figure D.9 TPS Lognormal Distribution

REFERENCES

[1] Haefeli, R., Littler, E., Hurley, J., Winter, M., Martin Marietta Corporation, "Technology Requirements for Advanced Earth-Orbital Transportation System", NASA Contractor Report, NASA CR-2866, October 1977.

[2] Wilhite, A., Gholston, S., Farrington, P., Swain, J., University of Alabama in Huntsville, "Evaluating Technology Impacts on Mission Success of Future Launch Vehicles", IAF-01-V.4.04, 52nd International Astronautical Congress, Toulouse, France, October 2001.

[3] Palisade Corporation Software, @RISK™ Risk Analysis and Simulation Software, Evolver Tool Software, 'Decision Tools 4.5', 2002.

[4] Smart, C., "NAFCOM Cost Risk Module", The NASA Engineering Cost Group and Science Application International Corporation, Huntsville, AL., pages 2-8, 2004.

[5] Walpole, R., Myers, R., Myers, S, Ye, K, Probability & Statistics for Engineers and Scientist, 7th edition, Prentice Hall, 2002.

[6] Box, G., Draper, N., Empirical Modeling–Building and Response Surfaces, John Wiley & Sons, New York, 1987.

[7] Montgomery, D., Design and Analysis of Experiments, 5th ed., John Wiley & Sons, New York, 2001.

[8] Obitko, M., Czech Technical University in Prague, 'http://cs.felk.cvut.cz/~xobitko/ga/', September 1998.

[9] Schoonover, P., Crossley, W., Heister, S., "Application of a Genetic Algorithm to the Optimization of Hybrid Rockets", Journal of Spacecraft and Rockets, Vol. 37, No. 5, pages 622-629, September-October 2000.

[10] Wilhite, A., McKinney, L., Farrington, P., and Lovell, N., "Launch System Trajectory Performance Modeling and Sensitivity Analysis Using Response Surface Methods", University Report, pages 2-3, University of Alabama in Huntsville, 2004.

[11] Manski, D., Martin, James A., "Optimization of the Propulsion Cycles for Advanced Shuttles Part 1: Propulsion Mass Model Methodology", AIAA-89-2279, July 1989.

[12] Wilhite, A., NASA Langley Research Center, "Engine Weight Study", 2004.

[13] Paulson, E., Burkhardt, W., Mysko, S., Jenkins, J., "Simplified Liquid Rocket Engine Performance and Weight Model", JANNAF CS/APS/PSHS & MSS, Colorado Springs, CO, pages 4-6, September 1-5, 2003.

[14] Wells, N., "Bell Parametrics", Rocketdyne a Division of North American Rockwell Corporation, Model ILRV, pages 4-33, December 1969.

[15] Leahy, J., "P-STAR: A Propulsion Sizing, Thermal Analysis and Weight Relationship Model", NASA George C. Marshall Space Flight Center, AL, 2003.

[16] Huzel, D., Huang, D., "Engineering for Design of Liquid Propellant Rocket Engines", Progress in Astronautics and Aeronautics, AIAA, Vol. 147, pages 71-79, 1992.

[17] The NASA Engineering Cost Group and Science Application International Corporation, 'The NASA/Air Force Cost Model (1999 version)', Huntsville, AL, 1999.

[18] Software and Engineering Associates, Inc., 'Cequel', 2001-2004.

[19] McBride, B., Gordon, S., "Computer Program for Calculation of Complex Chemical Equilibrium Compositions and Applications, II: Users Manual and Program Description", NASA RP–1311, 1996.

[20] Sutton, G., Rocket Propulsion Elements An Introduction to the Engineering of Rockets, 6th ed., John Wiley & Sons, New York, 1992.

[21] Coleman, H., Steele, G., Experimentation and Uncertainty Analysis for Engineers, 2nd ed., John Wiley & Sons, New York, 1999.